University of Latvia
Faculty of Biology

Reinis Rutkis
Doctoral Thesis

Study of *Zymomonas mobilis* uncoupled energy metabolism

Submitted for the degree of Doctor of Biology
Subfield of Microbiology

Supervisor: Prof. Uldis Kalnenieks

Riga, 2013

The doctoral thesis was carried out in University of Latvia, Faculty of Biology, and at the Institute of Microbiology and Biotechnology.
From 2006 to 2013.

This work has been supported by the European Social Fund within the project «Support for Doctoral Studies at University of Latvia». The research was supported by grant 09.1306 of Latvian Council of Science and by Latvian ESF projects European Structural Fund Nr. 2009/0207/1DP/1.1.1.2.0/ 09/APIA/VIAA/128 „Latvian Interdisciplinary Interuniversity Scientific Group of Systems Biology' and 2009/0138/1DP/1.1.2.1.2/09/IPIA/VIAA/004.

The thesis contains the introduction, review of literature, materials and methods, results and discussion chapters, conclusions, theses for defence and reference list.

Form of the thesis: Collection of research articles in biology, microbiology subfield

Supervisor: Professor Uldis Kalnenieks,
Institute of Microbiology and Biotechnology,
University of Latvia, Riga, Latvia

Reviewers:
1) Professor Indrikis Muižnieks
Faculty of Biology
University of Latvia,

2) Professor Raivo Vilu,
Department of Chemistry,
Tallin University of Technology

3) Professor Tālis Juhna,
Institute of Heat, Gas and Water technologies,
Riga Technical University

The thesis will be defended at the public session of the Doctoral Committee of Biology, University of Latvia, at 13:00, lecture hall nr. 2, on the 8th of April, 2014, at the Faculty of Biology, University of Latvia, Kronvalda Blvd 4, Riga, Latvia.

The thesis is available at the Library of the University of Latvia, Kalpaka blvd. 4.
This thesis is accepted for the commencement of the degree of Doctor of Biology on 24.10. 2013 by the Doctoral Committee of Biology, University of Latvia.

Secretary of the Doctoral Committee _____/Daina Eze/
Chairman of the Doctoral Committee _____/Pauls Pumpēns/

ABSTRACT

Facultatively anaerobic, Gram-negative ethanol producing bacterium *Z. mobilis* is of great interest from a biotechnological perspective. Showing an extremely rapid catabolism, which is quite loosely matched to the needs of cellular biosynthesis, *Z. mobilis* is considered as a classical example of the ucoupled energy metabolism. Ucoupled energy metabolism or uncoupled growth phenomenon, is largely what makes this bacterium an outstanding ethanol producer. However, the mechanisms of uncoupled growth so far are not fully understood. Although *Z. mobilis* possess high respiratory capacity, the respiratory system still remains poorly understood and it does not appear to be primarily required for energy conservation. The aim of the dissertation was (I) to examine the structure and function of electron transport chain and its relation to the uncoupled growth, (II) via creating computional kinetic model of the Entner-Doudoroff pathway, to investigate the possible regulatory factors of *Z. mobilis* rapid catabolism. Results of the research allow to conclude that: (I) the respiratory chain of *Z. mobilis* contains only one functional NAD(P)H dehydrogenase and at least two electron pathways to oxygen, (II) inhibition of respiration stimulates *Z. mobilis* aerobic growth due to reduction of toxic acetaldehyde in the media, (III) one of the functions of *Z. mobilis* respiratory chain might be to prevent endogenous oxidative stress, (IV) The absence of oxidative phosphorylation activity in aerobically growing *Z. mobilis* primarily results from insufficient degree of energy coupling between the proton-motive force and the F_0F_1 type H^+-dependent ATPase, (V) metabolic control analysis revealed that the majority of flux control resides outside the Entner-Doudoroff pathway, suggesting that glycolytic flux during the uncoupled growth is largely controled by ATP-consuming reactions, (VI) Increase of ATP-consuming reactions within physiological capacity, making growth more uncoupled, might serve as the appropriate strategy to increase the glycolytic flux in *Z. mobilis*.

Work was performed at the Institute of Microbiology and Biotechnology, University of Latvia.

KOPSAVILKUMS

Fakultatīvi anaerobajai, Gram-negatīvai, etanolu producējošai baktērijai *Z. mobilis* ir nozīmīgs biotehnoloģisks potenciāls. Uzrādot augstu no biosintēzes neatkarīgu katabolisma ātrumu, *Z. mobilis* baktērijas ir uzskatāmas par tipisku atjūgtā enerģētiskā metabolisma piemēru. Lielā mērā tieši atjūgtais enerģētiskais metabolisms vai citiem vārdiem, atjūgtās augšanas fenomens padara šo baktēriju par potenciāli izcilu etanola producentu. Neskatoties uz to, atjūgtās augšanas mehanismi līdz šim ir nepilnīgi izpētīti. Turklāt, lai arī *Z. mobilis* piemīt aktīva elpošanas ķēde, tās primārā loma līdz galam nav skaidra un visdrīzāk nav saistāma ar enerģijas ražošanu. Šīs disertācijas mērķi bija (I) izpētīt *Z. mobilis* elpošanas ķēdes strukturālās un funkcionālās īpatnības un tās saistību ar atjūgto augšanu, (II) konstruēt Entnera-Dudorova ceļa kinētisko datormodeli un ar tā palīdzību skaidrot *Z. mobilis* straujā katabolisma galvenos regulatoros faktorus. Darbā iegūtie rezultāti ļauj secināt, ka: (I) *Z. mobilis* elpošanas ķēde satur vienu funkcionāli aktīvu NAD(P)H dehidrogenāzi un vismaz divus elektronu transporta atzarus uz skābekli, (II) pateicoties zemākai acetaldehīda koncentrācijai vidē, elpošanas ķēdes inhibēšana stimulē *Z. mobilis* aerobo augšanu, (III) viena no elpošanas ķēdes funkcijām iespējams ir saistāma ar *Z. mobilis* aizsardzību pret endogēno oksidatīvo stresu, (IV) Oksidatīvās fosforilēšanas aktivitātes trūkums aerobi augošās *Z. mobilis* šūnās ir skaidrojams ar nepietiekamu protondzinējspēka un F_0F_1 tipa H^+-atkarīgās ATFāzes enerģētisku sajūgšanu, (V) *Z. mobilis* glikolīzes ātrums tiek kontrolēts ne tikai E-D ceļā, bet gan galvenokārt ir atkarīgs no ATF patēriņa, kas atjūgtās augšanas gadījumā daļēji tiek nodrošināts ar F_0F_1 tipa H^+-atkarīgās ATFāzes palīdzību, (VI) ATP patērējošo reakciju aktivitātes palielināšana *Z. mobilis* fizioloģiskās kapacitātes robežās var kalpot kā efektīvākā stratēģija glikolīzes ātuma palielināšanai E-D ceļā.

Darbs ir izstrādāts Latvijas Universitātes Mikrobioloģijas un Biotehnloģijas institūtā.

TABLE OF CONTENTS

ABBREVIATIONS

ADH	Alcohol dehydrogenase
ACET	Acetaldehyde
AK	Adenylate kinase
ATPcons	ATP consuming reactions
A.U.	Arbitrary units
bPG	1,3-bisphosphoglycerate
DCCD	Dicyclohexylcarbodiimide
E-D pathway	Entner-Doudoroff pathway
EMP pathway	Embden Meyerhof Parnas pathway
ENO	Enolase
ETOHcy	Cytoplasmic ethanol
ETOHex	Extracellular ethanol
ETOHexp	Ethanol transport
FT-IR	Fourier transform infrared
GAP	Glyceraldehyde 3-phosphate
GAPD	Glyceraldehyde 3-phosphate dehydrogenase
GF	Glucose facilitator
GK	Glucokinase
GLUCcy	Cytoplasmic glucose
GLUCex	Extracellular glucose
GLUC6P	Glucose 6-phosphate
GPD	Glucose 6-phosphate dehydrogenase
HCA	Hierarchical cluster analysis
KDPG	2-keto-3-deoxy-6-phosphogluconate
KDPGA	2-keto-3-deoxy-6-phosphogluconate aldolase
MCA	Metabolic control analysis
PDC	Pyruvate decarboxylase
PEP	Phosphoenolpyruvate
PGD	6-phosphogluconate dehydratase
PGK	3-phosphoglycerate kinase
PGL	6-phosphogluconolactonase
PGLACTON	6-phosphogluconolactone
PGLUCONATE	6-phosphogluconate
PGM	Phosphoglycerate mutase
P3G	3-phosphoglycerate
P2G	2-phosphoglycerate
PYK	Pyruvate kinase
PYR	Pyruvate
Δp	Proton-motive force
q	Specific rate of glucose consumption (g/g/h)
$Y_{X/S}$	Aerobic biomass yield, g (dry wt)/mole (glucose)
μ	Specific growth rate (h^{-1})

INTRODUCTION

Zymomonas mobilis is a facultatively anaerobic, Gram-negative bacterium with a very efficient and rapidly operating homoethanol fermentation pathway. Its rapid catabolism, in combination with tolerance to high ethanol and sugar concentrations, have kept *Z. mobilis* in the focus of biotechnological interest. One of the shortages of *Z. mobilis* is its limited carbon substrate range as it can only use glucose, fructose and sucrose for ethanol fermentation. As a result, studies on *Z. mobilis* genetic manipulation to extend substrate range for ethanol production has been intense during the last decades. Also, recently reported complete genome sequences of various *Z. mobilis* strains greatly contribute not only to biotechnological development, but also to better understanding of *Z. mobilis* unusual physiology.

Despite the extensive physiological studies, various aspects of *Z. mobilis* metabolism still remain poorly understood. *Z. mobilis* produces little cell mass, grow with a low energetic efficiency, and biomass synthesis is by far not the main consumer of ATP produced in the Entner-Doudoroff pathway. Thus, *Z. mobilis* is considered as a classical example of the ucoupled energy metabolism or uncoupled growth phenomenon, showing an extremely rapid catabolism, which is quite loosely matched to the needs of cellular biosynthesis. Excessive production of ATP in the E-D pathway raises a long-standing question, what might be the routes of its utilization.

Besides, *Z. mobilis* was shown to posses respiratory chain, the role of which in the bacteria‘s metabolism also has not been fully explained. *Z. mobilis* respiratory system does not appear to be primarily required for ATP synthesis during the different growth phases, since the rapid catabolism is loosely coupled with anabolic reactions. Data published so far, do not provide a coherent picture of the specific energetic mechanisms explaining the low energetic efficiency of its respiratory chain, and its relation to the uncoupled growth of *Z. mobilis.* In-depth structural and physiological studies of *Zymomonas mobilis* respiratory chain, supported by *in silico* metabolic modelling of central metabolic routes may reveal the relation between the high glycolytic flux and the uncoupled *Z. mobilis* metabolism both under aerobic and anaerobic conditions. Therefore the aim of the present thesis was, on the basis of experimental and theoretical studies, to explore the problems of *Z. mobilis* uncoupled energy metabolism, which have not received enough attention so far.

1 LITERATURE REVIEW

1.1 Characteristics of Z. mobilis

Zymomonas mobilis is a facultatively anaerobic Gram-negative bacterium, possesing a very efficient and rapidly operating homoethanol fermentation of glucose to equimolar amounts of ethanol and carbon dioxide. It belongs to the family of *Sphingomonadaceae* (White *et al*., 1996; Kosako *et al*., 2000), Group 4 of the alpha-subclass of the class Proteobacteria. The complete genome sequences of various *Z. mobilis* strains, has been reported recently (Seo *et al*., 2005; Kouvelis *et al*., 2009; Pappas *et al*., 2011; Desiniotis *et al*., 2012). The genome of *Z. mobilis* strain ATCC 29191 (Zm6), that was used in present study, consists of a single circular chromosome of 1,961,307 bp and three plasmids, p29191_1 to p29191_3, of 18,350 bp, 14,947 bp, and 13,742 bp, respectively. The entire genome has 1,765 protein-coding genes, 51 tRNA genes, and 3 rRNA gene clusters. Zm6 genome is smaller than that of reference strain ATCC 31821 (Zm4), yet it contains 41 genes that are unique compared to ZM4 (Desiniotis *et al*., 2012).

1.2 Z. mobilis central metabolism

Z. mobilis is an obligately fermentative microorganism. The network of *Z. mobilis* central metabolism (Fig. 1) is simpler, than in most model microorganisms, including *E. coli* and *Saccharomyces cerevisiae*. In conjunction with the pyruvate decarboxylase and two alcohol dehydrogenases *Z. mobilis* ferments glucose, fructose and sucrose to equimolar amounts of ethanol and carbon dioxide via the Entner-Doudoroff (2-keto-3-deoxy-6-phosphogluconate) pathway (Gibbs & DeMoss, 1954; Dawes *et al.*, 1966). The Embden–Meyerhof–Parnas (EMP) pathway is not operating in this bacterium, (Fuhrer *et al*., 2005). Although a weak phosphofructokinase activity has been reported (Viikari, 1988), it was not confirmed afterwards, coresponding gene is lacking in all sequenced *Z. mobilis* strains (Seo *et al*., 2005; Kouvelis *et al*., 2009; Pappas *et al*., 2011; Desiniotis *et al*., 2012). Early studies of the central metabolism of *Z. mobilis* by Dawes *et al.* (1970), revealed that the Krebs cycle in this bacterium is truncated and apparently functions only to provide precursors for biosynthesis. Lacking activities of α-ketoglutarate dehydrogenase, succinyl thiokinase, succinate dehydrogenase, fumarase (Dawes *et al*., 1970) and malate dehydrogenase (Bringer-

Meyer and Sahm, 1989) was later confirmed by genome analysis (Seo *et al*., 2005) Likewise, part of enzymes of the pentose phosphate pathway are missing, and also the glyoxylate shunt is absent in *Z. mobilis*. (De Graaf *et al*., 1999; Seo *et al*., 2005). The pyruvate dehydrogenase complex has been purified and characterised, and the sequence and localisation of the corresponding genes have been analysed (Neveling *et al*., 1998). Two anaplerotic enzyme activities, those of PEP carboxylase and malic enzyme, have been found in cell free extracts (Bringer-Meyer & Sahm, 1989). Besides the PEP carboxylase, *Z. mobilis* genome also contains genes for citrate lyase, malic enzyme and fumarate dehydratase (Seo *et al*., 2005). Therefore, the highly active Entner–Doudoroff glycolytic pathway, together with pyruvate decarboxylase and two alcohol dehydrogenase isoenzymes, form the true 'backbone' of the otherwise simple *Z. mobilis* central metabolism.

The enzymatic reactions producing building blocks for biosynthesis are extremely weak in comparison to the mainstream catabolic pathway (Bringer-Meyer & Sahm, 1989), thus serving as a basis for the uncoupled metabolism. In part, that explains the tiny percentage of the substrate carbon converted into biomass, and, at the same time, the very efficient conversion of glucose into ethanol. Up to 98% of the glucose metabolized by *Z.mobilis* is converted to ethanol and carbon dioxide, while only 3–5% of substrate carbon is converted into biomass (Swings & DeLey, 1977; Rogers *et al*., 1982).

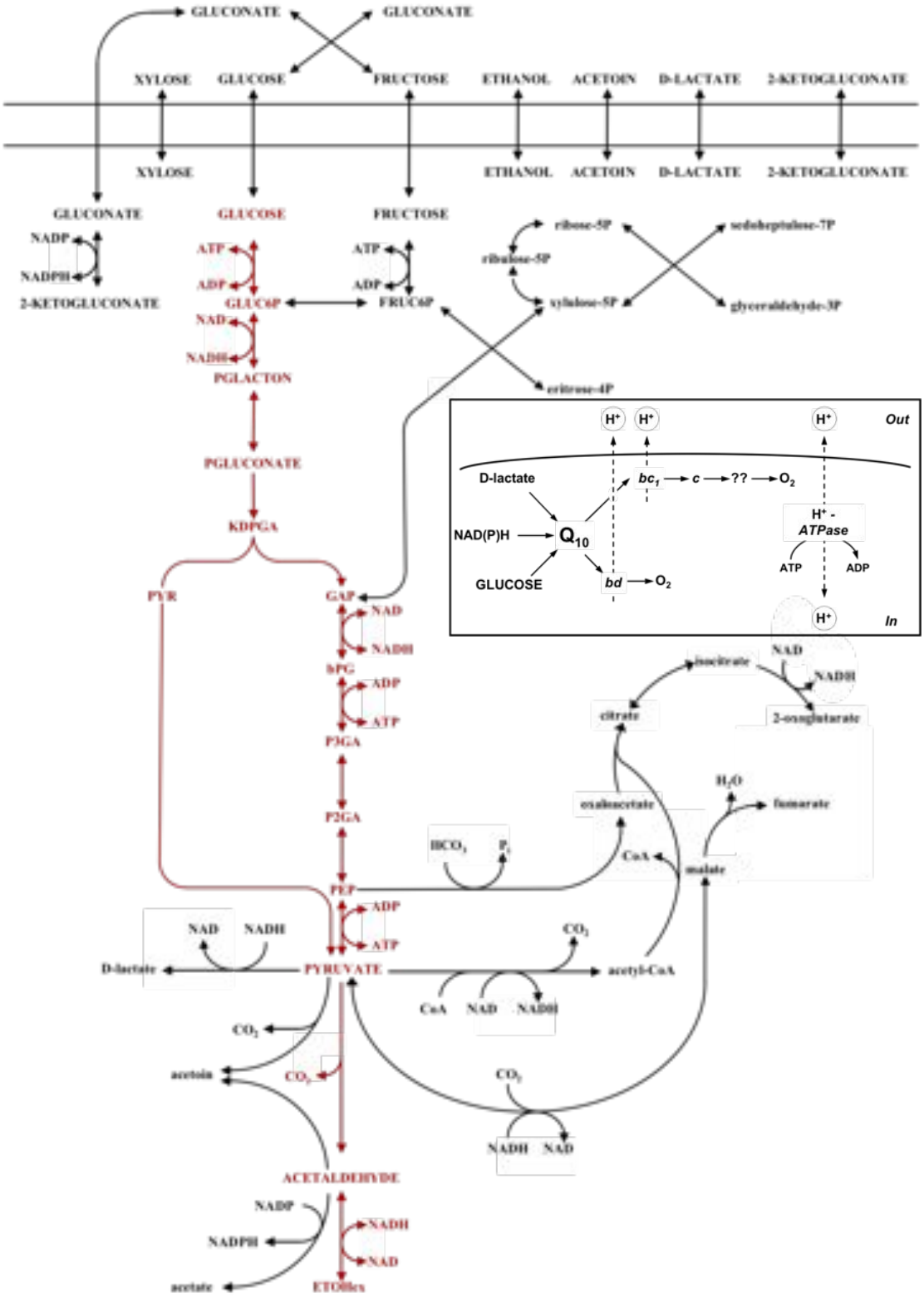

Fig. 1 The network of *Z. mobilis* central metabolism. Reactions of the Entner-Doudoroff pathway with sucsessive pyruvate decarboxylase and alcohol dehydrogenase reactions are highlighted in dark red color. Inset: putative aerobic electron transport chain of *Z. mobilis* proposed by Kalneieks, 2006.

1.3 Uncopled metabolism and Entner-Doudoroff pathway

The intrinsically rapid carbohydrate metabolism of *Z. mobilis* result from its unique physiology, particularly, from the properties and regulation of E-D pathway, that has been studied in great detail during the past decades (Barrow *et al*., 1984; Osman *et al*., 1987; De Graaf *et al*., 1999). All the enzymes of the E-D pathway have been purified and characterized kinetically, also the corresponding genes were cloned and sequenced allready in the 1980s and 1990s (Scopes 1983; 1984; 1985; Scopes *et al*., 1985; Scopes & Griffiths Smith 1984; 1986; Kinoshita *et al*., 1985; Pawluk *et al*., 1986; Viikari 1988; Sahm *et al*., 1992). In contrast to most other bacteria, *Z. mobilis* uses a facilitated diffusion system with a glucose facilitator protein (GLF) for intracellular glucose transport which does not utilise metabolic energy, and is suited for growth in sugar-rich media (DiMarco & Romano, 1985; Snoep *et al*., 1994; Weisser *et al*., 1995). Under anaerobic conditions exponentially growing *Z. mobilis* consumes glucose with specific uptake rate 4.0 – 5.6 g glucose g dry wt. $^{-1}$ h $^{-1}$ (Rogers *et al*., 1982; Viikari, 1988; Jones & Doelle, 1991; Arfman *et al*., 1992).

Z. mobilis is the only known microorganism that uses the E-D pathway under anaerobic conditions, in place of the EMP glycolytic pathway. Since EMP pathway produces two ATP per glucose while the E-D produces only one, it might seem that the EMP pathway is energetically superior. However, by introducing methods to analyze pathways in terms of thermodynamics and kinetics, it has been recently shown that the ED pathway is expected to require several-fold less enzymatic protein to achieve the same glucose conversion rate as the EMP pathway (Flamholz *et al*., 2013). According to the calculations of Flamholtz *et al*. (2013), the EMP pathway could generate an equivalent glycolytic flux in *Z mobilis* whith not less than 3.5 times of the protein investment. This seems fairly surprising and infeasible in *Z. mobilis*, knowing that enzymes involved in the fermentation (mainly in E-D pathway) comprise as much as 50% of total protein (Algar & Scopes, 1985; An *et al*., 1991). Furthermore simple calculation shows that, in comparison to yeast, catabolism of *Z. mobilis* generates ATP with a considerably higher specific rate. As an example, yeast produce 2 moles of ATP per mole of glucose in the EMP pathway, at the same time having a three to five (but not just two) times lower catabolic rate (Rogers *et al*., 1982). Therefore statements about the low energetic efficiency of the E-D pathway that pictures *Z. mobilis* as a bacterium, suffering from the lack of ATP, may be

considered as misleading, and ATP production in E-D pathway can be rather characterized as excessive.

The relatively low growth yield values, ranking between 2.3 and 10.5 g dry wt. (mol glucose) $^{-1}$ (Belaich & Senez, 1965; Lawford & Stevnsborg, 1986; Sahm & Bringer-Meyer, 1987; Kim *et al*., 2000; Lawford & Rousseau, 2000), with existing high catabolic rate in E-D pathway, do not coincide with the fact that energy production and consumption must always be well balanced. Biomass synthesis is by far not the main consumer of ATP produced in E-D pathway, since *Z. mobilis* produces little cell mass, grow with a low energetic efficiency (Belaich & Senez, 1965; Rogers *et al*., 1982) and is a typical example of uncoupled growth. Low growth yield values together with the rapid catabolism also point to the presence of ATP-dissipating reaction(s). Apparently, ATP dissipation is compulsory to permit glycolysis to proceed without a concomitant biomass synthesis. *Z. mobilis* possesses several ATP-hydrolysing enzymes that may be attributable to these needs, including periplasmic nucleotidase, acid and alkaline phosphatases, and the membrane F_0F_1-type H^+ dependent – ATPase (H^+ dependent – ATPase). The latter contributes up to the 20 % of the overall ATP turnover in the *Z. mobilis* cells under anaerobic conditions and has been considered as being partly responsible for the phenomenon of uncoupled growth (Reyes & Scopes, 1991). However, since the H^+ dependent – ATPase does not dissipate energy, but just converts it into the form of transmembrane proton-motive force (Δp), this finding does not solve the whole problem of energy dissipation.

Z. mobilis „catabolic highway“ appears to function with minimal allosteric control. E-D pathway lacks allosterically regulated pyruvate kinase and phosphofructokinase that is typical of microorganisms possesing EMP pathway (Barrow *et al*., 1984; Strohhäcker *et al*., 1993; Snoep *et al*., 1996). Allosteric inhibition by phosphoenolpyruvate has been demonstrated for the second enzyme of the ED pathway, glucose-6-phosphate dehydrogenase (Scopes, 1997) that, according to studies by Snoep et al. (1996), appears to exert a considerable control over the glycolytic flux in E-D pathway. On the other hand, when ethanol is present at high concentration (around 10% w/w), the flux control is shifted to enolase and phosphoglycerate mutase (Barrow *et al*., 1984; Strohhacker *et al*., 1993; Snoep *et al*.,

1996). Most likely these deviations in flux control may be assocoated with changes in enzymatic activities reported during bach fermentations (Osman *et al*., 1987).

1.4 Z. mobilis aerobic metabolism and respiratory chain.

Typicaly under aerobic conditions proton export in facultatively aerobic microorganisms is accomplished by respiratory chain, and therefore, H^+-dependent ATPase operates in the direction of ATP synthesis. Indeed, since *Z. mobilis* possesses both, H^+ dependent – ATPase and active, constitutive aerobic respiratory chain (Fig. 1. inset) supporting high oxygen uptake rates (Strohdeicher *et al*. 1990; Kalnenieks *et al*. 1998), one may suggest its aerobic metabolism to supply energy for growth, as it does for example in *E. coli*. However the physiology of aerobic metabolism in *Z. mobilis* is unusual for bacteria, since aerobic biomass yields do not exceed the anaerobic ones, and ATP outcome in oxidative phosphorylation is significantly lower than in *E. coli* and other microorganisms. It has not been reported yet, whether the lack of oxidative phosphorylation stems from innefficy of energy-coupling in a particular branch of respiratory chain, or lies at the level of energy-coupling membrane or H^+ dependent – ATPase. For example, high proton leakage of cytoplasmic membrane (Osman & Ingram, 1985; Osman *et al*., 1987) and accordingly, impaired maintenance of the proton-motive force, may contribute to poor energy-coupling.

Also, it was reported that respiratory metabolism is inhibitory for growth because of the accumulation of acetaldehyde and other toxic byproducts in oxic conditions (Viikari, 1986; Viikari & Berry 1988, Kalnenieks *et al*., 2000).

Finally, taking into account the active E-D pathway, the low energetic efficiency of *Z. mobilis* respiration raises the question - in which direction the H^+-dependent ATPase actually operates under aerobic conditions, when there is excess ATP available as the result of high glycolytic flux in E-D pathway.

Despite that long ago it was established that *Z. mobilis* possesses a constitutive respiratory chain (Belaich & Senez, 1965; Pankova *et al*., 1985; Strohdeicher *et al*., 1990), the organization of its components and the routes for electron transfer to oxygen have not been fully resolved. The genome sequence of *Z. mobilis* (Seo *et al*., 2005; Kouvelis *et al*., 2009; Pappas *et al*., 2011; Desiniotis *et al*., 2012) reveals genes encoding several NAD(P)H dehydrogenases, as well as electron transport dehydrogenases for D- lactate and glucose, several c-type cytochromes, the bc_1

complex and the cytochrome *bd* - the only one so far identified terminal oxidase (Kalnenieks *et al*. 1998; Sootsuwan *et al*. 2008). The known *Z. mobilis* genome sequences lack regions homologous to any known bacterial cytochrome *c* oxidase genes, also not supporting existence of *a*- or *o*-type terminal oxidases, which otherwise could be considered as terminal oxidases of the putative alternative pathway(s) (Seo *et al*., 2005). Therefore whether the electron transport to oxygen is branched, and what might be second terminal oxidase in a putative cytochrome bc_1 respiratory branch remains an open question

Energy generation is the central, yet not the sole function of bacterial electron transport chains (Poole and Cook 2000). The aerobic respiration in bacteria generates reactive species of oxygen (ROS) (Gonzalez-Flecha & Demple 1995), but may also protect the cell interior from molecular oxygen (as demonstrated for nitrogen-fixing bacteria, see Kelly *et al.*, 1990), and also from oxidative stress by diverting electrons from hydrogen peroxide-generating reactions (Korshunov & Imlay 2010). Low energetic efficiency of respiration potentially suggests respiratory-protective and ROS-protective roles of the electron transport in *Z. mobilis*, as a physiological alternative to oxidative energy generation. However such a hypothesis so far has attracted little attention.

1.5 Biotechnology and metabolic engineering of Z. mobilis

Rapid catabolism, which is quite loosely matched to the needs of cellular biosynthesis known as uncoupled growth phenomenon, is largely the mode of metabolism that makes *Z. mobilis* an outstanding ethanol producer. (Belaich & Senez, 1965; Lawford & Stevnsborg, 1986; Jones & Doelle, 1991). Almost five times faster glucose uptake rate than that obtained with yeast, in combination with tolerance to high ethanol and sugar concentrations, have kept *Z. mobilis* in the focus of biotechnological interest over several decades. Although, microorganism was originally discovered in fermenting tropical plant saps, e.g., in the traditional pulque drink of Mexico (Swings & DeLey, 1977), its potential application is not in alcoholic beverages, but rather for use in bio-ethanol production. One of the shortages of *Z. mobilis* is its limited carbon substrate range as it can only use glucose, fructose and sucrose for ethanol fermentation. As a result studies on *Z. mobilis* genetic manipulation have focussed on extending substrate range for ethanol production during the past decades. Recombinant *Z. mobilis* strains capable of fermenting

pentose sugars is regarded as an important alternative to yeast and recombinant *Escherichia coli* for bio-ethanol synthesis from agricultural and forestry waste (Dien *et al*., 2003; Lau *et al*., 2010). Other end products of *Z. mobilis* metabolism, for example, sorbitol and fructose polymer levan (Viikari, 1988; Sprenger, 1996), also represent interest for the food industry and healthcare. Recently published stoichiometric analysis of *Z. mobilis* central metabolism, reveals several metabolic engeneering strategies for obtaining other high-value products, such as glycerate, succinate and glutamate, also suggesting possibility of glycerol conversion to ethanol (Pentjuss *et al*., 2013). However, analysis of the stoichiometric matrix just uncovers these possibilities and futher in-depth studies of the regulation of *Z. mobilis* central metabolism are required to proceed with metabolic engineering.

1.6 Modeling of Z. mobilis central metabolism.

In spite of progress in the molecular biology of *Z. mobilis,* not always attempts to optimize metabolic processes by overexpression of enzymes that are thought to be important in the rate of ethanol formation, have led to counterintuitive effects, such as decrease of glycolytic flux (Arfman *et al*., 1992, Snoep *et al*., 1995). Optimizing metabolic flux towards desired end product(s) requires understanding how the nonlinear enzymatic rate equations are impacted by heterologous enzyme expression levels. Earlier studies focusing on the rate of ethanol formation and thus on glycolytic flux in *Z. mobilis* have led to contradictory suggestions. As an example studies by Osman *et al*. (1987), suggested that glycolytic flux is determined by the activities of certain enzymes of the E-D pathway (Osman *et al*. 1987) or even the concentration of ethanol in media (Osman & Ingram 1985). Later it has been convincingly demonstrated that *Z. mobilis* glycolytic flux increases during growth under uncoupled growth conditions (Lawford & Stevnsborg, 1986). Such reports clearly underline the need for quantitative metabolic control analysis prior to selection of enzymes that might exert flux control in *Z. mobilis*. It can be directly achieved by means of kinetic *in silico* modeling of *Z. mobilis* central metabolism, and E-D pathway in particular.

In spite of the diverse studies of *Z. mobilis* central metabolism during the past decades, accumulated knowledge has scarcely yet been exploited as the basis for building a comprehensive kinetic model of E-D pathway. The only recent attempt focusses on the aspects of interaction between the engineered pentose phosphate pathway and the native *Z. mobilis* E-D glycolysis for xylose fermentation, assuming

constant intracellular concentrations of the essential metabolic cofactors ADP, ATP, $NAD(P)^+$, and NAD(P)H (Altintas *et al*., 2006). Whilst such a simplification certainly reduces model complexity, it significantly limits general applicability of the model and in particular, for the study of *Z. mobilis* uncoupled metabolism. Thus, a credible kinetic model of *Z. mobilis* E-D pathway would not just shed light to the control of the metabolic processes, but may also serve to understand better the regulation of uncoupled growth phenomenon in this bacterium.

2. MATERIALS AND METHODS

2.1 Bacterial strains, Media and Cultivation

2.1.1 Bacterial strains

Bacterial strains used in the present study are listed and characterized in Table 1. Last column depicts publications in wich each strain was used.

Table. 1. Bacterial strains used in this study.

Strain	Characteristics	Source	Publications
Zm6	Parent strain	ATCC 29191	I, II, III, IV, V
Zm6-*ndh*	Zm6 strain with a chloramphenicol insert in the ORF of respirator type II NADH degydrogenase gene (*ndh*) (ZMO 1113)	Kalnenieks et al. (2008)	I, II, III
Zm6-*cydB*	Zm6 strain with chloramphenicol insert in the ORF the of subunit (*cydB*) gene (ZMO 1572) the cytochrome bd terminal oxidase	Strazdina et al. (2012)	I, II, III, IV, V
Zm6-*cytB*	Zm6 strain with chloramphenicol insert in the ORF of the cyto-chrome *b* subunit gene (ZMO 0957) of of the bc_1 complex	Strazdina et al. (2012)	I, II, III, IV, V
Zm6-*kat*	Zm6 strain with a chloramphenicol insert in the ORF of catalase gene (ZMO 0918)	Strazdina et al. (2012)	I, II, III
E.coli JM-109		ATCC 53323 "Promega"	I, II, III, IV, V

2.1.2 Media

Z. mobilis ZM6 (ATCC 29191), Zm6-*ndh,* Zm6-*cytB*, Zm6-*cydB* and Zm6-*kat* were grown in the standard culture medium containg (per 1iter): 5 g yeast extract, 50g glucose, 1g KH_2PO_4, 1 g $(NH_4)_2SO_4$, 0.5 g $MgSO_4$ * $7H_2O$. Media for *Z. mobilis* mutant strains was additionally suplemented with chloramphenicol (30 μg ml^{-1}).

E. coli JM109 was routinely grown on LB medium per liter containing 10 g tryptone, 5 g yeast extract and 10 g NaCl. In experiments were specific rate of glucose consumption was measured media was supplemented with 35g glucose.

2.1.3 Cultivation

All *Z. mobilis* cultures were grown in shaken flasks or were cultivated in Labfors fermenter (Infors).

Anaerobic *Z. mobilis* cultivation in 200 ml shaken flasks (50 ml culture volume) was caried out at 30°C, pH 6.0, while aerobic conditions were maintained on

a shaker at 150 rpm. For some cultivations, gassing with nitrogen or air was performed, as stated in Results.

Continuous cultivation was carried out in a Labfors fermenter (Infors) of 2.5 l working volume, containing 1 l of culture, and a dilution rate of 0.18 h^{-1}. Aerobic conditions were maintained by aeration with an air flow of 1.5 l min^{-1} and stirring rate 300 rpm. Anaerobic conditions was established by gassing the culture with nitrogen gas, at a flow rate of 1.4 l min^{-1}, and stirring rate 100 rpm.

E. coli JM109 was grown in 200 ml shaken flasks on a shaker at 150 rpm.

2.1.4 Preparation of cell-free extracts and membrane vesicles.

For preparation of cell-free extracts, cells were sedimented by centrifugation at 5,000 rpm for 15 min, washed, and resuspended in 100 mM potassium phosphate buffer, containing 2 mM magnesium sulfate, pH 6.9, to about 6.8–7.0 mg (dry wt) ml^{-1}. Cells were disrupted by 2.5 min long bead-vortexing in in the desintegrator at 3000 rpm with 106 μm (diameter) glass beads. Typically, cell free extracts of 4.6–4.9 mg protein ml^{-1} were obtained. Subsequent removal of unbroken cells and separation of cytoplasmic membranes by ultracentrifugation were performed as before (Kalnenieks *et al*., 1993, 1998).

2.2 Analytical methods

2.2.1 Enzymatic assays

Samples for ATP determination were quenched in ice-cold 10% trichloroacetic acid and assayed by the standard luciferin-luciferase method using LKB "Wallac 1251" luminometer (Anderson *et al*., 1985).

Acetaldehyde concentration was determined by the alcohol dehydrogenase assay, as described previously (Kalnenieks *et al.,* 2000).

NAD(P)H concentrations were determined with an LKB "Wallac 1251" luminometer, using the "Roche" bacterial luciferase assay, basically following the standard protocol.

Catalase activity in cellfree extracts was assayed spectrophotometrically, by monitoring absorbance decline at 240 nm (Gonzalez-Flecha & Demple, 1994).

Cytochrome c peroxidase activity was monitored by the decline in absorbance at the α-band of ferrocytochrome c at 550 nm on addition of cell-free extract and H_2O_2 (Ellfolk & Soininen, 1970).

Glutathione reductase activity was measured by decrease of NADPH absorbance at 340 nm on addition of oxidized glutathione (GSSG) in the presence of permeabilized cells (Bergmeyer *et al*., 1974).

2.2.2 Determination of glucose and ethanol

Glucose and Ethanol concentrations were measured with high preassure liquid chromotography - HPLC (Agilent 1100 series), using a Biorad Aminex HPX—87H column.

2.2.3. Monitoring of pO_2 and *pCO_2*

Concentration of dissolved oxygen was monitored by Clark-type oxygen electrodes. An autoclavable Ingold electrode was used in the fermenter. Radiometer electrode was used in washed cell or membrane vesicle suspensions and measurments were caried out in a thermostatted electrode cell (30 ^{o}C). Whole cell oxygen uptake was measured for cells taken from steady-state cultures, pelleted, washed, and resuspended in 100 mM phosphate buffer, pH 6.9, supplemented with 10 g glucose l^{-1}.

Carbon dioxide production by cell suspensions was monitored with "Radiometer" CO2 electrode in thermostatted electrode cell (30 ^{o}C).

2.2.4 Determination of H_2O_2 production

H_2O_2 production by cells was determined fluorimetrically by monitoring Amplex UltraRed fluorescence during its reaction with H2O2, catalyzed by horseradish peroxidase (Korshunov & Imlay, 2010). Fluorescence was measured with a FluoroMax-3 spectrofluorimeter (Jobin–Yvon), using 520-nm wavelength for excitation, and 620-nm wavelength for emission. To quantitate the generated hydrogen peroxide, fluorescence increase was calibrated by addition of 1 mM H_2O_2 in 5-ll increments.

2.2.5 Determination of protein concentration

Protein concentration in cell-free extracts and membrane samples was determined according to Markwell (Markwell *et al*., 1978).

2.2.6. Cell concentration

Cell concentration was determined spectrophotometrically as OD550, and dry cell mass of the suspensions was calculated by reference to a calibration curve.

2.2.7 Cytochrome spectroscopy

Cytochrome spectroscopy was done at the University of Sheffield, Prof. Rebert K. Poole's laborotory. Room-temperature reduced minus oxidized cytochrome absorption spectra were taken using membrane samples (1 ml) at a protein concentration of 5–6 mg ml^{-1} with small amounts of solid dithionite as reductant and potassium ferricyanide as oxidant. Spectra were recorded with a custom-built SDB4 dual-wavelength scanning spectrophotometer (University of Pennsylvania School of Medicine Biomedical Instrumentation Group and Current Designs, Philadelphia, PA), as described previously (Kalnenieks *et al*., 1998). The timecourse of cytochrome d reduction after addition of NADH was recorded by rapid, repetitive scanning in the wavelength range between 610 and 650 nm, using the dual-wavelength scanning spectrophotometer. The degree of cytochrome *d* reduction was calculated as the average value of the absorbance differences at wavelength pairs 630/614 and 630/646 nm.

2.2.8 FT-IR analysis

FT-IR analysis was performed using 5 – –15 µL of washed cell water suspension poured out by drops on a silicon plate and dried at T < 50 °C. Absorption spectra were recorded on an HTS-XT microplate reader (Bruker, Germany) over the range 4000 – 400 cm^{-1}, with a resolution of 4 cm^{-1}. Quantitative analysis of carbohydrates, nucleic acids, proteins, and lipids in biomass was carried out as described previously (Grube *et al.,* 2002) Data were processed with OPUS 6.5 software. Hierarchical cluster analysis (HCA) was used to create dendrograms from *Z. mobilis* and its knockout mutant IS absorption spectra using Ward's algorithm.

2.4 Genetic engineering of mutant strains

2.4.1 DNA extraction and purfication

Genomic DNA from 1ml of overnight *Z. mobilis* cultures was isolated using a Promega Wizard Genomic DNA purification kit, following the manufacturer's instructions or by a standart phenol/chloroform extraction. The QIAprep Spin Miniprep kit (Qiagen) was used for plasmid DNA isolation from *Z. mobilis* and *E. coli.* Purification of the amplified DNA fragments and purification of DNA from restriction and modifying reactions were done with the QIAquick PCR purification kit (Qiagen). The QIAquick gel extraction kit (Qiagen) was used for the recovery of plasmids and PCR products from agarose gels.

2.4.2 PCR

PCRs were carried out in a Thermo Hybaid gradient thermocycler or in Eppendorf Mastercycler, using Accuzyme (Bioline) or Fermentas DNA polymerase. *Z. mobilis ndh*, *cytB*, *cydB*, *kat* genes and chloramphenicol acetyltransferase (*cat*) gene were amplified by PCR, using primers according to Table 2. The engineered restriction sites for BamHI, HindIII and EcoR1 are underlined. Primers for PCR reactions were supplied by Operon and Invitrogen.

Table. 2. Primers used for amplification of mobilis *ndh, cytB, cydB, kat* genes and chloramphenicol acetyltransferase (*cat*).

Praimer	Sequence	Rest. Site	Gene	Corresponding strain
Z.m.ndh1	AGAGAATAGAGCGGATCCATGTCGAAGAAT	*Bam*HI	ZMO 1113	Zm6-*ndh*
Z.m.ndh1	ATCAGTATAATAAAGCTTTAGGGCGTAACA	*Hind*III		
Z.m.b1	GAACTTATTATGAAGCTTTCACCACCCCCT	*Hind*III	ZMO0957	Zm6-*cytB*
Z.m.b2	TTGAGCATATCAGGATCCCGTTCTTTTCTT	*Bam*HI		
Z.m.d1	ATGAAGCTTCTTGGATCCTGACCCATAGTC	*Bam*HI	ZMO1572	Zm6-*cydB*
Z.m.d2	TACCCGTCACTGCTGGTAAGCTTGCCGTGG	*Hind*III		
Z.m.cat1	AAGAGGGATCCTATGACTAGACCCAATCTT	*Bam*HI	ZMO0918	Zm6-*kat*
Z.m.cat2	GAAGCAGCAAGCTTTATAACAGGCTATCGG	*Hind*III		
cm1	TTTGCTTTCGAATTCCTGCCATTCATCCGC	*Eco*R1	*cat*	Zm6-*kat*
cm2	CACTACCGGGCGAATTCTTTGAGTTATCGAC	*Eco*R1		

2.4.3 qRT- PCR

An RNeasy Mini kit (Qiagen) was used for mRNA purification. Reverse transcription was done with the Revert Aid Premium First Strand cDNA Synthesis kit and Maxima SYBR green/ROX qPCR Master Mix (both from Fermentas) was used for the PCR. The quantitative real-time PCRs (qRT- PCR) were carried out in duplicate in a real-time thermal cycler (Model 7300, Applied Biosystems). qRT-PCR data in all cases were normalized against the respective amounts of cDNA of the 'housekeeping' gene glyceraldehyde-3-phosphate dehydrogenase (ZMO 0177). Primer pairs for 14 genes (Table 3) were designed to give PCR products of 200 (±8) bp length.

Primers for qRT-PCR reactions were supplied by Invitrogen.

Table. 3. Primer pairs and the corresponding genes used for qRT-PCR analysis.

Praimer	Sequence	Gene	Gene Product
ahpC_f ahpC_r	GGATTACGGCCAACATTCAA ATTACGCTTGGCGGAAATCT	ZMO1732	Alkyl hydroperoxide reductase
kat_f kat_r	AGGGAATTGGGATTTAGTCG AAGAGGAATACCACGATCAG	ZMO0918	Catalase
cydA_f cydA_r	TATGAATTCGGGACGAACTG CCAAGTCATGGAAATCAAGG	ZMO1571	Cytochrome bd subunit I
gapdeh_f gapdeh_r	AAGCTTGGCGTTGATATCGT GTGCAAGATGCGTTAGAAAC	ZMO0177	Glyceraldehyde-3-P dehydrogenase
gor_f gor_r	TTTTATAAAGCGCGCGATCG GATCGGGTTTTCGGTCATAA	ZMO1211	NADPH-glutathione reductase
grx_f grx_r	GTTATAAGCTGGTGCCGATT AATTCTGGCAAAGGTGCCAT	ZMO0070	Glutaredoxin 2
ldh_f ldh_r	TGAGCAGGTTATCTGTTTGC TGATACGAGCATAAAGGGTC	ZMO0256	D-lactate dehydrogenase
ndh_f ndh_r	AGAAGGCCATAAAATCAGCG TTGAGCAATCATGGTTCTGG	ZMO1113	Type II NADH dehydrogenase
per_f per_r	CAAAGAGTTAAAAGGCGTGC TCTACAAAACCAATCAGGGC	ZMO1573	Putative iron-dependent peroxidase
perC_f perC_r	TTTTCCTGTTCGTTGATCGC CCATGATTGGGCAGAAGTTA	ZMO1136	Cytochrome c peroxidase
rnfA_f rnfA_r	ATCCAACCGAGGAAGCAAAA ATTCTGATTATCGCTTCGGC	ZMO1814	NADH : ubiquinone oxidoreductase of RnfABCDGE type, RnfA subunit
sod_f sod_r	CCATCTTTCAAAACGAGCCA TTGTTCAACAATGCGGCACA	ZMO1060	Superoxide dismutase
tor_f tor_r	ATGCCTTTGATGCTGGTTTG TTATTGCTGGGGAAGATAGC	ZMO1142	Thioredoxin reductase
trx_f trx_r	TTTTGAAAAGCAGCAGGGTC TAAAATCACCGGTGCCTGTT	ZMO1097	Thioredoxin

2.4.4 Cloning Techniques

Restriction and ligation was done essentially by standard procedures (Sambrook et al., 1989). Plasmids constructed and used in the present work are listed in Table 4. *E. coli* was transformed by the $CaCl_2$ procedure as described by Sambrook *et al.* (1989). Z. mobilis was transformed by electroporation (Liang & Lee, 1998).

All DNA constructs were confirmed by DNA sequencing, done by Beckman Coulter Genomics (former Lark Technologies).

Table 4. Plasmids used in the study.

Plasmid	Characteristics	Source	Publications
pGEM-3Zf(?)	Amp^r	Promega	I, II
pBT	Cm^r	Stratagene	I, II
pGEMndh	pGEM-Zf(+) derivative, carrying a 1.3 kb fragment of PCR-ampl. genomic DNA with the ORF of the *ndh* gene (ZMO 1113) cloned between the *Hind*III and *Bam*HI sites of the multiple cloning site	Kalnenieks et al (2008)	I
pGEMndh :: cm	pGEMndh derivative, carrying 1.3 kb fragment of pBT with 0.7 kb of the chloramphenicol resistance ORF inserted in the *Age*I site of *ndh*	Kalnenieks et al (2008)	I
pGEMb	pGEM-Zf(+) derivative, carrying a 1.3-kb fragment of PCR-ampl. genomic DNA with the ORF of the cytochrome b subunit gene (ZMO 0957) of the *bc*1 complex, cloned between the *Hind*III and *Bam*HI sites of the MCS	Strazdina et al. (2012)	II
pGEMb :: cm^r	pGEMb derivative, carrying in the *Age*I site of the cloned gene a 1.3- kb *Age*I restriction fragment of pBT, with an 0.7-kb chloramphenicol resistance ORF	Strazdina et al. (2012)	II
pGEMd	pGEM-Zf(+) derivative, carrying a 1.55-kb fragment of PCR- amp genomic DNA with part of the ORF of *cydA* (ZMO 1571) and the whole of *cydB* (ZMO 1572), cloned between the *Hind*III and *Bam*HI sites of the MCS	Strazdina et al. (2012)	II
pGEMd::cm^r	pGEMd derivative, carrying in the AgeI site of *cydB* (ZMO 1572) a 1.3-kb *Age*I restriction fragment of pBT, with an 0.7-kb chloramphenicol resistance ORF	Strazdina et al. (2012)	II
pGEMcat	pGEM-Zf(+) derivative, carrying a 1.4-kb fragment of PCR- ampl. genomic DNA with the ORF of the catalase gene (ZMO 0918) cloned between the *Hind*III and *Bam*HI sites of the multiple cloning site. Lacks *EcoR*I site in the MCS in result of elimination of an 0.35-kb fragment between *Eco*24I restriction sites of pGEM-3Zf(+)	Strazdina et al. (2012)	II
pGEMcat::cm^r	pGEMcat derivative, carrying an 0.8-kb PCR-amplified fragment of pBT with 0.7 kb of the chloramphenicol resistance ORF, inserte in the *Eco*RI site of the cloned gene	Strazdina et al. (2012)	II

2.5 Metabolic modeling

2.5.1 System characteristics, simplifying assumptions and moieties

The model includes all enzymes of the Entner-Doudoroff pathway, glucose facilitator, alcohol dehydrogenases and reaction simulating ethanol export (Fig. 2).

A set of COPASI-generated differential equations was used to describe the time dependence of the metabolite concentrations (not shown). To reduce the model complexity, we have made two simplifying assumptions, derived from the stoichiometries of the E-D pathway and alcohol dehydrogenase reactions. These assumptions are attributable to adenine nucleotides and nicotinamide nucleotide pools.

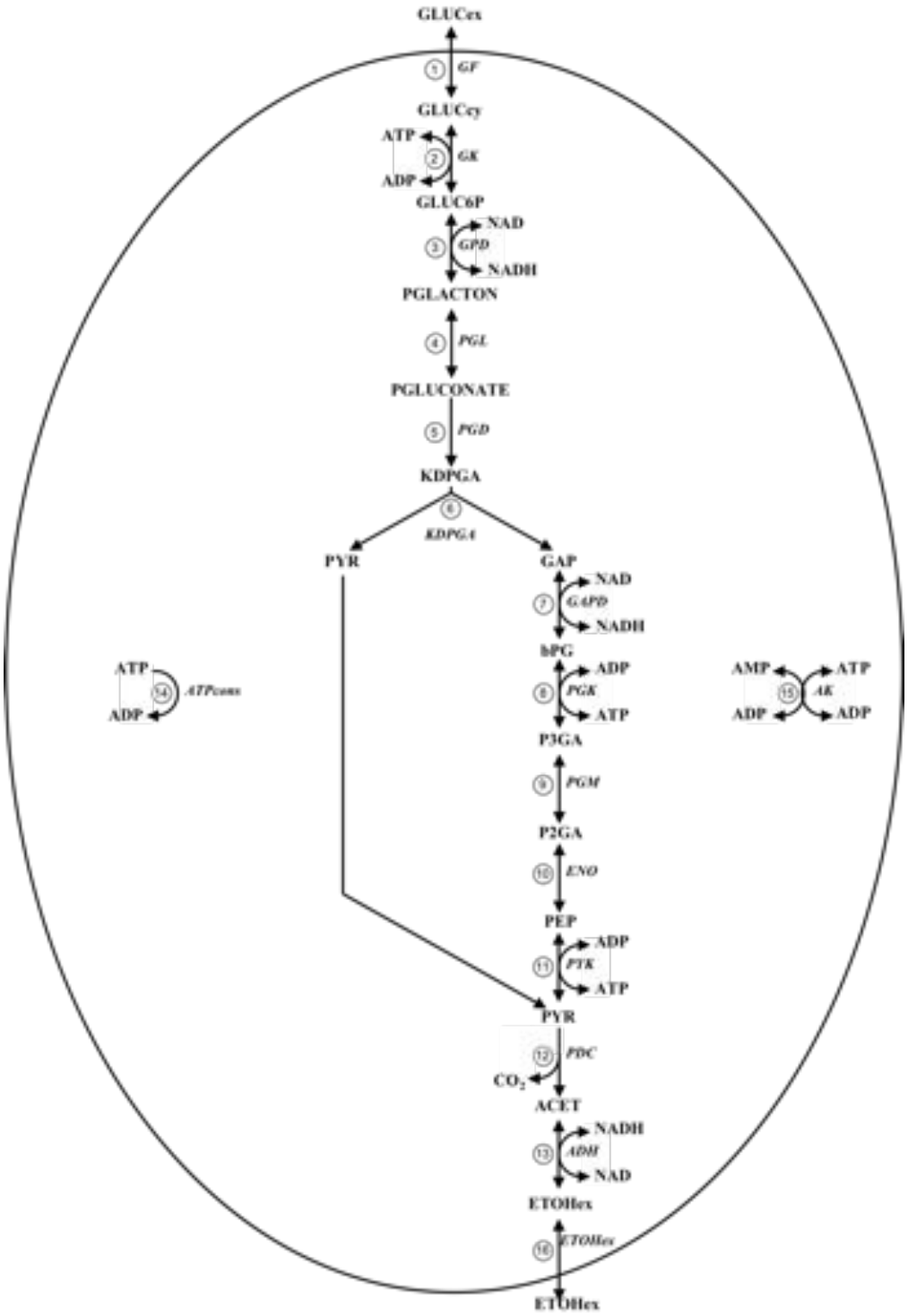

Fig. 2. Reactions included in the model of Entner Doudoroff (ED) glucose utilization pathway. The numbered enzymes in these pathways are: (1) glucose facilitator (GF); (2) glucokinase (GK); (3) glucose-6-P dehydrogenase (GPD); (4) 6-phospho- gluconolactonase (PGL); (5) 6-phosphogluconate dehydratase (PGD); (6) 2-keto-3-deoxy-6-phosphogluconate aldolase (KDPGA); (7) glyceraldehyde-3-P dehydrogenase (GAPD); (8) 3-phosphoglycerate kinase (PGK); (9) phosphoglycerate mutase (PGM); (10) enolase (ENO); (11) pyruvate kinase (PYK); (12) pyruvate decarboxylase (PDC); (13) alcohol dehydrogenase (ADH); (14) ATP consuming reactions (ATPcons); (15) adenylate kinase (AK); (16) ethanol export (ETOHex).

According to earlier reports, we have assumed following total adenylate moiety:

$$ATP + ADP + AMP = 3500\ \mu M \qquad \text{(Eq. 1)}$$

Like in other glycolytic models, we have lumped all ATP hydrolysing reactions into one general ATP-consuming reaction, whose initial properties are set according to experimental data, considering that membrane-bound F_0F_1 type ATPase is responsible for a significant part of ATP turnover in *Z. mobilis* (Reyes & Scopes, 1991). We have added adenylate kinase reaction to balance ADP and ATP pools according to experimental observations within the described moiety.

Second assumption relates to NAD(P)(H) metabolism. Like in earlier studies, we have assumed that NAD(H) made up most of the 4500 μM intracellular NAD(P)(H) pool, detected in *Z.mobilis* by NMR, without taking into account NADP(H) (De Graaf *et al.*, 1999).

$$NAD^+ + NADH = 4500\ \mu M \qquad \text{(Eq. 2)}$$

2.5.2 Enzyme kinetics

The rate equations for the individual enzymatic reactions are presented together with the transport reactions in Table 5. The numbers of these equations correspond with those depicted in Figure R. All the equations were modeled according to the available literature data on *Zymomonas mobilis* enzyme kinetics by using standard approaches, with an exeption of G-6-P dehydrogenase, where, in order to fit exprimental data, we have used the universal rate equation for systems biology derived by the Triple-J Group for Molecular Cell Physiology (Rohwer *et al.*, 2006).

2.5.3 Parameter optimisation

To combine all *in vitro* kinetic parameters and equations into one kinetic model, maximum velocities of all reactions were optimized according to steady-state intermediate concentrations obtained by ^{31}P NMR. Metabolite concentrations were determined from spectra of extracts prepared 3-4 min after addition of glucose to cell suspensions, which correspond to quasi steady-state concentrations (Strohhäcker *et al.*, 1993). Initial values of the maximum velocities (V_f) were derived from the data of

Table 5. Rate equations used in this study. Reaction numbers correspond to those depicted in Fig. 2.

Nr.	Reaction	Rate equation
1	v_{GP} =	$\frac{\frac{V_f}{K_{mGLUC_{cyt}}} * (GLUC_{cyt} - \frac{GLUC_{ex}}{K_{eq}})}{1 + \frac{GLUC_{ex}}{K_{mGLUC_{cyt}}} + \frac{GLUC_{cyt}}{K_{mGLUC_{cyt}}}}$
2	v_{HK} =	$\frac{\frac{V_f}{K_{mGLUC_{cyt}} * K_{mATP} * (1 + \frac{G6P_{cyt}}{K_{iGLUC6P}})} * (GLUC_{cyt} * ATP - \frac{GLUC6P * ADP}{K_{eq}})}{1 + \frac{GLUC_{cyt}}{K_{mGLUC_{cyt}}} + \frac{GLUC6P}{K_{mGLUC6P}} * (1 + \frac{ATP}{K_{mATP} * (1 + \frac{G6P_{cyt}}{K_{iGLUC6P}})} + \frac{ADP}{K_{mADP}})}$
3	v_{GPD} =	$\frac{V_f * \frac{GLUC6P}{K_{mGLUC6P}} + \frac{NAD}{K_{mNAD} * (1 + \frac{ATP}{K_{iATP}})} * (1 - \frac{PGLACTON * NADH}{GLUC6P * NAD * K_{eq}}) *}{(\frac{1 + (\frac{PEP}{K_{aPEP}})^h}{1 + \sigma^{2h} (\frac{PEP}{K_{aPEP}})^h} + \frac{1 + \sigma^{2h} (\frac{PEP}{K_{aPEP}})^h}{1 + \sigma^{4h} (\frac{PEP}{K_{aPEP}})^h}) * ((\frac{GLUC6P}{K_{mGLUC6P}} + \frac{PGLACTON}{K_{mPGLACTON}})^h +$ ...
		... $\frac{* (\frac{GLUC6P}{K_{mGLUC6P}} + \frac{PGLACTON}{K_{mPGLACTON}})^{h-1} * (\frac{NAD}{K_{mNAD} * (1 + \frac{ATP}{K_{iATP}})} + \frac{NADH}{K_{mNADH}})^{h-1}}{+ (\frac{NAD}{K_{mNAD} * (1 + \frac{ATP}{K_{mATP}})} + \frac{NADH}{K_{mNADH}})^h) * (\frac{GLUC6P}{K_{mGLUC6P}} + \frac{PGLACTON}{K_{mPGLACTON}})^h * (\frac{NAD}{K_{mNAD} * (1 + \frac{ATP}{K_{mATP}})} + \frac{NADH}{K_{mNADH}})^h}$
4	v_{PGL} =	$\frac{\frac{V_f}{K_{mPGLACTON} * (1 + \frac{G6P_{cyt}}{K_{iGLUC6P}})} * (PGLACTON - \frac{PGLUCONATE}{K_{eq}})}{1 + \frac{PGLACTON}{K_{mPGLACTON} * (1 + \frac{G6P_{cyt}}{K_{iGLUC6P}})} + \frac{PGLUCONATE}{K_{mPGLUCONATE}}}$
5	v_{PGD} =	$\frac{V_f * \frac{PGLUCONATE}{K_{mPGLUCONATE} * (1 + \frac{PEP}{K_{iPEP}})}}{1 + \frac{PGLUCONATE}{K_{mPGLUCONATE} * (1 + \frac{PEP}{K_{iPEP}})}}$
6	v_{GAPDH} =	$\frac{\frac{V_f * KDPG}{K_{mKDPG}} - \frac{V_f * GAP * PYR}{K_{eq} * K_{mKDPG}}}{1 + \frac{KDPG}{K_{mKDPG}} + \frac{PYR}{K_{mPYR}} + \frac{GAP}{K_{mGAP}} + \frac{KDPG * GAP}{K_{mKDPG} * K_{iGAP}} + \frac{PYR * GAP}{K_{mPYR} * K_{mGAP}}}$
7	v_{GPD} =	$\frac{\frac{V_f}{K_{mGAP} * K_{mNAD}} * (GAP * NAD - \frac{BPG * NADH}{K_{eq}})}{(1 + \frac{GAP}{K_{mGAP}} + \frac{BPG}{K_{mBPG}}) * (1 + \frac{NAD}{K_{mNAD}} + \frac{NADH}{K_{mNADH}})}$
8	v_{PGK} =	$\frac{\frac{V_f}{K_{mBPG} * K_{mADP}} * (BPG * ADP - \frac{P3G * ATP}{K_{eq}})}{(1 + \frac{BPG}{K_{mBPG}} + \frac{P3G}{K_{mP3G}}) * (1 + \frac{ADP}{K_{mADP}} + \frac{ATP}{K_{mATP}})}$
9	v_{PGM} =	$\frac{\frac{V_f}{K_{mP3G}} * (P3G - \frac{P2G}{K_{eq}})}{1 + \frac{P3G}{K_{mP3G}} + \frac{P2G}{K_{mP2G}}}$
10	v_{ENO} =	$\frac{\frac{V_f}{K_{mP2G}} * (P2G - \frac{PEP}{K_{eq}})}{1 + \frac{P2G}{K_{mP2G}} + \frac{PEP}{K_{mPEP}}}$
11	v_{PYK} =	$\frac{\frac{V_f}{K_{mPEP} * K_{mADP}} * (PEP * ADP - \frac{PYR * ATP}{K_{eq}})}{(1 + \frac{PEP}{K_{mPEP}} + \frac{PYR}{K_{mPYR}}) * (1 + \frac{ADP}{K_{mADP}} + \frac{ATP}{K_{mATP}})}$
12	v_{PDC} =	$\frac{V_f * \frac{PYR}{K_{mPYR}}}{1 + \frac{PYR}{K_{mPYR}}}$
13	v_{ADH} =	$\frac{\frac{V_f * NADH * ACET}{K_{eNADH} * K_{mACET}} - \frac{V_f * K_{eq} * NAD * ETOH}{K_{eq} * K_{mNADH} * K_{mACET} * K_{eNAD}}}{1 + \frac{NADH}{K_{eNADH}} + \frac{K_{mNADH} * ACET}{K_{eNADH} * K_{mACET}} + \frac{NADH * ACET}{K_{eNADH} * K_{mACET}} + \frac{NAD}{K_{eNAD}} + \frac{K_{mNAD} * ETOH}{K_{mETOH} * K_{eNAD}} + \frac{ETOH * NAD}{K_{mETOH} * K_{eNAD}}}$
14	v_{ATPase} =	$\frac{V_f * ATP}{K_{mATP} + ATP}$
15	v_{AK} =	$\frac{\frac{V_f}{K_{mADP}} * (ADP^2 - \frac{ATP * AMP}{K_{eq}})}{(1 + \frac{ADP}{K_{mADP}} + \frac{ATP}{K_{mATP}}) * (1 + \frac{ADP}{K_{mADP}} + \frac{AMP}{K_{mAMP}})}$
16	v_{EXPORT} =	$K * (ETOH_{cyt} - ETOH_{ex})$

18th hour of batch fermentation, ensuring that the intermediate concentrations and V_f values used correspond roughly to the same physiological condition of the cells, where according to ^{31}P NMR studies, specific glucose uptake rate slightly exceeds 5 g/g/h (grams glucose on gram dry weight per hour) (Osman *et al*., 1987, De Graaf *et al*., 1999). We selected 5 g/g/h as the target value, representing glycolytic flux for parameter optimization. For calculations we assumed that 1 mg dry wt of biomasss corresponds to 2.2 microliters of intracellular volume in average (Strohhacker *et al*., 1993). According to previous reports, most of the enzymes from the ED pathway change their activity up to 5 times during bach fermentation, therefore the upper and lower boundaries of V_f values that we have set for each reaction during parameter optimization was within the factor of 5 above and below the initial value (Osman et *al*., 1987). Km(i) values, that have been assumed or obtained from other databases attributable to other microorganisms, were optimized within the factor of 3 above and below the initial value. Parameter optimization was carried out using COPASI software V 4.8 with various optimization algorithms (Hoops *et al*., 2006).

2.5.4 Quantifying the flux control

The control of an particular enzyme on a glycolytic flux under steady-state conditions was defined by flux control coefficient C_i^J expressed in percents,

$$C_i^J = \frac{\delta J}{\delta v_i}.\frac{v_i}{dJ}.100\% = \frac{\delta lnJ}{\delta lnv_i}.100\% \qquad \text{(Eq. 3)}$$

in which v_i is the rate of enzyme i, J is a steady-state pathway flux. The flux control coefficients of an enzymes and transporters was calculated by COPASI, and obtained results always obeyed the summation theorem,

$$\sum C_i^J = 100\% \qquad \text{(Eq. 4)}$$

in which the summation is over all enzymes i in the pathway.

The effect of changing the activity (amount) of a single enzyme on the pathway flux, was determined according to Small & Kascer (1993),

$$f = \frac{1}{1 - \frac{r-1}{r*100} C_i^J} \qquad \text{(Eq. 5)}$$

in which f is a flux increase value and r is the increase of the enzyme activity.

2.5.5 Quantifying ATP homoeostasis

The extent to which metabolite concentrations can be maintained relatively constant as fluxes change is a measure of metabolic homoeostasis (Hofmeyr *et al,* 1993; Cornish-Bowden & Hofmeyr, 1994; Thomas & Fell, 1996, 1998). This can be quantified by the ratio of the metabolite's concentration control coefficient to the flux control coefficient of the same enzyme, which has been defined as the co-response coefficient (Hofmeyr *et al,* 1993; Cornish-Bowden & Hofmeyr, 1994). Thus for metabolite S_j, flux J and enzyme i:

$$\Omega_i^{S_j:J} = \frac{C_i^{S_j}}{C_i^J} = \frac{\partial \ln S_j}{\partial \ln J} \qquad \text{(Eqn. 6)}$$

The final term in the above equation results from the terms $\partial \ln v_i$ and the scaling factor 100 cancelling from the equation. This is useful since it is not necessary to know the change in enzyme activity used to perturb the systém in order to calculate the co-response coefficient from simultaneous measurements of metabolite concentration and flux, provided that the perturbation is produced by modulation of a single enzyme, *i*. This contrasts with experimental determinations of flux and concentration control coefficients, which do require a measure of the enzyme activity change involved. Hence the co-response coefficient may be
obtained from the slope of a log-log graph of concentration against flux. Alternatively, for a small enough perturbation, the coresponse coefficient may approximated from the difference between adjacent points as:

$$\Omega_i^{S_j:J} \approx \frac{\Delta S_j}{\Delta J} \qquad \text{(Eqn. 7)}$$

In this paper, we determine the ATP:$J_{glycolysis}$ co-response coefficient with respect to ATPase, i.e. $\Omega_{ATPase}^{ATP:J_{glycolysis}}$ in this way.

3. RESULTS

3.1 NADH dehydrogenase deficiency results in low respiration rate and improved aerobic growth of Zymomonas mobilis

Microbiology (2008), 154, 989–994 DOI 10.1099/mic.0.2007/012682-0

NADH dehydrogenase deficiency results in low respiration rate and improved aerobic growth of *Zymomonas mobilis*

Uldis Kalnenieks,[1] Nina Galinina,[1] Inese Strazdina,[1] Zane Kravale,[1] James L. Pickford,[2] Reinis Rutkis[1] and Robert K. Poole[2]

[1]Institute of Microbiology and Biotechnology, University of Latvia, Kronvalda Boulv. 4, LV-1586, Riga, Latvia

[2]Department of Molecular Biology and Biotechnology, The University of Sheffield, Firth Court, Western Bank, Sheffield S10 2TN, UK

Correspondence
Uldis Kalnenieks
kalnen@lanet.lv

Received 24 August 2007
Revised 13 November 2007
Accepted 27 November 2007

The respiratory chain of the ethanol-producing bacterium *Zymomonas mobilis* is able to oxidize both species of nicotinamide cofactors, NADH and NADPH. A mutant strain with a chloramphenicol-resistance determinant inserted in *ndh* (encoding an NADH:CoQ oxidoreductase of type II) lacked the membrane NADH and NADPH oxidase activities, while its respiratory D-lactate oxidase activity was increased. Cells of the mutant strain showed a very low respiration rate with glucose and no respiration with ethanol. The aerobic growth rate of the mutant was elevated; exponential growth persisted longer, resulting in higher biomass densities. For the parent strain a similar effect of aerobic growth stimulation was achieved previously in the presence of submillimolar cyanide concentrations. It is concluded (i) that the respiratory chain of *Z. mobilis* contains only one functional NAD(P)H dehydrogenase, product of the *ndh* gene, and (ii) that inhibition of respiration, whether resulting from a mutation or from inhibitor action, stimulates *Z. mobilis* aerobic growth due to redirection of the NADH flux from respiration to ethanol synthesis, thus minimizing accumulation of toxic intermediates by contributing to the reduction of acetaldehyde to ethanol.

INTRODUCTION

Zymomonas mobilis is a Gram-negative facultatively anaerobic bacterium with an efficient and very rapidly operating homoethanol fermentation pathway (Rogers *et al.*, 1982). Recombinant *Z. mobilis* capable of simultaneous fermentation of pentose and hexose sugars is regarded as having great promise for fuel ethanol production from wood hydrolysates (Dien *et al.*, 2003). Not surprisingly, the fermentative catabolism of this bacterium has been studied in great detail due to its potential biotechnological significance (Viikari & Berry, 1988; Conway, 1992; Sprenger, 1996). However, major uncertainties still persist in our understanding of the structure and function of its electron-transport chain (Kalnenieks, 2006). Inhibitor analysis points to a branched structure of the electron-transport pathway, with several alternative dehydrogenases and terminal oxidases (Strohdeicher *et al.*, 1990; Kalnenieks *et al.*, 1996, 1998). Accordingly, the genome sequence of *Z. mobilis* (Seo *et al.*, 2005) reveals genes encoding several NAD(P)H dehydrogenases, as well as electron-transport dehydrogenases for D-lactate and glucose, several c-type cytochromes, the *bd* terminal oxidase and the bc_1 complex (CoQ:cytochrome *c* oxidoreductase). Most probably, some of the genes that encode key components of the respiratory chain still await identification, in particular those of the oxidase(s) terminating the putative bc_1 electron-transport branch. Serious ambiguities can be noted when the genomic information is compared to the existing biochemical data on the respiratory dehydrogenases for NADH and NAD(P)H (Strohdeicher *et al.*, 1990; Kalnenieks *et al.*, 1996, 1998; Seo *et al.*, 2005). Thus, although the site I energy-coupling (Kalnenieks *et al.*, 1995) and kinetic parameters for NADH oxidation in membranes (Kalnenieks *et al.*, 1996) suggest presence of the NADH dehydrogenase complex I, nevertheless the six genes of the *Z. mobilis* genome encoding the putative NADH:ubiquinone oxidoreductase complex do not bear homology to those of the *nuo* operon of *Escherichia coli*. They appear to be closely homologous to the genes of the *rnf* operon, encoding a recently discovered membrane electron-transport complex, which is involved in electron transport to nitrogenase in the photosynthetic bacterium *Rhodobacter capsulatus* (Schmehl *et al.*, 1993). Genes for the type II NADH dehydrogenase (*ndh*), and for several other NAD(P)H dehydrogenases, have also been annotated in the genome, but the corresponding activities in the respiratory chain have so far not been identified.

Electron transport in *Z. mobilis* provokes special interest because of its unusual physiological manifestations. Although the cytoplasmic membrane of *Z. mobilis* carries a functional H^+-ATP synthase complex (Reyes & Scopes, 1991), this bacterium does not use its respiratory chain to supply energy for aerobic growth in the same way as the majority of aerobic and facultatively anaerobic micro-organisms do. Indeed, its respiratory metabolism seems to be inhibitory for this bacterium, largely because of the accumulation of acetaldehyde and other toxic byproducts (Viikari, 1986; Viikari & Berry, 1988). A pronounced stimulation of aerobic growth takes place when respiration is partially inhibited by addition of cyanide at submillimolar concentrations (Kalnenieks *et al.*, 2000). Oxygen uptake in aerobic cultures of *Z. mobilis* proceeds at a relatively high rate, while the biomass yields under oxic conditions are low, typically well below 10 g dry weight per mole of glucose (Belaich & Senez, 1965; Bringer *et al.*, 1984; Pankova *et al.*, 1985). It is not clear whether the respiratory chain per se plays any role in the energetics of growth or stationary-phase survival, and whether there might be some alternative physiological functions of electron transport (Kalnenieks, 2006). Obviously, without a clear picture of the electron-transport pathways, it will not be possible to explain the function of the respiratory chain in *Z. mobilis*.

Respiratory knockout mutants have contributed greatly to research on bacterial electron transport during the last two decades (Calhoun *et al.*, 1993; Poole & Cook, 2000), helping to reveal the structure and energy-coupling efficiency of particular electron-transport branches. To our knowledge, no respiratory mutants have so far been reported for *Z. mobilis*. This largely explains the gaps in our understanding of the electron transport in this bacterium. Here we report the construction and study of a *Z. mobilis* mutant that is deficient in the NADH : CoQ oxidoreductase of type II (Ndh). The mutant shows profound alterations of the respiratory phenotype, namely a dramatic decrease of the respiration rate and yet an improvement of the aerobic growth capacity.

METHODS

Bacterial strains, plasmids and transformation. *E. coli* JM109 and plasmid pGEM-3Zf(+) were purchased from Promega. Strain JM109 was used as the host for cloning of the recombinant plasmids. *Z. mobilis* ATCC 29191 (Zm6) was maintained and cultivated as described previously (Kalnenieks *et al.*, 1993, 2003). Plasmids constructed and used in the present work are listed in Table 1. *E. coli* was transformed by the $CaCl_2$ procedure as described by Sambrook *et al.* (1989). *Z. mobilis* was transformed by electroporation (Liang & Lee, 1998).

PCR and DNA manipulations. Genomic DNA from *Z. mobilis* was isolated using a Promega Wizard Genomic DNA purification kit, following the manufacturer's instructions. The QIAprep Spin Miniprep kit (Qiagen) was used for plasmid isolation. The *Z. mobilis* *ndh* gene (*Z. mobilis* ZM4 genome sequence; GenBank accession AE008692) was amplified by PCR, using primers Z.m.ndh1 (AGAGAATAGAGGGGATCCATGTCGAAGAAT) and Z.m.ndh2 (ATCAGTATAATTAAGCTTTAGGGCGTAACA) supplied by Sigma Genosys. The engineered restriction sites for *Bam*HI and *Hin*dIII, respectively, are underlined. PCRs were carried out in a ThermoHybaid gradient thermocycler, using Accuzyme DNA polymerase (Bioline). Purification of the amplified DNA fragment was done with the QIAquick PCR purification kit (Qiagen). The QIAquick gel extraction kit (Qiagen) was used for the recovery of plasmids and PCR products from agarose gels. T4 DNA ligase (Fermentas) was used in ligation assays. Restriction, ligation and cloning was done essentially by standard procedures (Sambrook *et al.*, 1989). All DNA constructs were confirmed by DNA sequencing, done by Lark Technologies.

Cultivation and preparation of membranes. Batch cultivations were carried out at 30 °C, either in 300 ml shaken flasks, 120 ml culture volume, on a shaker at 120 r.p.m., or in a Labfors fermenter (Infors) of 1 l working volume with air flow 2.5 l min^{-1} and stirring rate 300 r.p.m. For some cultivations, gassing with nitrogen or air was performed, as stated in Results. The growth medium contained glucose (50 g l^{-1}), yeast extract (5 g l^{-1}), potassium dihydrogen phosphate (1 g l^{-1}), ammonium sulfate (1 g l^{-1}) and magnesium sulfate (0.5 g l^{-1}), pH 5.5. To compare various modes of aeration, the oxygen volumetric mass transfer coefficient (K_La, s^{-1}) was determined by the gassing-out method, as described by Demirtas *et al.* (2003). For preparation of cytoplasmic membrane vesicles, cells were sedimented by centrifugation at 5000 r.p.m. for 15 min, resuspended in 100 mM potassium phosphate buffer, containing 2 mM magnesium sulfate, pH 6.9, and disrupted by disintegration with abrasive quartz beads, 125–150 μm diameter, in a homogenizer at 1000 r.p.m. for 3.5 min. Separation of cytoplasmic membranes was performed as described previously (Kalnenieks *et al.*, 1993).

Analytical methods. Concentration of dissolved oxygen was monitored by Clark-type oxygen electrodes. An autoclavable Ingold electrode was used in the fermenter, and a Radiometer electrode with a thermostatted electrode cell for oxygen uptake measurements in washed cell or membrane vesicle suspensions. Ethanol concentration

Table 1. Plasmids used in the study

Plasmid	Characteristics	Source
pGEM-3Zf(+)	Amp^r	Promega
pBT	Cm^r	Stratagene
pGEMndh	pGEM-3Zf(+) derivative, carrying a 1.3 kb fragment of PCR-amplified genomic DNA with the ORF of the *ndh* gene cloned between the *Hin*dIII and *Bam*HI sites of the multiple cloning site	Present work
pGEMndh : : cm^r	pGEMndh derivative, carrying a 1.3 kb fragment of pBT with 0.7 kb of the chloramphenicol resistance ORF inserted in the *Age*I site of *ndh*	Present work

was determined by gas chromatography (Varian). Acetaldehyde was assayed via the alcohol dehydrogenase reaction, and glucose was assayed by the glucose oxidase method, as described previously (Kalnenieks *et al.*, 2000). Protein concentration in membrane samples was determined according to Markwell *et al.* (1978). Cell concentration was determined as OD_{550}, and dry cell mass of the suspensions was calculated by reference to a calibration curve. All results are means of at least three replicates.

RESULTS AND DISCUSSION

Construction of the *ndh*-deficient strain

Amplification and cloning of *ndh*, using pGEM-3Zf(+) plasmid vector, and the strategy for construction of the *ndh*-deficient *Z. mobilis* strain was essentially the same as used previously for construction of a strain deficient in alcohol dehydrogenase (ADH II) activity (Kalnenieks *et al.*, 2006). The amplified 1.33 kb DNA fragment, starting 18 bp upstream and ending 162 bp downstream of the ORF of *Z. mobilis ndh*, was double-digested with *Bam*HI and *Hin*dIII, and was directionally cloned between the *Bam*HI and *Hin*dIII restriction sites of the multiple cloning site of plasmid pGEM-3Zf(+), yielding plasmid pGEMndh (Table 1). Plasmid pBT was digested with *Age*I (*Bsh*TI) to obtain three fragments, of approximately 1.6, 1.3 and 0.3 kb. The 1.3 kb *Age*I digestion fragment carried the chloramphenicol-resistance determinant (659 bp ORF of the chloramphenicol acetyltransferase gene). *Age*I digestion was chosen because plasmid pGEMndh contained only one *Age*I restriction site that was localized in the *ndh* insert. After digestion of pGEMndh with *Age*I, the 1.3 kb fragment of pBT was cloned in the middle of *ndh* to yield plasmid pGEMndh::cm^r. Plasmid pGEMndh::cm^r was used to transform *Z. mobilis* by electroporation, and selection for homologous recombinants was carried out on plates containing chloramphenicol (50 μg ml^{-1}). Several colonies were screened for the *ndh*::*cm*^{r} genotype by PCR on the genomic DNA template with primers Z.m.ndh1 and Z.m.ndh2.

Effect of *ndh* disruption on the respiratory oxidase activities

Data on the respiratory oxidase activities in membrane preparations obtained from cultures of strains Zm6 and the mutant *ndh*::*cm*^{r} grown under various conditions of aeration are presented in Fig. 1. In agreement with previous data (Bringer *et al.*, 1984; Kim *et al.*, 1995), NADH oxidase was the major respiratory activity in Zm6 membranes. In cultures grown either without aeration (in shaken flasks under nitrogen gas) (Fig. 1a), or under moderate aeration (K_La 0.27 s^{-1}) on the shaker at 120 r.p.m. (Fig. 1b), its activity was close to 0.3 U (mg membrane protein)$^{-1}$. NADPH oxidase activity constituted approximately 25–50 % of this value. Both oxidase activities were approximately doubled when Zm6 was grown with hyperventilation (Fig. 1c) in shaken flasks at 120 r.p.m., additionally gassed with air (1 l min^{-1}, K_La 1.18 s^{-1}). Minor D-lactate oxidase (Kalnenieks *et al.*, 1998) and glucose oxidase activities (Strohdeicher *et al.*, 1990) were also detectable; both of them were likewise induced by aeration (Fig. 1b, c).

Remarkably, disruption of *ndh* by insertion of the chloramphenicol-resistance determinant resulted in a total loss of NADH and NADPH oxidase activities in the mutant cell membranes under all tested culture aeration regimes. However, membranes from mutant cells grown under aerated conditions overexpressed the membrane D-lactate oxidase (Fig. 1b, c). D-Lactate oxidase activity in aerobically grown *ndh*::*cm*^{r} appeared to be the dominant oxidase activity, and was higher than in Zm6 under all aeration conditions. It is tempting to think that the elevated D-lactate oxidase in aerated cells has some physiological importance for the aerobic metabolism of *Z. mobilis ndh*::*cm*^{r}. In the mutant strain D-lactate dehydrogenase might serve to compensate for the lack of respiratory NAD(P)H oxidation. A somewhat similar effect was reported for a *Corynebacterium glutamicum* type II NADH dehydrogenase-deficient strain, in which elevated levels of membrane L-lactate oxidase were found (Nantapong *et al.*, 2004). In principle, D-lactate in *Z.*

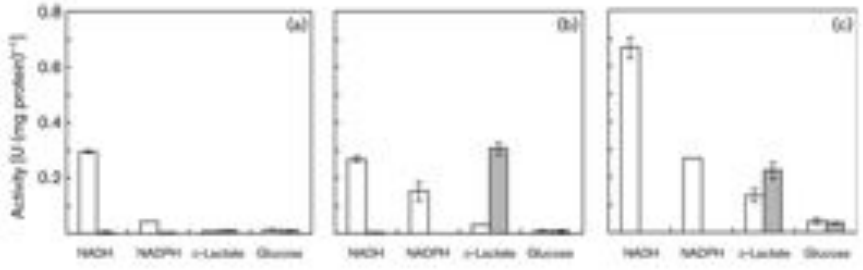

Fig. 1. Activity of the respiratory oxidases in membrane preparations, obtained from cells of Zm6 (white bars) and *ndh*::*cm*^{r} (shaded bars) cultivated anaerobically (a), aerobically on a shaker (b), and aerobically with additional gassing with air (c) (see text for details). Data are means ± SEM.

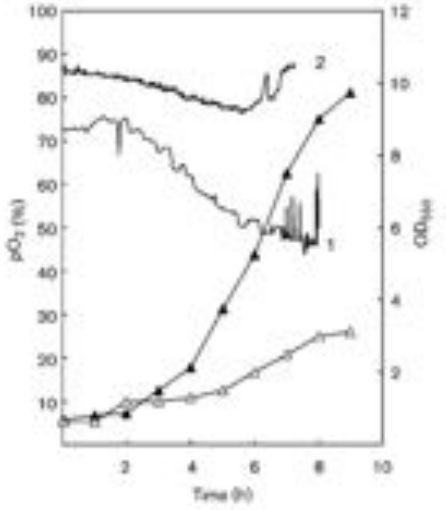

Fig. 2. Aerobic batch cultivation of Zm6 (△) and *ndh*::*cm*^{r} (▲) in a fermenter with continuous monitoring of pO_2 (1, Zm6; 2, *ndh*::*cm*^{r}).

mobilis might be produced from pyruvate and NADH by the cytoplasmic lactate dehydrogenase, and then reoxidized by the respiratory D-lactate dehydrogenase, forming a kind of 'lactate shunt' for NADH reoxidation. However, the rate of oxygen uptake in the mutant strain is very low (see Fig. 2 and Table 2), indicating low activity of the putative lactate shunt. Furthermore, NADH reoxidation in the respiratory chain of glycolysing *Z. mobilis* has an obvious alternative – the highly active alcohol dehydrogenase reaction. The increased D-lactate oxidase activity in the mutant strain under aerobic conditions, therefore, might have some other, so far unknown function.

Our results indicate that the *ndh* gene product is the sole functional respiratory NAD(P)H dehydrogenase of *Z. mobilis*. On the other hand, the existing kinetic data (Kalnenieks *et al.*, 1996) as well as genome information (Seo *et al.*, 2005) seem to support the presence of more than one NAD(P)H dehydrogenase in its electron-transport chain. Kinetic analysis of NADH oxidation in membrane preparations revealed two components with different K_m values for NADH (Kalnenieks *et al.*, 1996). The apparent K_m for the activity that prevails in anaerobically grown cells was found to be close to 7 μM, as for the energy-coupling NADH dehydrogenase complex I in *E. coli*, encoded by the *nuo* operon (Matsushita *et al.*, 1987; Leif *et al.*, 1995). The apparent K_m of the other component, prevailing in aerobically grown cells, was around 60 μM (Kim *et al.*, 1995; Kalnenieks *et al.*, 1996), which is a typical value for the energy non-generating type II NADH dehydrogenase, encoded by *ndh* (Yagi, 1991). At present the mechanistic basis for the observed '*nuo*-like' (or the low-K_m) component seems obscure, because: (i) the *Z. mobilis* genome does not contain any sequences homologous to *nuo*, and (ii) as demonstrated in the present work, inactivation of *ndh* eliminates the entire respiratory NAD(P)H dehydrogenase activity in both aerobic and anaerobic culture.

Bacterial respiratory dehydrogenases are predominantly NADH-specific (Yagi, 1991), yet the ability to oxidize NADPH in the respiratory chain has been reported for several bacteria. For *C. glutamicum* (Matsushita *et al.*, 2001) and for *Azotobacter vinelandii* (Bertsova *et al.*, 2001) it was demonstrated that NADPH oxidation in the respiratory chain is accomplished by the type II NADH dehydrogenase (*ndh*), in full accordance with our present observations on *Z. mobilis*. Apart from *ndh*, the *Z. mobilis* genome (Seo *et al.*, 2005) contains a gene homologous to *mdaB* of *E. coli*, encoding an NADPH-specific quinone reductase. Homologues of the MdaB protein are known to act as antioxidant factors in many pathogenic bacteria, helping to cope with the oxidative stress accompanying inflammation processes (Wang & Maier, 2004). The putative function of the MdaB homologue in *Z. mobilis* has not been investigated so far.

Aerobic growth of the mutant strain

Some of the aerobic batch cultivation experiments were carried out in a lab-scale fermenter with continuous monitoring of pO_2. Remarkably, Ndh deficiency in *Z. mobilis* resulted in an increase of biomass yield, i.e. $Y_{X/S}$,

Table 2. Aerobic yields and specific rates of oxygen consumption of *Z. mobilis* strains Zm6 and *ndh*::*cm*^{r}

Yields (aerobic biomass yield, $Y_{X/S}$; g dry weight per mole glucose consumed; and ethanol yield, $Y_{P/S}$; g ethanol synthesized per g glucose consumed) were calculated for early stationary-phase cultures (9 h after inoculation) grown in the fermenter. The specific rates of oxygen consumption (Q_{O_2}; μmol oxygen per minute per g dry weight) refer to washed cell suspensions in 100 mM phosphate buffer (pH 6.9) with added glucose or ethanol (10 g l^{-1}). Data are means ± SEM.

Strain	$Y_{X/S}$ [g dry wt (mol glucose)$^{-1}$]	$Y_{P/S}$ [g ethanol (g glucose)$^{-1}$]	Q_{O_2} (glucose) [U (g dry wt)$^{-1}$]	Q_{O_2} (ethanol) [U (g dry wt)$^{-1}$]
Zm6	4.1 (± 1.5)	0.22 (± 0.04)	0.103 (± 0.020)	0.215 (± 0.002)
ndh::*cm*^{r}	8.6 (± 1.6)	0.39 (± 0.09)	0.013 (± 0.005)	0.000

cell yield normalized with respect to glucose consumption (Table 2), and stimulation of aerobic growth. The mutant strain also grew substantially faster than Zm6, at the end of the exponential phase typically reaching a threefold higher biomass concentration (Fig. 2). However, the downshift of pO_2 that occurred during the growth of Zm6 was much larger than that seen in the mutant, indicating a higher respiration rate of the parent culture. Accordingly, the mutant culture showed an increased aerobic ethanol yield ($Y_{P/S}$, Table 2), because more reducing equivalents were diverted towards ethanol synthesis. As expected, the oxygen uptake rate of a washed *ndh*::*cm*^{r} cell suspension was close to zero (Table 2). No oxygen consumption could be detected with ethanol, implying that in *Z. mobilis*, ethanol oxidation proceeds solely via NAD^+-dependent alcohol dehydrogenases. The remaining respiratory activity of cell suspensions with glucose most probably is related to some type of lactate shunt, as discussed above.

In general, the aerobic growth of the *ndh*-deficient mutant strain resembles that of Zm6 in the presence of cyanide (Kalnenieks *et al.*, 2000, 2003). However, the results obtained with the *ndh*-deficient mutant are less ambiguous, and help to draw a more precise picture of the aerobic growth stimulation of *Z. mobilis*. Cyanide typically caused the growth stimulation of Zm6 after a prolonged lag phase, when, following an initial period of complete inhibition, the re-emerging respiration reached 30–50 % of the respiration rate in the control culture (Kalnenieks *et al.*, 2000). Hence, an important question was left: (i) does the stimulating effect result simply from inhibition of the bulk oxygen consumption, or (ii) is some specific, energetically efficient and cyanide-resistant branch of the respiratory chain contributing to the aerobic growth? Our present results with the *ndh*::*cm*^{r} strain tend to support the first alternative, because the oxygen uptake in the mutant strain would be too low for any measurable impact of oxidative phosphorylation. We therefore suggest that the observed elevation of the aerobic growth rate and biomass yield ($Y_{X/S}$) of *Z. mobilis* does not result from extra ATP generation by oxidative phosphorylation, but occurs whenever the NADH flux is redirected from respiration to ethanol synthesis, so that less acetaldehyde, the toxic precursor of ethanol (Wecker & Zall, 1987), is accumulated in the culture.

The key role of acetaldehyde was reinforced by the present finding that vigorous aeration (hyperventilation) of the shaken flask cultures of Zm6 improved the aerobic growth rate. As described above, the batch cultivations in shaken flasks were carried out under strictly anaerobic conditions (gassing of cultures with oxygen-free nitrogen gas), aerobically on the shaker, and aerobically on the shaker with hyperventilation. Under strictly anaerobic conditions, the growth curves of Zm6 and *ndh*::*cm*^{r} were identical (not shown). However, the aerobic behaviour of the two strains differed substantially (Fig. 3). In shaken flasks without hyperventilation Zm6 accumulated acetaldehyde and grew much more slowly than the mutant. At the early stationary phase, acetaldehyde concentration reached

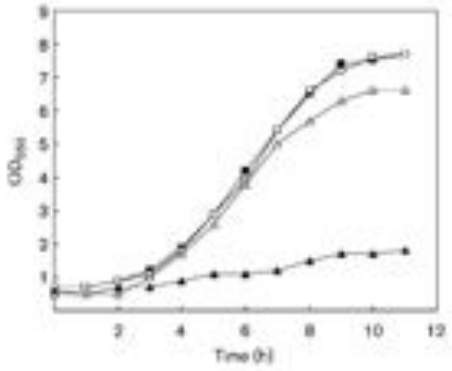

Fig. 3. Aerobic batch cultivation of Zm6 (▲, ■) and *ndh*::*cm*^{r} (△, □) in shaken flasks at 120 r.p.m. (▲, △) and in shaken flasks with additional aeration at 1 l min^{-1} (■, □).

33 mM (1.4 g l^{-1}). In the mutant strain, due to its low respiration rate, accumulation of acetaldehyde was negligible; its concentration at the end of the batch cultivation did not exceed 0.6 mM. Hyperventilation of the shaken flask cultures barely affected the growth of *ndh*::*cm*^{r}, yet greatly improved that of Zm6. Acetaldehyde concentration in both hyperventilated cultures was low: 0.5 mM for Zm6 and 0.4 mM for *ndh*::*cm*^{r}. We may conclude that either a low rate of acetaldehyde generation (as in *ndh*::*cm*^{r}) or an efficient removal of acetaldehyde (as in the hyperventilated Zm6) is of prime importance for aerobic growth stimulation in *Z. mobilis* to take place.

Notably, however, the aerobic growth stimulation of Zm6 never extended beyond the limits imposed by its fermentative catabolism. The hyperventilation of the shaken flask cultures clearly demonstrated that, even at very low acetaldehyde concentrations, the respiratory chain did not contribute to the aerobic batch growth of *Z. mobilis*: hyperventilated Zm6 and *ndh*::*cm*^{r} showed identical growth curves (Fig. 3). Thus, acetaldehyde acting as a potent inhibitor of growth is not the key factor that causes the deficiency of oxidative phosphorylation in growing *Z. mobilis*.

ACKNOWLEDGEMENTS

This work was funded by grant 04.1101 of the Latvian Council of Science and by Royal Society fellowship 2005/R3 (to U.K.). The authors are grateful to Dr Malda M. Tonna for valuable help in cultivation experiments.

REFERENCES

Belaich, J. P. & Senez, J. C. (1965). Influence of aeration and pantothenate on growth yields of *Zymomonas mobilis*. *J Bacteriol* **89**, 1195–1206.

Bertsova, Y. V., Bogachev, A. V. & Skulachev, V. P. (2001). Noncoupled NADH:ubiquinone oxidoreductase of *Azotobacter vinelandii* is required for diazotrophic growth at high oxygen concentrations. *J Bacteriol* **183**, 6869–6874.

Bringer, S., Finn, R. K. & Sahm, H. (1984). Effect of oxygen on the metabolism of *Zymomonas mobilis*. *Arch Microbiol* **139**, 376–381.

Calhoun, M. W., Oden, K. L., Gennis, R. B., de Mattos, J. T. & Neijssel, J. (1993). Energetic efficiency of *Escherichia coli*: effects of mutations in components of the aerobic respiratory chain. *J Bacteriol* **175**, 3020–3025.

Conway, T. (1992). The Entner–Doudoroff pathway: history, physiology and molecular biology. *FEMS Microbiol Rev* **9**, 1–27.

Demirtas, M. U., Kolhatkar, A. & Kilbane, J. J., 2nd (2003). Effect of aeration and agitation on growth rate of *Thermus thermophilus* in batch mode. *J Biosci Bioeng* **95**, 113–117.

Dien, B. S., Cotta, M. A. & Jeffries, T. W. (2003). Bacteria engineered for fuel ethanol production: current status. *Appl Microbiol Biotechnol* **63**, 258–266.

Kalnenieks, U. (2006). Physiology of *Zymomonas mobilis*: some unanswered questions. *Adv Microb Physiol* **51**, 73–117.

Kalnenieks, U., de Graaf, A. A., Bringer-Meyer, S. & Sahm, H. (1993). Oxidative phosphorylation in *Zymomonas mobilis*. *Arch Microbiol* **160**, 74–79.

Kalnenieks, U., Galinina, N., Irbe, I. & Toma, M. M. (1995). Energy coupling sites in the electron transport chain of *Zymomonas mobilis*. *FEMS Microbiol Lett* **133**, 99–104.

Kalnenieks, U., Galinina, N., Toma, M. M. & Skards, I. (1996). Electron transport chain in aerobically cultivated *Zymomonas mobilis*. *FEMS Microbiol Lett* **143**, 185–189.

Kalnenieks, U., Galinina, N., Bringer-Meyer, S. & Poole, R. K. (1998). Membrane D-lactate oxidase in *Zymomonas mobilis*: evidence for a branched respiratory chain. *FEMS Microbiol Lett* **168**, 91–97.

Kalnenieks, U., Galinina, N., Toma, M. M. & Poole, R. K. (2000). Cyanide inhibits respiration yet stimulates aerobic growth of *Zymomonas mobilis*. *Microbiology* **146**, 1259–1266.

Kalnenieks, U., Toma, M. M., Galinina, N. & Poole, R. K. (2003). The paradoxical cyanide-stimulated respiration of *Zymomonas mobilis*: cyanide sensitivity of alcohol dehydrogenase (ADH II). *Microbiology* **149**, 1739–1744.

Kalnenieks, U., Galinina, N., Toma, M. M., Pickford, J. L., Rutkis, R. & Poole, R. K. (2006). Respiratory behaviour of a *Zymomonas mobilis adh*II::*kan*^{r} mutant supports the hypothesis of two alcohol dehydrogenase isoenzymes catalysing opposite reactions. *FEBS Lett* **580**, 5084–5088.

Kim, Y. J., Song, K.-B. & Rhee, S.-K. (1995). A novel aerobic respiratory chain-linked NADH oxidase system in *Zymomonas mobilis*. *J Bacteriol* **177**, 5176–5178.

Leif, H., Sled, V. D., Ohnishi, T., Weiss, H. & Friedrich, T. (1995). Isolation and characterization of the proton-translocating NADH:ubiquinone oxidoreductase from *Escherichia coli*. *Eur J Biochem* **230**, 538–548.

Liang, C.-C. & Lee, W.-C. (1998). Characteristics and transformation of *Zymomonas mobilis* with plasmid pKT230 by electroporation. *Bioprocess Eng* **19**, 81–85.

Markwell, M. A. K., Haas, S. M., Bieber, L. L. & Talbert, N. E. (1978). A modification of the Lowry procedure to simplify protein determination in membrane and lipoprotein samples. *Anal Biochem* **87**, 206–210.

Matsushita, K., Ohnishi, T. & Kaback, R. H. (1987). NADH-ubiquinone oxidoreductases of the *Escherichia coli* aerobic respiratory chain. *Biochemistry* **26**, 7732–7737.

Matsushita, K., Otofuji, A., Iwahashi, M., Toyama, H. & Adachi, O. (2001). NADH dehydrogenase of *Corynebacterium glutamicum*. Purification of an NADH dehydrogenase II homolog able to oxidize NADPH. *FEMS Microbiol Lett* **204**, 271–276.

Nantapong, N., Kugimiya, Y., Toyama, H., Adachi, O. & Matsushita, K. (2004). Effect of NADH dehydrogenase disruption and over-expression on respiration-related metabolism in *Corynebacterium glutamicum* KY 9714. *Appl Microbiol Biotechnol* **66**, 187–193.

Pankova, L. M., Shvinka, Y. E., Beker, M. E. & Slava, E. E. (1985). Effect of aeration on *Zymomonas mobilis* metabolism. *Mikrobiologiia* **54**, 141–145.

Poole, R. K. & Cook, G. M. (2000). Redundancy of aerobic respiratory chains in bacteria? Routes, reasons and regulation. *Adv Microb Physiol* **43**, 165–224.

Reyes, L. & Scopes, R. K. (1991). Membrane-associated ATPase from *Zymomonas mobilis*: purification and characterization. *BBA* **1068**, 174–178.

Rogers, P. L. K., Lee, J., Skotnicki, M. L. & Tribe, D. E. (1982). Ethanol production by *Zymomonas mobilis*. *Adv Biochem Eng* **23**, 37–84.

Sambrook, J., Fritsch, E. F. & Maniatis, T. (1989). *Molecular Cloning: a Laboratory Manual*, 2nd edn. Cold Spring Harbor, NY: Cold Spring Harbor Laboratory.

Schmehl, M., Jahn, A., Meyer zu Vilsendorf, A., Hennecke, S., Masepohl, B., Schuppler, M., Marxer, M., Oelze, J. & Klipp, W. (1993). Identification of a new class of nitrogen fixation genes in *Rhodobacter capsulatus*: a putative membrane complex involved in electron transport to nitrogenase. *Mol Gen Genet* **241**, 602–615.

Seo, J.-S., Chong, H., Park, H. S., Yoon, K.-O., Jung, C., Kim, J. J., Hong, J. H., Kim, H., Kim, J. H. & other authors (2005). The genome sequence of the ethanologenic bacterium *Zymomonas mobilis* ZM4. *Nat Biotechnol* **23**, 63–68.

Sprenger, G. A. (1996). Carbohydrate metabolism in *Zymomonas mobilis*: a catabolic highway with some scenic routes. *FEMS Microbiol Lett* **145**, 301–307.

Strohdeicher, M., Neuß, B., Bringer-Meyer, S. & Sahm, H. (1990). Electron transport chain of *Zymomonas mobilis*: Interaction with the membrane-bound glucose dehydrogenase and identification of ubiquinone 10. *Arch Microbiol* **154**, 536–543.

Viikari, L. (1986). By-product formation in ethanol fermentation by *Zymomonas mobilis*. *Technical Research Centre of Finland, Publication* **27**.

Viikari, L. & Berry, D. R. (1988). Carbohydrate metabolism in *Zymomonas*. *Crit Rev Biotechnol* **7**, 237–261.

Wang, G. & Maier, R. J. (2004). An NADPH quinone reductase of *Helicobacter pylori* plays an important role in oxidative stress resistance and host colonization. *Infect Immun* **72**, 1391–1396.

Wecker, M. S. A. & Zall, R. R. (1987). Production of acetaldehyde by *Zymomonas mobilis*. *Appl Environ Microbiol* **53**, 2815–2820.

Yagi, T. (1991). Bacterial NADH-quinone oxidoreductases. *J Bioenerg Biomembr* **23**, 211–225.

Edited by: R. van Spanning

3.2 Electron transport and oxidative stress in Zymomonas mobilis respiratory mutants

Arch Microbiol (2012) 194:461–471
DOI 10.1007/s00203-011-0785-7

ORIGINAL PAPER

Electron transport and oxidative stress in *Zymomonas mobilis* respiratory mutants

Inese Strazdina · Zane Kravale · Nina Galinina · Reinis Rutkis · Robert K. Poole · Uldis Kalnenieks

Received: 27 July 2011 / Revised: 19 November 2011 / Accepted: 16 December 2011 / Published online: 7 January 2012

Abstract The ethanol-producing bacterium *Zymomonas mobilis* is of great interest from a bioenergetic perspective because, although it has a very high respiratory capacity, the respiratory system does not appear to be primarily required for energy conservation. To investigate the regulation of respiratory genes and function of electron transport branches in *Z. mobilis*, several mutants of the common wild-type strain Zm6 (ATCC 29191) were constructed and analyzed. Mutant strains with a chloramphenicol-resistance determinant inserted in the genes encoding the cytochrome *b* subunit of the bc_1 complex (Zm6-*cytB*), subunit II of the cytochrome *bd* terminal oxidase (Zm6-*cydB*), and in the catalase gene (Zm6-*kat*) were constructed. The *cytB* and *cydB* mutants had low respiration capacity when cultivated anaerobically. Zm6-*cydB* lacked the cytochrome *d* absorbance at 630 nm, while Zm6-*cytB* had very low spectral signals of all cytochromes and low catalase activity. However, under aerobic growth conditions, the respiration capacity of the mutant cells was comparable to that of the parent strain. The catalase mutation did not affect aerobic growth, but rendered cells sensitive to hydrogen peroxide. Cytochrome *c* peroxidase activity could not be detected. An upregulation of several thiol-dependent oxidative stress-protective systems was observed in an aerobically growing *ndh* mutant deficient in type II NADH dehydrogenase (Zm6-*ndh*). It is concluded that the electron transport chain in *Z. mobilis* contains at least two electron pathways to oxygen and that one of its functions might be to prevent endogenous oxidative stress.

Keywords *Zymomonas mobilis* · Respiratory chain · Cytochrome *bd* · Cytochrome bc_1

Communicated by Gregory Cook.

I. Strazdina · Z. Kravale · N. Galinina · R. Rutkis · U. Kalnenieks (✉)
Institute of Microbiology and Biotechnology, University of Latvia, Kronvalda bulv. 4, 1586 Riga, Latvia
e-mail: kalnen@lanet.lv

R. K. Poole
Department of Molecular Biology and Biotechnology, The University of Sheffield, Firth Court, Western Bank, Sheffield S10 2TN, UK

Introduction

Zymomonas mobilis is a facultatively anaerobic, obligately fermentative bacterium with a highly active ethanol fermentation pathway (Rogers et al. 1982, 2007; Sprenger 1996). Nevertheless, *Z. mobilis* possesses an active, constitutive aerobic respiratory chain (Strohdeicher et al. 1990; Kalnenieks et al. 1998), supporting oxygen uptake rates substantially higher than those of *Saccharomyces cerevisiae*, *Escherichia coli*, or *Pseudomonas putida* (Kalnenieks 2006; Sootsuwan et al. 2008). The physiology of aerobic electron transport in *Z. mobilis* is unusual for bacteria. Although the cytoplasmic membrane of *Z. mobilis* carries a functional H^+-ATP synthase complex (Reyes and Scopes 1991), and non-growing cells and membrane preparations show oxidative phosphorylation activity (Kalnenieks et al. 1993), the bacterium does not use its respiratory chain to supply energy for aerobic growth in the manner typical of aerobic and facultatively anaerobic microorganisms. The aerobic biomass yields of *Z. mobilis* do not exceed the anaerobic yields, which are typically around 8–10 g dry wt (mol glucose)$^{-1}$ for batch cultures growing on rich media (Belaich and Senez 1965; Bringer et al. 1984). Indeed, respiratory metabolism is inhibitory for growth because of

the accumulation of acetaldehyde and other toxic byproducts (Viikari 1986; Viikari and Berry 1988), and a stimulation of aerobic growth is evident when respiration is inhibited by addition of cyanide at submillimolar concentrations (Kalnenieks et al. 2000), or on mutation of the respiratory NADH dehydrogenase (Kalnenieks et al. 2008). However, the reasons for the low energetic efficiency of respiration in growing *Z. mobilis* are not clear.

The organization of respiratory components and the routes for electron transfer to oxygen are not fully resolved in *Z. mobilis*, but Fig. 1 shows a current working model. There is only one functional respiratory NAD(P)H dehydrogenase in the *Z. mobilis* electron transport chain, belonging to the type II respiratory dehydrogenase (Ndh) family (Kalnenieks et al. 2008; Seo et al. 2005; Yang et al. 2009a), and only one terminal cytochrome *bd*-type quinol oxidase has been identified so far (Kalnenieks et al. 1998; Sootsuwan et al. 2008). The known *Z. mobilis* genome sequences contain genes encoding a cytochrome bc_1 complex and cytochrome *c* (Seo et al. 2005; Yang et al. 2009a; Kouvelis et al. 2009), yet lack sequences homologous to any known bacterial cytochrome *c* oxidase genes. Sootsuwan et al. (2008) proposed that the cytochrome bc_1 branch most likely is terminated by a cytochrome *c* peroxidase, as the cytochrome *c* peroxidase gene is present in the genome. In the present work, we aimed to investigate the function of cytochrome *bd* and the cytochrome bc_1 complex in respiration, and to find out whether the cytochrome bc_1 complex supplies electrons to a cytochrome *c* peroxidase.

Energy generation is the central, yet not the sole function of bacterial electron transport chains (Poole and Cook 2000). The aerobic respiration in bacteria generates reactive species of oxygen (ROS) (Gonzalez-Flecha and Demple 1995), but may also protect the cell interior from molecular oxygen (as demonstrated for nitrogen-fixing bacteria, see Kelly et al. 1990), and also from oxidative stress by diverting electrons from hydrogen peroxide-generating reactions (Korshunov and Imlay 2010). The potential respiratory-protective and ROS-protective roles of the electron transport in *Z. mobilis*, as a physiological alternative to oxidative energy generation, are of interest but so far have attracted little attention.

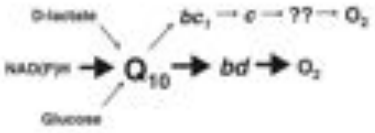

Fig. 1 The current model of respiratory chain of *Zymomonas mobilis*. A route to oxygen via cytochrome *bd* is established and supported in this work. The nature of any other terminal oxidase is unknown

To address these problems, we have carried out a comparative study of respiration, and regulation of respiratory and ROS-protective genes in several *Z. mobilis* mutants, namely an Ndh-deficient strain, a strain deficient in the cytochrome *b* subunit of the bc_1 complex, a strain deficient in the subunit II of the cytochrome *bd* terminal oxidase, and a catalase-deficient strain. The results demonstrated significant effects of the knockout mutations in cytochrome *bd* and in cytochrome bc_1 complex on respiration, yet did not verify the presence of a cytochrome *c* peroxidase activity. At the same time, some unexpected pleiotropic effects of the respiratory gene mutations were observed.

Materials and methods

Bacterial strains, plasmids, and transformation

Escherichia coli JM109 and plasmid pGEM-3Zf(+) were purchased from Promega. Strain JM109 was used as the host for cloning of the recombinant plasmids. *Z. mobilis* ATCC 29191 (Zm6) and its mutant derivative, deficient in type II respiratory NADH dehydrogenase (the *ndh* mutant; Zm6-*ndh*) were maintained and cultivated as described previously (Kalnenieks et al. 1993, 2008). The plasmids and strains constructed and used in the present work are listed in Table 1. *E. coli* was transformed by the $CaCl_2$ procedure described by Sambrook et al. (1989). *Z. mobilis* was transformed by electroporation (Liang and Lee 1998).

PCR, cloning techniques, and mutant construction

Genomic and plasmid DNA isolation from *Z. mobilis* were performed as before (Kalnenieks et al. 2006, 2008). The *Z. mobilis* catalase gene (*Z. mobilis* ZM4 genome sequence, locus tag ZMO 0918) was amplified by PCR using the primer pair Z.m.cat1 (AAGAGGGATCCTATGACTAGA CCCAATCTT) and Z.m.cat2 (GAAGCAGCAAGCTTT ATAACAGGCTATCGG). The engineered restriction sites for *Bam*HI and *Hin*dIII, respectively, are underlined. To obtain a mutant defective in the *kat* gene (Zm6-*kat*), the 1.45-kb region of the chromosomal DNA containing the *kat* ORF (ZMO 0918) was amplified, double-digested with *Bam*HI and *Hin*dIII, and directionally cloned between the *Bam*HI and *Hin*dIII restriction sites of the multiple cloning site (MCS) of plasmid pGEM-3Zf(+). In addition, the *Eco*RI site was removed from the MCS, by eliminating a 0.35-kb fragment between the *Eco*24I restriction sites of pGEM-3Zf(+) yielding plasmid pGEMcat (Table 1). A 0.8-kb fragment of plasmid pBT (Table 1), containing the 659-bp ORF of the chloramphenicol acetyltransferase gene, was amplified using a primer pair with *Eco*RI sites

Table 1 Plasmids and strains used in the study

Plasmid/strain	Characteristics	Source
pGEM-3Zf(+)	Amp^r	Promega
pBT	Cm^r	Stratagene
pGEMb	pGEM-Zf(+) derivative, carrying a 1.3-kb fragment of PCR-amplified genomic DNA with the ORF of the cytochrome *b* subunit gene (ZMO 0957) of the bc_1 complex, cloned between the *Hin*dIII and *Bam*HI sites of the MCS	Present work
pGEMb::cm′	pGEMb derivative, carrying in the *Age*I site of the cloned gene a 1.3-kb *Age*I restriction fragment of pBT, with an 0.7-kb chloramphenicol resistance ORF	Present work
pGEMd	pGEM-Zf(+) derivative, carrying a 1.55-kb fragment of PCR-amplified genomic DNA with part of the ORF of *cydA* (ZMO 1571) and the whole of *cydB* (ZMO 1572), cloned between the *Hin*dIII and *Bam*HI sites of the MCS	Present work
pGEMd::cm′	pGEMd derivative, carrying in the *Age*I site of the *cydB* (ZMO 1572) a 1.3-kb *Age*I restriction fragment of pBT, with an 0.7-kb chloramphenicol resistance ORF	Present work
pGEMcat	pGEM-Zf(+) derivative, (1) carrying a 1.4-kb fragment of PCR-amplified genomic DNA with the ORF of the catalase gene (ZMO 0918) cloned between the *Hin*dIII and *Bam*HI sites of the multiple cloning site, (2) lacking *Eco*RI site in the MCS in result of elimination of an 0.35-kb fragment between *Eco*24I restriction sites of pGEM-3Zf(+)	Present work
pGEMcat::cm′	pGEMcat derivative, carrying an 0.8-kb PCR-amplified fragment of pBT with 0.7 kb of the chloramphenicol resistance ORF, inserted in the *Eco*RI site of the cloned gene	Present work
Zm6	Parent strain	ATCC 29191
Zm6-ndh	*Zm6* strain with a cm′ insert in the ORF of respiratory type II NADH dehydrogenase gene (*ndh*) (ZMO 1113)	Kalmokoff et al. (2008)
Zm6-cytB	*Zm6* strain with a cm′ insert in the ORF of the cytochrome *b* subunit gene (ZMO 0957) of the bc_1 complex	Present work
Zm6-cydB	*Zm6* strain with a cm′ insert in the ORF of the subunit II (*cydB*) gene (ZMO 1572) of the cytochrome *bd* terminal oxidase	Present work
Zm6-kat	*Zm6* strain with a cm′ insert in the ORF of catalase gene (ZMO 0918)	Present work

(underlined): cm1 (TTTGCTTTCGAATTCCTGCCATTC ATCCGC) and cm2 (CACTACCGGGCGAATTCTTTGA GTTATCGAG). The PCR product was digested with *Eco*RI and inserted in the *Eco*RI site of the cloned *kat* gene, yielding plasmid pGEMcat::cm′ (Table 1). This plasmid was used to transform *Z. mobilis* by electroporation, and homologous recombinants were selected on plates containing chloramphenicol (120 μg ml^{-1}). Several colonies were screened for the *kat*::*cm*′ genotype by PCR on the genomic DNA template with primers Z.m.cat1 and Z.m.cat2; insertion of the chloramphenicol-resistance determinant in the catalase gene was verified by sequencing the PCR product.

The gene encoding the cytochrome *b* subunit of the respiratory chain bc_1 complex (*Z. mobilis* ZM4 genome sequence, locus tag ZMO 0957) was amplified using the primer pair Z.m.b1 (GAACTTATTATGAAGCTTTCAC CACCCCCT) with the engineered site for *Hin*dIII underlined, and Z.m.b2 (TTGAGCATATCAGGATCCCGT TCTTTTCTT) with the *Bam*HI site underlined. In the *Z. mobilis* ZM4 genome annotation, the expected product of ZMO 0957 is described as 'cytochrome b/b6 domain-containing protein' of the cytochrome bc_1 complex. ZMO 0957 is homologous to the *cytB* gene of the taxonomically related *Sphingobium japonicum*; therefore, by analogy, we named this gene '*cytB*'. To construct a *cytB* mutant defective in the cytochrome *b* subunit of the bc_1 complex, the 1.26-kb region of the chromosomal DNA containing the gene ZMO 0957 was amplified and cloned as described for the catalase gene construct, yielding plasmid pGEMb (Table 1). Plasmid pBT was digested with *Age*I (*Rsh*TI) to obtain three fragments of approximately 1.6, 1.3, and 0.3 kb length. The 1.3-kb fragment carried the ORF of the chloramphenicol acetyltransferase gene. The *Age*I digestion of pBT was chosen because plasmid pGEMb contained only one *Age*I restriction site that was localized in the cloned ORF of the *cytB* gene. After digestion of pGEMb with *Age*I, the 1.3-kb fragment of pBT was inserted in the

middle of the cloned gene to yield plasmid pGEMb::cm^r (Table 1). Transformation of *Z. mobilis* and screening for the mutation were done exactly as described for the *kat* gene.

A 1.55-kb genomic DNA fragment, with part of the gene encoding the cytochrome *bd* subunit I and the whole of the gene encoding the cytochrome *bd* subunit II (*Z. mobilis* ZM4 genome sequence, locus tags ZMO 1571 and ZMO 1572), was amplified, using the primer pair Z.m.d1 (ATG AAGCTTCTTGGATCCTGACCCATAGTC) and Z.m.d2 (TACCCGTCACTGCTGGTAAGCTTGCCGTGG), with the engineered restriction sites for *Bam*HI and *Hin*dIII, respectively, underlined. In order to disrupt subunit II of the cytochrome *bd* terminal oxidase, the amplified 1.55-kb DNA fragment, containing part of ZMO 1571 (homologous to the *cydA* gene of *E. coli*) and the whole ZMO 1572 ORF (homologous to the *cydB* gene of *E. coli*, respectively), was directionally cloned in the MCS of pGEM-3Zf(+), yielding plasmid pGEMd (Table 1). The plasmid pGEMd contained a single *Age*I restriction site, which was localized in ZMO 1572. Further steps in the *cydB* mutant construction were identical to those described above for the *cydB* mutant. After transformation, several colonies were screened for the *cydB*::cm^r genotype by PCR on the genomic DNA template with primers Z.m.d1 and Z.m.d2, and the insertion of the chloramphenicol-resistance determinant in the *cydB* gene was verified by sequencing the PCR product.

Primers for PCR reactions were supplied by Operon and Invitrogen. PCRs were carried out in an Eppendorf Mastercycler, using Fermentas *Taq*DNA polymerase. Other DNA manipulations were done as described previously (Kalnenieks et al. 2008), using Qiagen kits. All DNA constructs were confirmed by DNA sequencing, done by Beckman Coulter genomics.

Quantitative PCR analysis

Primer pairs for 14 genes (Table 2) were designed to give PCR products of 200 (±8) bp length. An RNeasy Mini kit (Qiagen) was used for mRNA purification. Reverse transcription was done with the Revert Aid Premium First Strand cDNA Synthesis kit (Fermentas), and Maxima

Table 2 Genes and the corresponding primer pairs used for qRT-PCR analysis

Gene product	Gene	Primers	Sequences (5′–3′)
Alkyl hydroperoxide reductase	ZMO 1732	ahpC_f	ggattacggccaacatcaa
		ahpC_r	attacgctggcggaaatct
Catalase	ZMO 0918	kat_f	agggaatgggattagtcg
		kat_r	aagaggaatacccacgatcag
Cytochrome *bd* subunit I	ZMO 1571	cydA_f	tatgaattcgggacgaactg
		cydA_r	ccaagtcatggaaatcaagg
Glyceraldehyde-3-P dehydrogenase	ZMO 0177	gapdeh_f	aagcttggcgtgaatcgt
		gapdeh_r	gtgccaagatgcgttagaaac
NADPH-glutathione reductase	ZMO 1211	gor_f	tttataaagcgcgcgatcg
		gor_r	gatcgggttttcggtcataa
Glutaredoxin 2	ZMO 0070	grx_f	gttataagctggtgccgatt
		grx_r	aattctggcaaaggtgccat
D-lactate dehydrogenase	ZMO 0256	ldh_f	tgagcaggttatctgtttgc
		ldh_r	tgatacgagcataaaggggtc
Type II NAD(H) dehydrogenase	ZMO 1113	ndh_f	agaaggccataaaatcagcg
		ndh_r	ttgagcaatcatggttctgg
Putative iron-dependent peroxidase	ZMO 1573	per_f	caaagagttaaaaggcggtgc
		per_r	tctacaaaaccaatcaggggc
Cytochrome *c* peroxidase	ZMO 1136	perC_f	tttccgttcgtgatcgtc
		perC_r	ccatgattgggcagaagtta
NADH:ubiquinone oxidoreductase of RnfABCDGE type, RnfA subunit	ZMO 1814	rnfA_f	atccaaccgaggaagcaaaa
		rnfA_r	attctgattatcgcttcgggc
Superoxide dismutase	ZMO 1060	sod_f	ccatcttccaaaacgagccca
		sod_r	ttgttcaacaatgcggcaca
Thioredoxin reductase	ZMO 1142	tor_f	atgccttgatgctggttttg
		tor_r	ttattgctgggcaagatagc
Thioredoxin	ZMO 1097	trx_f	tttgaaaagcagcaggggtc
		trx_r	taaaatcaccggtgccctgtt

SYBR green/ROX qPCR Master Mix (Fermentas) was used for the PCR. The quantitative real-time PCRs (qRT-PCR) were carried out in duplicate in a real-time thermal cycler (Model 7300, Applied Biosystems). In order to compare gene transcription between the strains and cultivation conditions, qRT-PCR data in all cases were normalized against the respective amounts of cDNA of the glyceraldehyde-3-phosphate dehydrogenase gene (ZMO 0177). Choice of ZMO 0177 as the 'housekeeping' gene for *Z. mobilis* was justified by the data of Yang et al. (2006b), showing that transcription of this gene is constitutive, and is not affected significantly by aeration or by accumulation of metabolic end products.

Continuous cultivation

Continuous cultivation was carried out in a Labfors fermenter (Infors) of 2.5-l working volume, containing 1 l of culture, at 30°C, pH 6.0, and a dilution rate of 0.18 h^{-1}. The growth medium contained glucose (20 g l^{-1}), yeast extract (5 g l^{-1}), and mineral salts, as described previously (Kalnenieks et al. 1993). Cultivations were started under anaerobic conditions and established by gassing the culture with nitrogen gas, containing only trace amounts of oxygen, at a flow rate of 1.4 l min^{-1}, and stirring rate 100 rpm. During the steady state under these conditions, the metabolism was strictly anaerobic: ethanol yield in the parent strain Zm6 reached 0.49–0.50 g g $glucose^{-1}$ (close to the theoretical maximum value; Rogers et al. 1982), and no acetaldehyde could be detected in the medium. When the anaerobic steady state had established, samples were taken for qRT-PCR, as well as for product analysis, and for whole-cell oxygen uptake assay, catalase, and peroxide-generation assays. After that, aeration was started with an air flow of 1.5 l min^{-1} and stirring rate 300 rpm., and the chemostat was run overnight. It took typically 12–15 h to reach the aerobic steady state, and at that point, sampling was repeated. During the aerobic steady state, the parent strain Zm6 maintained pO_2 in the fermenter around 0–2%, ethanol yield reached 60% of the theoretical maximum, and 0.2 g acetaldehyde l^{-1} was present in the medium, corresponding to a moderately aerobic metabolism of *Z. mobilis* (for review see Kalnenieks 2006).

Preparation of cell-free extracts and membrane vesicles

For preparation of cell-free extract, cells were sedimented by centrifugation at 5,000 rpm for 15 min, washed, and resuspended in 100 mM potassium phosphate buffer, containing 2 mM magnesium sulfate, pH 6.9, to an OD_{550} of about 40 (after correction for dilution, measured in a Shimadzu spectrophotometer), corresponding to a biomass concentration of 6.8–7.0 mg (dry wt) ml^{-1}. Cells were broken by an 8-min ultrasonic treatment with pulses of 0.5-s duration, separated by 0.5-s intervals, using a Dr. Hielscher ultrasonic processor. Typically, cell-free extracts of 4.6–4.9 mg protein ml^{-1} were obtained. Subsequent removal of unbroken cells and separation of cytoplasmic membranes by ultracentrifugation were performed as before (Kalnenieks et al. 1993, 1998).

Cytochrome spectroscopy

Room-temperature reduced minus oxidized cytochrome absorption spectra were taken using membrane samples (1 ml) at a protein concentration of 5–6 mg ml^{-1} with small amounts of solid dithionite as reductant and potassium ferricyanide as oxidant. Spectra were recorded with a custom-built SDB4 dual-wavelength scanning spectrophotometer (University of Pennsylvania School of Medicine Biomedical Instrumentation Group and Current Designs, Philadelphia, PA), as described previously (Kalnenieks et al. 1998). The time-course of cytochrome *d* reduction after addition of NADH was recorded by rapid, repetitive scanning in the wavelength range between 610 and 650 nm, using the dual-wavelength scanning spectrophotometer. The degree of cytochrome *d* reduction was calculated as the average value of the absorbance differences at wavelength pairs 630/614 and 630/646 nm.

Enzyme assays

Catalase activity in cell-free extracts was assayed spectrophotometrically, by monitoring absorbance decline at 240 nm (Gonzalez-Flecha and Demple 1994). Cytochrome *c* peroxidase activity was monitored by the decline in absorbance at the α-band of ferrocytochrome *c* at 550 nm on addition of cell-free extract and H_2O_2 (Ellfolk and Soininen 1970). Glutathione reductase activity was measured by decrease of NADPH absorbance at 340 nm on addition of oxidized glutathione (GSSG) in the presence of permeabilized cells (Bergmeyer et al. 1974). The cells were permeabilized as described previously (Kalnenieks et al. 2005), following a slightly modified procedure of Osman et al. (1987).

Analytical methods

H_2O_2 production by cells was determined fluorimetrically by monitoring Amplex UltraRed fluorescence during its reaction with H_2O_2, catalyzed by horseradish peroxidase (Korshunov and Imlay 2010). Fluorescence was measured with a FluoroMax-3 spectrofluorimeter (Jobin–Yvon), using 520-nm wavelength for excitation, and 620-nm wavelength for emission. To quantitate the generated

hydrogen peroxide, fluorescence increase was calibrated by addition of 1 mM H_2O_2 in 5-µl increments. Ethanol and glucose in culture media were determined by HPLC (Agilent 1100 series), using a Biorad Aminex HPX—87H column. Acetaldehyde concentration was determined by the alcohol dehydrogenase assay, as described previously (Kalnenieks et al. 2000). Concentration of dissolved oxygen was monitored by Clark-type oxygen electrodes. An autoclavable Ingold electrode was used in the fermenter, and a Radiometer electrode with a thermostatted electrode cell for oxygen uptake measurements in cell or membrane vesicle suspensions. Whole-cell oxygen uptake was measured for cells taken from steady-state cultures, pelleted, washed, and resuspended in 100 mM phosphate buffer, pH 6.9, supplemented with 10 g glucose l^{-1}. Protein concentration in cell-free extracts and membrane samples was determined according to Markwell et al. (1978). Cell concentration was determined as OD_{550}, and dry cell mass of the suspensions was calculated by reference to a calibration curve. Results are means of at least three replicates. SEM values are given as error bars in the figures.

Results

Respiratory gene regulation in the NADH dehydrogenase-deficient strain

Previously, we have demonstrated that the *ndh* mutant (Zm6-*ndh*) grows aerobically with very low rate of respiration and high ethanol yield, reaching higher biomass concentrations than the parent strain (Kalnenieks et al. 2008). This is confirmed in the whole-cell respiration assays of Zm6-*ndh* shown in Fig. 2a. Here we studied respiratory gene expression in this mutant and showed that it differed significantly from that of the parent Zm6 and other strains. In Zm6, upon transition from anaerobic to aerobic culture conditions, the transcription of *cydA* (ZMO 1571) was down-regulated 12-fold, yet transcription of other respiratory genes was not affected significantly, changing less than twofold (not shown). In the aerobically grown Zm6-*ndh* strain, the *ldh* gene (ZMO 0256) encoding the membrane D-lactate dehydrogenase and *cydA* were up-regulated relative to Zm6 (Table 3), supporting our previous observation of the elevated activity of membrane D-lactate oxidase in an aerobically grown *ndh* mutant (Kalnenieks et al. 2008). However, the knockout of the *ndh* gene did not affect transcription of *nqfA* (ZMO 1814). In *Rhodobacter capsulatus*, this gene encodes an alternative NADH/ubiquinone oxidoreductase, which is a part of a membrane complex supplying electrons to nitrogenase (Schmehl et al. 1993). In *Z. mobilis*, its function is unknown.

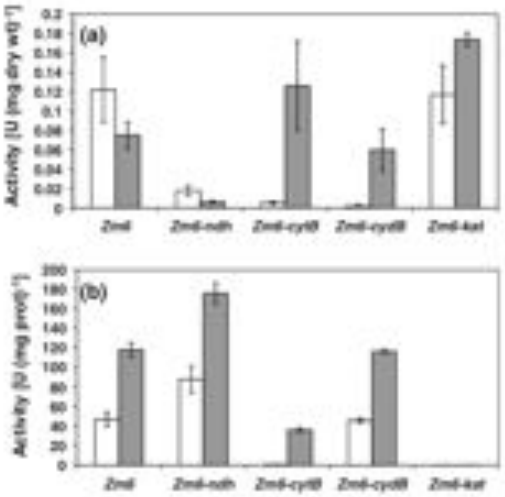

Fig. 2 Oxygen uptake rate and catalase activity in cells, harvested from chemostat cultures under anaerobic and aerobic steady-state conditions. Cells were sedimented, washed, and resuspended in 100 mM potassium phosphate buffer (pH 6.9) supplied with glucose (10 g l^{-1}). *Empty bars*—anaerobically cultivated cells; *filled bars*—aerobically cultivated cells. **a** oxygen uptake rate, **b** catalase activity in cell-free extracts, obtained by ultrasonic disruption

Table 3 The qRT-PCR ratios (mutant/Zm6) of the aerobic and anaerobic gene transcription, showing more than twofold difference between the mutant and parent strain

	(Zm6-*ndh*/ Zm6)		(Zm6-*cyd0*/ Zm6)		(Zm6-*cyd0*/ Zm6)		(Zm6-*kat*/ Zm6)	
	$+O_2$	$-O_2$	$+O_2$	$-O_2$	$+O_2$	$-O_2$	$+O_2$	$-O_2$
kat		0.2		0.25	4.59	4.41	n.d.	n.d.
ahpC				0.13	3.39			0.09
sod	3.2		4.0			2.2	4.6	
pcr				4.0				0.22
pcrC						0.18		
nqfA			3.5	2.1	0.47	0.49		
ndh	n.d.	n.d.				0.39	2.5	0.5
ldh	3.0			0.38				
cydA	6.1	0.27	2.1	0.23				0.05
grx	4.9						2.3	0.41
grx	60.0						0.04	
trx	2.1		3.0					
grr				0.08	2.25		0.38	0.5

n.d. not determined

Notably, we found some indications of oxidative stress in aerobically growing Zm6-*ndh*. The gene, encoding glutaredoxin 2 (ZMO 0070; *grx* in Table 3), was up-regulated 60-fold relative to the parent strain, the thioredoxin

gene (ZMO 1097; *trx* in Table 3) was up-regulated almost fivefold, and the thioredoxin reductase gene (ZMO 1142; *tor* in Table 3) more than twofold. As in the other mutant strains, the gene encoding superoxide dismutase (ZMO 1060; *sod*) was up-regulated more than threefold relative to Zm6. Although we did not see any change of glutathione reductase (ZMO 1211; *gor*) transcription, under aerobic growth conditions, the enzyme was more active in the Zm6-*ndh* strain: 0.030 U (mg dry wt)$^{-1}$, versus 0.009 U (mg dry wt)$^{-1}$ in Zm6 (not shown).

The respiratory chain in the cytochrome *bd* and cytochrome bc_1 mutants

Anaerobically cultivated cells of the Zm6-*cydB* strain, under oxic conditions in potassium phosphate buffer supplemented with 1% glucose, had insignificant oxygen uptake activity (Fig. 2a). This finding confirmed the previously postulated key role of the *bd*-type terminal oxidase in *Z. mobilis* respiration. It is in a good agreement with the genome data (Seo et al. 2005; Yang et al. 2009a) and is supported by spectroscopic evidence (Kalnenieks et al. 1998, 2000; Sootsuwan et al. 2008) demonstrating the presence of cytochrome *bd* both in aerobically and anaerobically grown Zm6 cells. Unexpectedly, however, anaerobically grown cells of the Zm6-*cytB* strain also had a near-zero oxygen consumption rate (Fig. 2a). Furthermore, when the cultures were shifted to aerobic growth conditions, oxygen uptake both in Zm6-*cydB* and Zm6-*cytB* gradually increased (not shown). After 11–12 h of aerobic growth, the respiration rate of the mutant cells reached a level comparable to that of Zm6, as shown in Fig. 2a.

Antimycin is considered a specific inhibitor of the cytochrome bc_1 complex (Trumpower and Gennis 1994). Antimycin sensitivity of *Z. mobilis* respiration has been reported previously by Strohdeicher et al. (1990). Here we compared antimycin sensitivity of oxygen uptake in membrane preparations obtained from aerobically grown Zm6, Zm6-*cytB*, and Zm6-*cydB* cells. There was no significant difference in antimycin sensitivity between Zm6 and Zm6-*cydB* (not shown); however, the *cytB* mutation increased the antimycin resistance of oxygen uptake in membrane preparations with NADH as the electron donor (Fig. 3, inset). Such an effect of the *cytB* mutation upon sensitivity of respiration toward an inhibitor of the cytochrome bc_1 complex indicates that part of electrons in the respiratory chain of the parent strain is transported to oxygen via the cytochrome bc_1 branch.

Reduced minus oxidized absorption spectra of cytochromes were recorded in membranes, prepared from cells in stationary-phase batch cultures. The results presented in Fig. 3 show that cytoplasmic membranes of anaerobically cultivated Zm6-*cydB* cells, as expected, lacked the

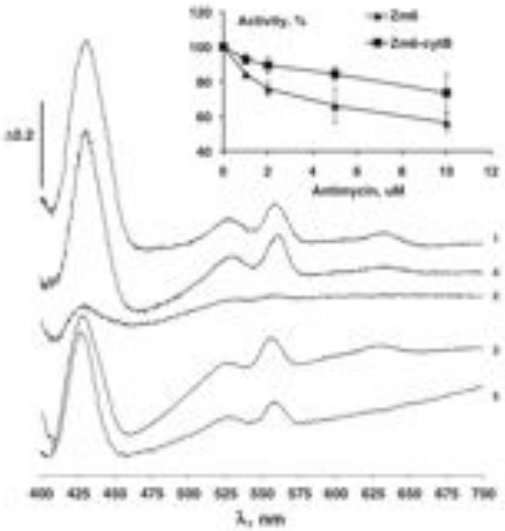

Fig. 3 Reduced minus oxidized difference spectra of membrane preparations. (*1*) Anaerobically cultivated Zm6, (*2*) anaerobically cultivated Zm6-*cytB*, (*3*) aerobically cultivated Zm6, (*4*) aerobically cultivated Zm6-*cytB*, (*5*) anaerobically cultivated Zm6-*cydB*. *Inset* antimycin titration of oxygen uptake in aerobically cultivated cell membrane preparations of Zm6 (*filled triangle*) and Zm6-*cytB* (*filled square*)

absorbance around 630 nm, characteristic for cytochrome *d*. However, anaerobically grown Zm6-*cytB* exhibited a general deficiency of cytochromes (Fig. 3), explaining the low respiratory rates measured (Fig. 2). In comparison to anaerobically cultivated Zm6 and Zm6-*cydB*, the Soret region in Zm6-*cytB* membranes was weak; there was almost no signal in the α-region of cytochromes *c* and *b* between 550 and 560 nm, and also no cytochrome *d* absorbance at 630 nm. Surprisingly, the amount of *cydA* transcript in the anaerobically cultivated Zm6-*cytB* strain was just fourfold lower than that of the anaerobically grown Zm6 (Table 3), but still higher than in aerobically grown Zm6, in which the absorbance of cytochrome *d* around 630 nm was clearly present (Fig. 3). Likewise, anaerobically cultivated Zm6-*cytB* cells lacked catalase activity (Fig. 2b), while the transcription of *kat* was very similar to that in anaerobically cultivated Zm6-*ndh* (Table 3), in which catalase activity was high. The rise of respiratory capacity of the *cytB* mutant during aerobic cultivation was accompanied by an increase of the spectral features of cytochromes (Fig. 3) and of catalase activity (Fig. 2b).

The time-course of cytochrome *d* reduction was monitored after addition of NADH to anaerobic suspensions of membrane vesicles, prepared from aerobically cultivated Zm6, Zm6-*cytB*, and Zm6-*cydB* cells (Fig. 4). As expected,

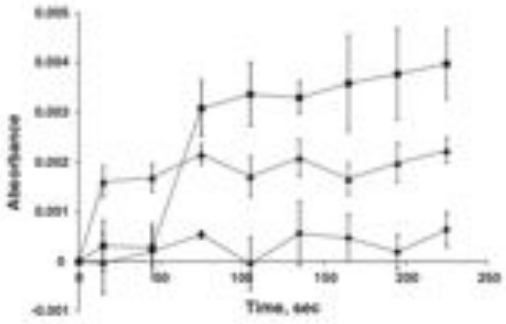

Fig. 4 Time-course of cytochrome *d* reduction in membranes prepared form aerobically grown Zm6 (*filled triangle*), Zm6-*cytB* (*filled square*), and Zm6-*cydB* (*filled diamond*). Cytochrome *d* spectral signals were recorded by repetitive scanning in the wavelength range between 610 and 650 nm at 30-s intervals, after addition of 3.5 mM NADH to anaerobic suspension of membranes. The degree of cytochrome *d* reduction was taken as the average of the absorbance differences at wavelength pairs 630/614 and 630/646 nm

in the membranes from the Zm6-*cydB* strain, the spectral signal of reduced cytochrome *d* remained close to zero during the whole experiment. On the contrary, for Zm6-*cytB*, after a short lag time, the cytochrome *d* absorbance reached even higher level, than in Zm6. This finding indicates that (1) in Zm6-*cytB*, electrons are diverted more toward the cytochrome *bd* terminal oxidase, than in the parent strain, and that (2) in *Z. mobilis*, the cytochrome bc_1 complex and cytochrome *bd* are localized in different electron transport branches (as in other bacteria with branched electron transport chains; see Poole and Cook 2000).

The *cytB* mutant was the only strain in which *ndh* (ZMO 1814) was up-regulated relative to Zm6, under both anaerobic and aerobic conditions (Table 3). However, the only functional respiratory NAD(P)H dehydrogenase of *Z. mobilis*—the type II NAD(P)H dehydrogenase *ndh*—was expressed at the same level as in the parent strain. In the *cydB* mutant, *ndh* was down-regulated relative to Zm6, while some of the ROS-protective genes, like those of catalase, *ahpC* (ZMO 1732), and glutathione reductase (ZMO 1211), were up-regulated under aerobic growth conditions. For catalase, the fourfold increase of gene transcription did not match with the observed enzymatic activity: In Zm6-*cydB*, it was the same as in Zm6 (Fig. 2b).

Properties of the catalase mutant and the apparent lack of cytochrome *c* peroxidase activity

Cytochrome *c* peroxidase is a periplasmic enzyme, loosely bound to the bacterial cytoplasmic membrane (Goodhew et al. 1990; Atack and Kelly 2006). During the preparation of cytoplasmic membrane vesicles, part of it may be lost, and hence, either cell-free extracts or permeabilized cells are better choices for cytochrome *c* peroxidase assays. However, *Z. mobilis* cells possess high catalase activity (Fig. 2b), which would interfere with the assay by rapidly removing the electron acceptor, H_2O_2. Therefore, a catalase mutant was constructed with the prime purpose of examining the activity of cytochrome *c* peroxidase in cell-free extracts. Although catalase activity was close to zero in the Zm6-*kat* strain (Fig. 2b), no cytochrome *c* peroxidase could be detected by the cytochrome *c* assay: H_2O_2-dependent oxidation of externally added cytochrome *c* did not occur in the cell-free extracts of the *kat* mutant (not shown).

In Fig. 5, the effect of millimolar H_2O_2 additions upon aerobic growth of the Zm6, Zm6-*cytB*, and Zm6-*kat* strains is presented. At the end of the exponential growth phase of shaken flask cultures, the cells were sedimented by centrifugation, resuspended in fresh culture medium (indicated by arrows) containing various concentrations of hydrogen peroxide, and aerobic cultivation was resumed. The results

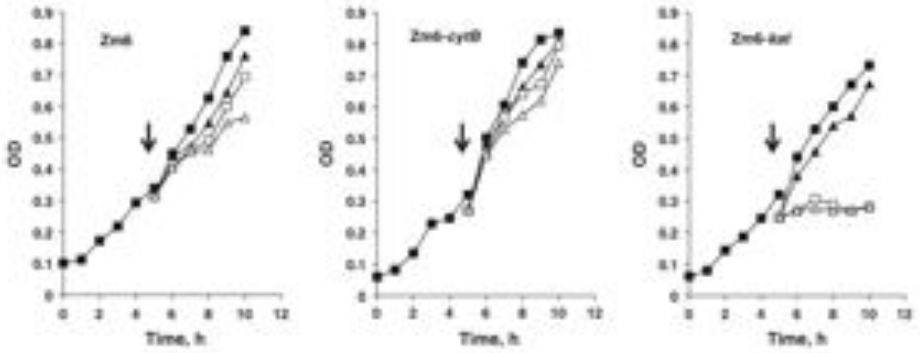

Fig. 5 The effect of *kat* and *cytB* knockout mutations on aerobic batch growth in the presence of externally added hydrogen peroxide (*filled square*) 0 mM, (*filled triangle*) 0.5 mM, (*open square*) 1 mM, and (*open triangle*) 2 mM

show no significant difference between the sensitivities of Zm6 and Zm6-*cydB* to the added H_2O_2. However, Zm6-*kat* appeared to be much more vulnerable and ceased to grow in the presence of 1 and 2 mM H_2O_2. Monitoring of hydrogen peroxide decomposition was done for the cultures transferred to the medium with 2 mM H_2O_2. For that purpose, samples were taken at 5-min intervals, cells were rapidly sedimented, and H_2O_2 was determined in the supernatant using the Amplex UltraRed dye. In Zm6 and Zm6-*cydB*, during the 5 min after transfer of cells into the fresh medium, the concentration of H_2O_2 dropped from 2 mM to around 20 μM, while in the *kat* mutant, it remained 1.69 mM even after 30 min of cultivation (not shown).

Taken together, these data do not support the function of the cytochrome *c* peroxidase (ZMO 1136) gene product in the degradation of hydrogen peroxide and cast doubt on whether a functional cytochrome *c* peroxidase terminates the cytochrome bc_1 branch of electron transport in *Z. mobilis*. At the same time, transcription of the corresponding gene (ZMO 1136) did take place in all strains. Neither aeration nor mutations exerted significant transcriptional regulation over this gene, with one exception: In anaerobically cultivated *cydB* mutant cells, the gene encoding ZMO1136 (*perC*) was down-regulated relative to Zm6 (Table 3).

Catalase deficiency in the aerobically cultivated Zm6-*kat* cells did not give rise to any coordinated upregulation of the alternative peroxide-scavenging systems. Although *ahpC* (ZMO 1732) and the putative iron-dependent peroxidase (ZMO 1573) during the anaerobic-to-aerobic transition of Zm6-*kat* were up-regulated by factors of about 10 and 5, respectively (Table 3), neither of them exceeded the transcript levels found in aerobically cultivated parent strain. An almost fivefold higher level of superoxide dismutase and twofold higher level of thioredoxin (ZMO 1097) transcript were accompanied by a threefold down-regulation of glutathione reductase and by 25-fold down-regulation of glutaredoxin in the *kat* mutant relative to the aerobically growing Zm6.

Aerobic growth parameters of the Zm6-*kat* strain in a chemostat did not differ significantly from those of Zm6. Washed cells from an aerobic *kat* mutant culture, suspended in phosphate buffer with glucose, showed an even higher oxygen uptake rate than that of strain Zm6 (Fig. 2a), in good agreement with the >twofold aerobic upregulation of *sdh* (Table 3). Catalase deficiency did not result in any significant elevation of H_2O_2 production by the Zm6-*kat* strain. In all strains, the specific rate of hydrogen peroxide export from the cells was found to be in the narrow range of 4–7 nmol (mg dry wt)$^{-1}$ min^{-1} and depended neither on the bulk oxygen consumption rate, nor on culture aeration (not shown).

Discussion

Oxygen-dependent regulation of gene expression represents a rapidly evolving field of research in microbiology, focussed largely on in-depth studies of a few species of model microorganisms. The ethanol-fermenting bacterium *Z. mobilis* is not among them, and little is known about its response to aeration. However, recently a genome-scale transcriptomic and metabolomic study of aeration in wild-type *Z. mobilis* (strain ZM4) was reported by Yang et al. (2009b). The authors explored the effects of aeration on exponential and stationary-phase cultures during controlled batch cultivations. In agreement with our present findings, these authors reported aerobic downregulation of *cydA* and *cydB* and found no significant effect of aeration upon catalase, peroxidase, superoxide dismutase, and glutathione reductase gene transcription. Yet, in contrast to the report of Yang et al. (2009b), in Zm6, we did not observe aerobic upregulation of alkyl hydroperoxide reductase *ahpC* (ZMO 1732), thioredoxin *trx* (ZMO 1097), and the NADH:ubiquinone oxidoreductase subunit *nqfA* (ZMO 1814). Also, we did not see aerobic downregulation of *sdh* (ZMO 1113). In part, these discrepancies might be due to strain differences, but also different levels of aeration. For *Z. mobilis*, ethanol yield may serve as a rough estimate for culture aeration. As mentioned in 'Materials and methods', in our study, the ethanol yield of Zm6 aerobic chemostat culture was close to 60% of the theoretical maximum. Yang et al. (2009b) reported only 27% of the maximum ethanol yield, which points to more vigorous aeration in their aerobic batch culture. Finally, we compared continuously growing cultures at a moderate dilution rate (D 0.18 h^{-1}), while Yang et al. (2009b) mostly analyzed transcription differences that they found in stationary-phase cultures.

Our results support the general conclusion of Yang et al. (2009b) that in growing *Z. mobilis*, there is little transcriptional response to changes of aeration per se, at least concerning the respiratory chain and the ROS-protective systems. The regulation of the respiratory and oxidative stress-protective gene transcription in *Z. mobilis* is poorly understood, and probably differs from the generally established mechanisms for Gram-negative facultative anaerobes. Yang et al. (2009b) reports a strong aerobic upregulation of the alternative sigma factor *rpoH* (ZMO 0749), a MerR family regulator (ZMO 1121), and some other putative regulatory elements. At the same time, the *Z. mobilis* genome lacks homologs of the *oxyR* and *soxR* genes (Seo et al. 2005; Yang et al. 2009a).

Here we demonstrate that respiratory mutations affect the aerobic physiology of this bacterium, in some cases in an unexpected manner. For the NADH dehydrogenase mutant, showing an improved aerobic growth capacity (Kalnenieks et al. 2008), which permanently keeps its

respiration rate low under oxic growth conditions, several thiol-dependent oxidative stress-protective systems are strongly up-regulated in the presence of oxygen. Such a regulatory response to aeration has not been observed in other *Z. mobilis* strains with medium or high respiration rate under aerobic conditions. It is possible that the rapid, yet energetically inefficient respiratory chain in *Z. mobilis* helps to prevent oxidative stress in aerobically growing culture. Furthermore, a knockout mutation of the cytochrome *b* subunit of the bc_1 complex in *Z. mobilis* gives rise to a complex, non-respiring phenotype, when cultivated under anoxic conditions. Notably, the absence of cytochrome spectral features and catalase activity under these conditions do not result from downregulation of the corresponding genes. Further research is needed to see whether, perhaps, heme biosynthesis or assembly of heme-containing enzymes is affected in the mutant strain under oxygen-limiting conditions.

The ability of both aerobically cultivated mutants, Zmb-*cydB* and Zmb-*cydB*, to consume oxygen, as well as the difference seen in the antimycin sensitivity of their respiration, and in the kinetics of the cytochrome *d* reduction with NADH, indicates the presence of at least two branches of electron transport in the *Z. mobilis* respiratory chain. The effects of the *cydB* mutation clearly demonstrate that cytochrome *bd* is involved in electron transport. Yet, the apparent lack of genes for other terminal oxidases raises the intriguing problem of what could be the nature of the oxidase activity manifested in the Zmb-*cydB* strain. We speculate that the cytochrome *c* peroxidase gene product might have an alternative oxidase activity. Construction and study of a cytochrome *c* peroxidase/*cydB* double knockout strain could help to verify this hypothesis. We were not able to demonstrate any cytochrome *c* peroxidase activity, or any relation of the cytochrome bc_1 branch to the hydrogen peroxide resistance of the *Z. mobilis* cells. However, recently, Charoensuk et al. (2011) reported an electron transport chain-linked peroxidase activity in a thermotolerant *Z. mobilis* strain. We, therefore, conclude that the cytochrome *c* peroxidase activity might largely depend on the strain and culture conditions.

Obviously, catalase in *Z. mobilis* plays a minor role in the scavenging of endogenously generated H_2O_2 and is not critical for aerobic growth. In general, the role of bacterial catalases in endogenous H_2O_2 degradation varies. For example, in *Bradyrhizobium japonicum* catalase is the primary detoxifier of endogenously produced hydrogen peroxide (Panek and O'Brian 2004), and aerobic growth of the catalase-negative strain of this bacterium is severely impaired. In the pathogen *Staphylococcus aureus*, KatA and AhpC are mutually compensatory, and both enzymes are responsible for scavenging of endogenously produced H_2O_2 (Cosgrove et al. 2007). *Z. mobilis* seems to be more like *E. coli* in this respect. In *E. coli*, AhpC (Seaver and Imlay 2001) and possibly Fe-containing alcohol dehydrogenase (AdhE) (Echave et al. 2003) scavenge the majority of endogenous H_2O_2, with a small fraction degraded by catalase. As in *E. coli*, catalase in *Z. mobilis* protects the cells against exogenous hydrogen peroxide. Knowing that *Z. mobilis* is a non-pathogenic bacterium, found in sugar-rich tropical plant saps (Swings and DeLey 1977), it is likely that in the natural environment, its catalase degrades H_2O_2 of plant origin.

Acknowledgments This work was funded by grant 09.1306 of Latvian Council of Science, The Royal Society Travel Grant TG 102318 (for UK), and by Latvian ESF project 2009/0207/1DP/1.1.1.2.0/09/APIA/VIAA/128.

References

Attack JM, Kelly DJ (2006) Structure, mechanism and physiological roles of bacterial cytochrome *c* peroxidases. Adv Microb Physiol 52:73–106

Belaich JP, Senez JC (1965) Influence of aeration and pantothenate on growth yields of *Zymomonas mobilis*. J Bacteriol 89:1195–1200

Bergmeyer HU, Gawehn K, Grassl M (1974) Glutathione reductase. In: Bergmeyer HU (ed) Methods of enzymatic analysis, vol 1. Academic Press, New York, pp 465–466

Bringer S, Finn RK, Sahm H (1984) Effect of oxygen on the metabolism of *Zymomonas mobilis*. Arch Microbiol 139:376–381

Charoensuk K, Irie A, Lertwattanasakul N, Sootsuwan K, Thanonkeo P, Yamada M (2011) Physiological importance of cytochrome *c* peroxidase in ethanologenic thermotolerant *Zymomonas mobilis*. J Mol Microbiol Biotechnol 20:70–82

Cosgrove K, Coutts G, Jonsson I-M, Tarkowski A, Kokai-Kun JF, Mond JJ, Foster SJ (2007) Catalase (KatA) and alkyl hydroperoxide reductase (AhpC) have compensatory roles in peroxide stress resistance and are required for survival, persistance, and nasal colonization in *Staphylococcus aureus*. J Bacteriol 189:1025–1035

Echave P, Tamarit J, Cabiscol E, Ros J (2003) Novel antioxidant role of alcohol dehydrogenase E from *Escherichia coli*. J Biol Chem 278:30193–30198

Ellfolk N, Soininen R (1970) *Pseudomonas* cytochrome *c* peroxidase. Acta Chem Scand 24:2126–2136

Gonzalez-Flecha B, Demple B (1994) Intracellular generation of superoxide as a by-product of *Vibrio harveyi* luciferase expressed in *Escherichia coli*. J Bacteriol 176:2293–2299

Gonzalez-Flecha B, Demple B (1995) Metabolic sources of hydrogen peroxide in aerobically growing *Escherichia coli*. J Biol Chem 270:13681–13687

Goodhew CF, Wilson IBH, Hunter DJB, Pettigrew GW (1990) The cellular location and specificity of bacterial cytochrome *c* peroxidases. Biochem J 271:707–712

Kalnenieks U (2006) Physiology of *Zymomonas mobilis*: some unanswered questions. Adv Microb Physiol 51:73–117

Kalnenieks U, de Graaf AA, Bringer-Meyer S, Sahm H (1993) Oxidative phosphorylation in *Zymomonas mobilis*. Arch Microbiol 160:74–79

Kalnenieks U, Galinina N, Bringer-Meyer S, Poole RK (1998) Membrane D-lactate oxidase in *Zymomonas mobilis*: evidence for a branched respiratory chain. FEMS Microbiol Lett 168:91–97

Kalnenieks U, Galinina N, Toma MM, Poole RK (2000) Cyanide inhibits respiration yet stimulates aerobic growth of *Zymomonas mobilis*. Microbiology 146:1259–1266

Kalnenieks U, Galinina N, Toma MM (2005) Physiological regulation of the properties of alcohol dehydrogenase II (ADH II) of *Zymomonas mobilis*: NADH renders ADH II resistant to cyanide and aeration. Arch Microbiol 183:450–455

Kalnenieks U, Galinina N, Toma MM, Pickford JL, Rutkis R, Poole RK (2006) Respiratory behaviour of a *Zymomonas mobilis adhB knw* mutant supports the hypothesis of two alcohol dehydrogenase isoenzymes catalysing opposite reactions. FEBS Lett 580: 5084–5088

Kalnenieks U, Galinina N, Strazdina I, Kravale Z, Pickford JL, Rutkis R, Poole RK (2008) NADH dehydrogenase deficiency results in low respiration rate and improved aerobic growth of *Zymomonas mobilis*. Microbiology 154:989–994

Kelly MJ, Poole RK, Yates MG, Kennedy C (1990) Cloning and mutagenesis of genes encoding the cytochrome *bd* terminal oxidase complex in *Azotobacter vinelandii*: mutants deficient in the cytochrome *d* complex are unable to fix nitrogen in air. J Bacteriol 172:6010–6019

Korshunov S, Imlay JA (2010) Two sources of endogenous hydrogen peroxide in *Escherichia coli*. Mol Microbiol 75:1389–1401

Kouvelis VN, Saunders E, Brettin TS, Bruce D, Detter C, Han C, Typas MA, Pappas KM (2009) Complete genome sequence of the ethanol producer *Zymomonas mobilis* NCIMB 11163. J Bacteriol 191:7140–7141

Liang C-C, Lee W-C (1998) Characteristics and transformation of *Zymomonas mobilis* with plasmid pKT230 by electroporation. Bioprocess Eng 19:81–85

Markwell MAK, Haas SM, Bieber LL, Talbert NE (1978) A modification of the Lowry procedure to simplify protein determination in membrane and lipoprotein samples. Anal Biochem 87:206–210

Osman YA, Conway T, Bonetti SJ, Ingram LO (1987) Glycolytic flux in *Zymomonas mobilis*: enzyme and metabolite levels during batch fermentation. J Bacteriol 169:3726–3736

Panek HR, O'Brian MR (2004) KatG is the primary detoxifier of hydrogen peroxide produced by aerobic metabolism in *Bradyrhizobium japonicum*. J Bacteriol 186:7874–7880

Poole RK, Cook GM (2000) Redundancy of aerobic respiratory chains in bacteria? Routes, reasons and regulation. Adv Microb Physiol 43:165–224

Reyes L, Scopes RK (1991) Membrane-associated ATPase from *Zymomonas mobilis*: purification and characterization. BBA 1068:174–178

Rogers PL, Lee KJ, Skotnicki ML, Tribe DE (1982) Ethanol production by *Zymomonas mobilis*. Adv Biochem Eng 23:37–84

Rogers PL, Jeon YJ, Lee KJ, Lawford HG (2007) *Zymomonas mobilis* for fuel ethanol and higher value products. Adv Biochem Eng Biotechnol 108:263–288

Sambrook J, Fritsch EF, Maniatis T (1989) Molecular cloning: a laboratory manual. 2nd edn. Cold Spring Harbor Laboratory, Cold Spring Harbor

Schmehl M, Jahn A, Meyer zu Vilsendorf A, Hennecke S, Masepohl B, Schuppler M, Marxer M, Oelze J, Klipp W (1993) Identification of a new class of nitrogen fixation genes in *Rhodobacter capsulatus*: a putative membrane complex involved in electron transport to nitrogenase. Mol Gen Genet 241:602–615

Seaver LC, Imlay JA (2001) Hydrogen peroxide fluxes and compartmentalization inside growing *Escherichia coli*. J Bacteriol 183: 7182–7189

Seo JS, Chong H, Park HS, Yoon KO, Jung C, Kim JJ, Hong JH, Kim H, Kim JH et al (2005) The genome sequence of the ethanologenic bacterium *Zymomonas mobilis* ZM4. Nat Biotechnol 23:63–68

Soemanwan K, Lertwattanasakul N, Thanonkeo P, Matsushita K, Yamada M (2008) Analysis of the respiratory chain in ethanologenic *Zymomonas mobilis* with a cyanide-resistant *bd*-type ubiquinol oxidase as the only terminal oxidase and its possible physiological roles. J Mol Microbiol Biotechnol 14:163–175

Spreinger G (1996) Carbohydrate metabolism in *Zymomonas mobilis*: a catabolic highway with some scenic routes. FEMS Microbiol Lett 145:301–307

Strohdeicher M, Neuß B, Bringer-Meyer S, Sahm H (1990) Electron transport chain of *Zymomonas mobilis*. Interaction with the membrane-bound glucose dehydrogenase and identification of ubiquinone 10. Arch Microbiol 154:536–543

Swings J, DeLey J (1977) The biology of *Zymomonas*. Bacteriol Rev 41:1–46

Trumpower BL, Gennis RB (1994) Energy transduction by cytochrome complexes in mitochondrial and bacterial respiration: the enzymology of coupling electron transfer reactions to transmembrane proton translocation. Annu Rev Biochem 63:675–716

Viikari L (1986) By-product formation in ethanol fermentation by *Zymomonas mobilis*. Technical Research Centre of Finland. Publication 27

Viikari L, Berry DR (1988) Carbohydrate metabolism in *Zymomonas*. Crit Rev Biotechnol 7:237–261

Yang S, Pappas KM, Hauser LJ, Land ML, Chen G-L, Hurst GB, Pan C, Kouvelis VN, Typas MA, Pelletier DA, Klingeman DL, Chang YJ, Samatova NF, Brown SD (2009a) Improved genome annotation for *Zymomonas mobilis*. Nat Biotechnol 27:893–894

Yang S, Tschaplinski TJ, Engle NL, Carroll SL, Martin SL, Davison BH, Palumbo AV, Rodriguez M Jr, Brown SD (2009b) Transcriptomic and metabolomic profiling of *Zymomonas mobilis* during aerobic and anaerobic fermentations. BMC Genomics 10:34

3.3 Application of FT-IR spectroscopy for fingerprinting of Zymomonas mobilis respiratory mutants

Hindawi Publishing Corporation
Spectroscopy: An International Journal
Volume 27 (2012), Issue 5-6, Pages 581–585
doi:10.1155/2012/163712

Application of FT-IR Spectroscopy for Fingerprinting of *Zymomonas mobilis* Respiratory Mutants

M. Grube, R. Rutkis, M. Gavare, Z. Lasa, I. Strazdina, N. Galinina, and U. Kalnenieks

Institute of Microbiology and Biotechnology, University of Latvia, 1010 Riga, Latvia

Correspondence should be addressed to M. Gavare, mareite24@inbox.lv

Abstract. *Z. mobilis* ATCC 29191 and its respiratory knockout mutants, *kat*-, *adh*-, *cydB*-, and *cydB*-, were grown under anaerobic and aerobic conditions. FT-IR spectroscopy was used to study the variations of the cell macromolecular composition. Quantitative analysis showed that the concentration ratios—nucleic acids to lipids, for *Z. mobilis* parent strain, *kat*-, *adh*-, *cydB*-, and *cydB*- strains, clearly distinguished *Z. mobilis* parent strain from its mutant derivatives and corresponded fairly well to the expected degree of biochemical similarity between the strains. Two different FT-IR-spectra hierarchical cluster analysis (HCA) methods were created to differentiate *Z. mobilis* parent strain and respiratory knockout mutant strains. HCA based on discriminative spectra ranges of carbohydrates, nucleic acids, and lipids allowed to evaluate the influence of growth environment (aeration, growth phase) on the macromolecular composition of cells and differentiate the strains. HCA based on IR spectra of inoculums, in a diagnostic region including the characteristic nucleic acid vibration modes, clearly discriminated the strains under study. Thus it was shown that FT-IR spectroscopy can distinguish various alterations of *Z. mobilis* respiratory metabolism by HCA of biomass spectra.

Keywords: FT-IR spectroscopy, *Zymomonas mobilis*, respiratory mutants, HCA, oxidative stress

1. Introduction

Discrimination between different strains of microorganisms can be based on the whole organism biochemical fingerprinting. For that purpose, Fourier-transform infrared (FT-IR) spectroscopy is one of the methods of choice, proven to be efficient for quantitative analysis of the cell macromolecular composition. FT-IR spectroscopy is a time- and chemicals-saving biophysical method that enables characterization, screening, discrimination, and identification of intact microbial cells or cell components. Main advantages of this whole-organism fingerprinting method are small sample amounts, and simple, time-saving sample preparation without chemical pretreatment, allowing to obtain real-time information about the macromolecular composition of cells.

It has been shown that FT-IR spectroscopy has a sufficient resolution power to distinguish between single-gene knockout mutants in yeast [1], *Bacillus subtilis* and its gerD and gerA mutants [2], well-defined discrimination of different phenotypes of *Staphylococcus aureus* in liquid media for diagnostic and research purposes [3]. FT-IR microspectroscopy of leaves was used to develop a rapid

method for screening of mutant plants for a broad range of cell wall phenotypes [4] and to identify different classes of *Arabidopsis* mutants [5]. Lately FT-IR spectroscopy was used to study the bacterium *Enterobacter cloacae* and several of its biofilm mutants [6].

For certain reasons, respiratory mutants of the Gram-negative bacterium *Zymomonas mobilis* might represent special interest for FT-IR analysis and strain fingerprinting. *Zymomonas mobilis* is a facultatively anaerobic, obligately fermentative bacterium with a highly active ethanol fermentation pathway. At the same time, it possesses aerobic respiratory chain, supporting high oxygen uptake rates. Due to still unknown mechanisms, respiration in this bacterium is poorly coupled to ATP synthesis [7]. Recently, we have constructed a type-II NADH dehydrogenase knockout strain (*ndh*-) [8], a knockout of the cytochrome *b* subunit of the bc_1 complex (*cytB*-), a knockout of the subunit II of *bd* terminal oxidase (*cydB*-), and catalase knockout (*kat*-) strain [9]. All these mutant strains are able to grow under aerobic conditions, but have distinct alterations of respiratory metabolism to various degrees. All the mutant strains show clear indications of oxidative stress; relative to the parent type they have 3-4 times upregulated transcription of superoxide dismutase, as measured by quantitative RT-PCR [9]. Apparently, the mechanism of oxidative stress should be different for each strain, as far as the alterations of respiratory metabolism differ. Macromolecular components, analyzed by FT-IR spectroscopy, like cell membrane lipids, proteins, and nucleic acids, are the primary molecular targets of reactive oxygen species during oxidative stress [10]. Hence, our aim was to investigate the macromolecular composition of these respiratory mutants by FT-IR spectroscopy, to see if it is possible to discriminate various alterations of respiratory metabolism by hierarchical cluster analysis of biomass spectra.

2. Materials and Methods

Z. mobilis ATCC 29191, the type-II NADH dehydrogenase knockout strain (*ndh*-) [8], the knockout of the cytochrome *b* subunit of cytochrome bc_1 complex (*cytB*-), the knockout of the subunit II of *bd* terminal oxidase (*cydB*-), and catalase knockout (*kat*-) strain [9] were constructed, by disruption of the respective genes with the chloramphenicol-resistance determinant, using homologous recombination [8, 9]. Inoculum biomass was grown under microaerophilic conditions in liquid medium with glucose for 24 h. The batch cultures were grown under anaerobic and aerobic conditions in plastic 20 mL test-tubes and in 50 mL glass flasks, respectively, and aerobic cultures were stirred at 200 rpm. Growth medium contained 20 g/L glucose, 5 g/L yeast extract and mineral salts, pH 6 and temperature +30°C. Biomass samples were collected at exponential (7 h) and stationary (24 h) growth phases. Cells were washed twice with distilled water and centrifuged. FT-IR analysis was performed using 5–15 μL of washed cell water suspension poured out by drops on a silicon plate and dried at $T < 50$°C. Absorption spectra were recorded on an HTS-XT microplate reader (Bruker, Germany) over the range 4000–400 cm^{-1}, with a resolution of 4 cm^{-1}. Quantitative analysis of carbohydrates, nucleic acids, proteins, and lipids in biomass was carried out as in [11]. Data were processed with OPUS 6.5 software. Hierarchical cluster analysis (HCA) was used to create dendrograms from *Z. mobilis* and its knockout mutant IS absorption spectra using Ward's algorithm.

3. Results and Discussion

FT-IR spectra of *Z. mobilis* ATCC 29191 parent type and its mutant biomass grown under aerobic or anaerobic conditions were analyzed by quantitative analysis and HCA.

Comparison of recorded absorption spectra showed changes of band profiles in spectral regions 1140–1110 and 1665–1645 cm^{-1}, thus indicating differences in the macromolecular composition of parent and mutant cells. Bands at 1183 (P=O; C–O), 1095 (P=O; carbohydrates), 1108, 1515 (protein, NH_3^+ of α-amino groups, tyrosine), 1521 (NH_3^+ of side-chain amino groups), 1660 and 1657 cm^{-1} (Amide I, β-sheet) changing the shape and/or intensities were used for discrimination [12]. The shift between 1515 and 1521 cm^{-1} specifies the changes in cell protein composition depending on the growth conditions—anaerobic/aerobic, exponential/stationary phase.

Quantitative analysis of all samples was done to gain data on the carbohydrate, nucleic acid, protein, and lipid concentrations in biomass (data not shown). Variations of concentrations were not wide (2–8% depending on a component), yet well-expressed analysis of these data showed that the cell macromolecular composition depends on the growth conditions. In all strains lipid concentrations were higher under aerobic growth conditions than anaerobic growth. For example the content of lipids in *Z. mobilis* parent strain cells was 4% dry weight (DW) and 2% DW under aerobic and anaerobic growth conditions correspondingly. It is known that the increase of lipid content is one of cells responses to stress. The content of total carbohydrates was higher in mutant strain cells and was influenced by growth conditions (+/− oxygen, 7 or 24 h). For example, the carbohydrate concentration in *cydB*- mutant at exponential phase (after 7 h) under aerobic environment was 21% DW but under anaerobic conditions 17% DW. Data analysis of quantitative results showed that discrimination of parent and mutant strains can be based on nucleic acid and lipid concentrations in inoculum's cells. As the concentrations of nucleic acids and lipids in parent and mutant inoculums biomasses were in various proportions, their ratio was used for the strain differentiation. Nucleic acid to lipid concentration ratios for *Z. mobilis* parent strain, *kat*-, *ndh*-, *cytB*-, and *cydB*- strains were 6.95, 4.42, 5.33, 5.16, and 5.13 (±0.3) correspondingly. Notably, the values of this ratio clearly distinguished *Z. mobilis* parent strain from its mutant derivatives and corresponded fairly well to the expected degree of biochemical similarity between the strains. Thus, the catalase knockout strain differed from all the respiratory chain mutants. There was more similarity found between *cytB*- and *cydB*- strains, each with partially disrupted electron transport, than between either of them and *ndh*-, having near-zero respiration rate.

Next step was to create HCA method for differentiation of *Z. mobilis* parent and knockout mutant strains. It was established that vector normalized, 2nd-derivative spectra in three spectral ranges 1185–950, 1483–1360, and 3022–2832 cm^{-1}, were functional for HCA of all samples at various growth conditions and phases. This dendrogram clearly showed two distinct clusters of aerobically and anaerobically grown strains. All inoculum samples of parent and knockout mutant strains were clearly discriminated and formed one subcluster. These results showed that the biochemical composition of cells is influenced and can be changed by choosing appropriate fermentation conditions.

Since the dendrogram of the above mentioned HCA and quantitative analysis data discriminated *Z. mobilis* parent and knockout mutant strains even using the spectra of inoculums, another HCA method was created. The second derivative inoculums spectra were analyzed in several regions: 1665–1645, 1544–1510, 1301–1086, 1220–1174, and 1120–1086 cm^{-1} to choose the diagnostic peaks or regions for HCA. As characteristic were chosen two regions: 1120–1086 and 1301–1086 cm^{-1}, and as diagnostic region was selected 1301–1086 cm^{-1} including the characteristic nucleic acid vibration modes. HCA dendrogram (Figure 1) clearly shows discrimination between *Z. mobilis* parent and knockout mutant strains, difference between *kat*- and respiratory mutants, differences between respiratory mutants and the similarity of *cydB*- and *cytB*- mutants.

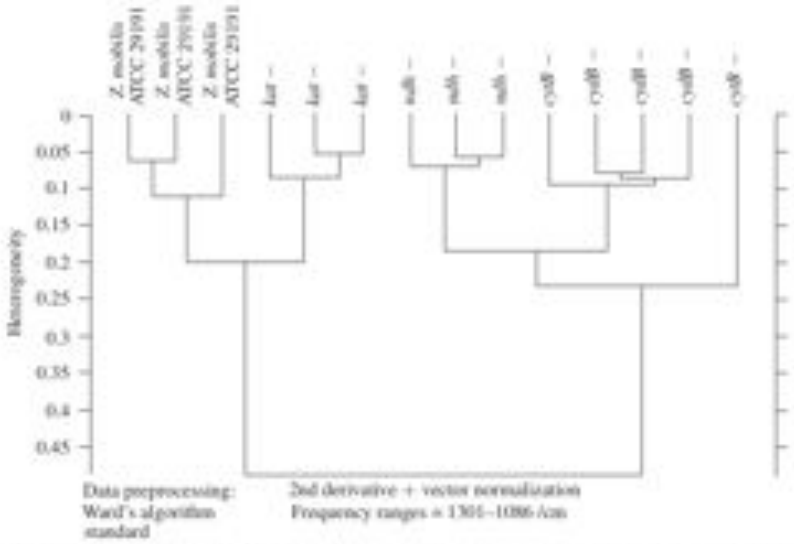

Figure 1: HCA of *Z. mobilis* ATCC 29191 and its knockout mutant inoculums spectra of 3 folds experiment (Ward's algorithm, Vector normalization, 2nd derivative, region 1301–1086 cm^{-1}).

These results are in agreement with quantitative analysis data and estimated from the mutant construction.

4. Conclusions

FT-IR quantitative analysis showed variations of the cell macromolecular composition depending on the strain peculiarities and growth conditions. Discrimination of *Z. mobilis* ATCC 29191 parent strain and its knockout mutant strains can be based on the ratio of nucleic acid to lipid concentrations. HCA showed to be effective for *Z. mobilis* ATCC 29191 parent strain and respiratory knockout mutant strain discrimination on the basis of inoculum IR-spectra and indicated the influence of growth environment (aeration, growth phase) on the macromolecular composition of cells.

Acknowledgment

This work was supported by the Project Nr. 2009/0207/1DP/1.1.1.2.0/09/APIA/VIAA/128 Establishment of Latvian Interdisciplinary Interuniversity Scientific Geoup of Systems Biology, http://www.sysbio.lv.

References

[1] S. G. Oliver, M. K. Winson, D. B. Kell, and F. Baganz, "Systematic functional analysis of the yeast genome," *Trends in Biotechnology*, vol. 16, no. 9, pp. 373–378, 1998.

[2] H. Y. Cheung, J. Cui, and S. Q. Sun, "Real-time monitoring of Bacillus subtilis endospore components by attenuated total reflection Fourier-transform infrared spectroscopy during germination," *Microbiology*, vol. 145, no. 5, pp. 1043–1048, 1999.

[3] K. Becker, N. Al Laham, W. Fegeler, R. A. Proctor, G. Peters, and C. Von Eiff, "Fourier-transform infrared spectroscopic analysis is a powerful tool for studying the dynamic changes in staphylococcus aureus small-colony variants," *Journal of Clinical Microbiology*, vol. 44, no. 9, pp. 3274–3278, 2006.

[4] L. Chen, N. C. Carpita, W. D. Reiter, R. H. Wilson, C. Jeffries, and M. C. McCann, "A rapid method to screen for cell-wall mutants using discriminant analysis of Fourier transform infrared spectra," *Plant Journal*, vol. 16, no. 3, pp. 385–392, 1998.

[5] G. Mouille, S. Robin, M. Lecomte, S. Pagant, and H. Höfte, "Classification and identification of Arabidopsis cell wall mutants using Fourier-Transform InfraRed (FT-IR) microspectroscopy," *Plant Journal*, vol. 35, no. 3, pp. 393–404, 2003.

[6] R. J. Delle-Bovi, A. Smits, and H. M. Pylypiw, "Rapid method for the determination of total monosaccharide in enterobacter cloacae strains using Fourier transform infrared spectroscopy," *American Journal of Analytical Chemistry*, vol. 2, pp. 212–216, 2011.

[7] U. Kalnenieks, "Physiology of *Zymomonas mobilis*: some unanswered questions," *Advances in Microbial Physiology*, vol. 51, pp. 73–117, 2006.

[8] U. Kalnenieks, N. Galinina, I. Strazdina et al., "NADH dehydrogenase deficiency results in low respiration rate and improved aerobic growth of *Zymomonas mobilis*," *Microbiology*, vol. 154, no. 3, pp. 989–994, 2008.

[9] I. Strazdina, Z. Kravale, N. Galinina, R. Rutkis, R.K. Poole, and U. Kalnenieks, "Electron transport and oxidative stress in *Zymomonas mobilis* respiratory mutants," *Archives of Microbiology*. In press.

[10] S. V. Avery, "Molecular targets of oxidative stress," *Biochemical Journal*, vol. 434, no. 2, pp. 201–210, 2011.

[11] M. Grube, M. Bekers, D. Upite, and E. Kaminska, "IR-spectroscopic studies of *Zymomonas mobilis* and levan precipitate," *Vibrational Spectroscopy*, vol. 28, no. 2, pp. 277–285, 2002.

[12] D. Naumann, "Infrared spectroscopy in microbiology," in *Encyclopedia of Analytical Chemistry*, R. A. Meyers, Ed., pp. 102–131, John Wiley & Sons, Chichester, UK, 2000.

3.4 The inefficient aerobic energetics of Zymomonas mobilis: identifying the bottleneck

Journal of Basic Microbiology
Environment · Health · Techniques

Research Paper

The inefficient aerobic energetics of *Zymomonas mobilis*: Identifying the bottleneck

Reinis Rutkis, N. Galinina, I. Strazdina and U. Kalnenieks

Institute of Microbiology and Biotechnology, University of Latvia, Riga, Latvia

To investigate the mechanisms of *Zymomonas mobilis* uncoupled aerobic metabolism, growth properties of the wild-type strain Zm6 were compared to those of its respiratory mutants *cyt8* and *cyd8*, and the effects of the ATPase inhibitor DCCD on growth and intracellular ATP concentration were studied. The effects of the ATPase inhibitor DCCD on growth and intracellular ATP concentration strongly indicated that the apparent lack of oxidative phosphorylation in aerobically growing *Z. mobilis* culture might be caused by the ATP hydrolyzing activity of the H^+-dependent ATPase in all analyzed strains. Aerobic growth yields of the mutants, and their capacity of oxidative ATP synthesis with ethanol were closely similar, not supporting presence of one major, yet energetically inefficient electron transport branch causing the observed poor aerobic growth and lack of oxidative phosphorylation in *Z. mobilis*. We suggest that rapidly operating Entner–Doudoroff pathway generates too high phosphorylation potential for the weakly coupled respiratory system to shift the H^+-dependent ATPase toward ATP synthesis.

Abbreviations: DCCD – dicyclohexylcarbodiimide; **Δp** – proton-motive force; **E–D pathway** – Entner–Doudoroff pathway

Keywords: H^+-dependent ATPase / Oxidative phosphorylation / Respiratory mutants / *Zymomonas mobilis*

Received: October 28, 2013; accepted: February 7, 2014

DOI 10.1002/jobm.201300859

Introduction

Zymomonas mobilis is a facultatively anaerobic, ethanol-producing bacterium that possesses a constitutive aerobic respiratory chain and H^+-dependent F_1F_o-type ATPase [1–6]. However, the respiratory system does not appear to participate in ATP synthesis, since aerobic biomass yields do not exceed the anaerobic values, which are around 8–10 g dry wt. $(mol\ glucose)^{-1}$ for batch cultures [7–9]. Earlier reports suggesting that aerobic metabolism is inhibitory due to the accumulation of acetaldehyde [8, 10, 11] do not explain the low yield, since elimination of acetaldehyde by air sparging during aerobic batch cultivation increases *Z. mobilis* aerobic growth yields to the same level with those observed anaerobically [12]. At the same time, oxidative phosphorylation activity was demonstrated in non-growing cells with ethanol, and in membrane preparations with NADH [13]. These findings suggested the need to look deeper for other mechanisms that possibly can explain *Z. mobilis* poor aerobic metabolism.

Biomass synthesis is by far not the main consumer of ATP produced in the Entner–Doudoroff pathway, since *Z. mobilis* produces little cell mass, grows with a low energetic efficiency, and represents a typical example of "uncoupled growth" [7, 14]. The relatively low growth yield values together with the high glucose uptake rate, reaching 4.0–5.6 g glucose h^{-1} $(g\ dry\ wt.)^{-1}$, raise the question of the reactions dissipating the excess ATP produced in glycolysis [11, 14–16]. Apparently, the rate of the excess ATP hydrolysis must be equal to the difference between ATP production by catabolic reactions and its utilization by anabolic processes. *Z. mobilis* possess several ATP-hydrolyzing enzymes: periplasmic nucleotidase(s), acid and alkaline phosphatases, and the membrane H^+-dependent ATPase [2]. However, nothing is known about the possible involvement of membrane transport in putative ATP hydrolyzing futile

Correspondence: Dr. Reinis Rutkis, Institute of Microbiology and Biotechnology, University of Latvia, Kronvalda Boulv. 4, 1586 Riga, Latvia
E-mail: reinis.rutkis@gmail.com
Phone: +371 29129436
Fax: +371 67034885

cycles in this bacterium. The H^+-dependent ATPase contributes up to the 20% of the overall ATP turnover in *Z. mobilis* cells and has been considered as partly responsible for the "uncoupled growth" [2]. The previously reported increase of *Z. mobilis* anaerobic growth yield in the presence of the H^+-dependent inhibitor DCCD [17], indicates that H^+-dependent ATPase hydrolyzing activity indeed competes with the biosynthetic ATP demand in anaerobically growing culture.

While in the anaerobic conditions, largely due to necessity to maintain proton-motive force (Δp), ATP hydrolysis predominantly may be attributed to the H^+-dependent ATPase, the ATP turnover under aerobic conditions seems more obscure. Typically, growth of a facultatively aerobic microorganism is stimulated by additional ATP generated in the oxidative phosphorylation. Hence, a plausible reason for the low aerobic growth yield of *Z. mobilis* may be related to an impaired aerobic ATP turnover: either the H^+-dependent ATPase for some reasons is unable to turn to ATP synthesis, or the newly synthesized ATP gets rapidly hydrolyzed by other reactions. Thus, the capacity of the respiratory system of *Z. mobilis* to generate high enough Δp for aerobic ATP synthesis is an open question. Recently, using aerobically cultivated cytochrome bc_1 and cytochrome bd knock-out mutants (Zm6-cytB and Zm6-cydB), it has been shown that electron transport chain in *Z. mobilis* contains at least two electron pathways to oxygen [18]. Yet, the terminal oxidase for the cytochrome bc_1 containing branch has not been identified, and the relative energetic efficiency of these branches has not been studied. It is worth to mention that difficulty to reach sufficiently high Δp might be enhanced by the earlier reported high proton leakage of *Z. mobilis* energy-coupling membrane at elevated ethanol concentrations or by other Δp dissipating mechanisms [19, 20]. Once the critical level of the non-specific dissipation of Δp is reached, it naturally leads to ATP hydrolysis because of the Δp-compensatory role of the H^+-dependent ATPase. Yet, it is possible that the respiratory chain in *Z. mobilis* can generate sufficient Δp, and oxidative phosphorylation actually takes place, but the ATP is dissipated by other mechanisms, not involving H^+-dependent ATPase directly. In the present paper, we used respiratory knock-out mutants and the H^+-dependent ATPase inhibitor DCCD to discriminate between these possibilities.

Materials and methods

Chemicals

Dicyclohexylcarbodiimide (DCCD), ATP, and ADP were purchased from Sigma–Aldrich (Deisenhofen, Germany). The ATP bioluminescence assay kit, was supplied by Roche Diagnostics GmbH (Germany).

Bacterial strains and cultivation

Bacterial strains used in the present study and their genotypes are listed in Table 1. The bacteria were grown at 30 °C in the standard culture medium containg (per 1liter): 5 g yeast extract, 50 g glucose, 1 g KH_2PO_4, 1 g $(NH_4)_2SO_4$, 0.5 g $MgSO_4 \cdot 7H_2O$. All *Z. mobilis* cultures were grown in 200 ml flasks (50 ml culture volume) shaken at 150 r.p.m., at 30 °C with atmospheric sparging of air. Within the series of aerobic batch cultivations of wild-type strain Zm6 and *Z. mobilis* respiratory mutants, DCCD was added at 50, 100, and 200 μM concentrations directly before the exponential growth phase.

Escherichia coli JM109 was routinely grown on LB medium supplemented with 35 g glucose per liter, in 200 ml flasks (50 ml culture volume) shaken at 150 r.p.m., at 37 °C.

Preparation of non-growing cell suspensions and membrane vesicles

For the preparation of non-growing cell suspension, cells were harvested at late exponential phase, sedimented, washed, and resuspended in 100 mM potassium phosphate buffer (pH 6.9), containing 2 mM magnesium sulfate, to a biomass concentration of 6.8–7.0 g (dry wt.) L^{-1}.

For the preparation of cell-free extracts, cells were sedimented from 200 ml suspension (OD 9.0 at 550 nm) by centrifugation at 5000 rpm (3000*g*) for 15 min, washed, and resuspended in 100 mM potassium phosphate buffer, containing 2 mM magnesium sulfate, pH

Table 1. Bacterial strains used in this study.

Strain	Characteristics	Source
Zm6	Parent strain	ATCC 29191
Zm6-cytB	Zm6 strain with chloramphenicol resistance determinant inserted in the ORF of the cytochrome b subunit gene (ZMO 0957) of the bc_1 complex	Strazdina *et al.* [18]
Zm6-cydB	Zm6 strain with chloramphenicol resistance determinant inserted in the ORF of subunit II (cydB) gene (ZMO 0957) of the cytochrome bd terminal oxidase	Strazdina *et al.* [18]
E. coli JM-109		ATCC 53323 "Promega"

6.9, to about 6.8–7.0 mg (dry wt.) ml^{-1}. Cell walls were broken by vortexing the above suspension in the disintegrator at 3000 rpm (1400*g*) for 2.5 min, using 106 μm diameter glass beads. Typically, cell free extracts of 4.6–4.9 mg protein per milliliter were obtained. Subsequent removal of unbroken cells and separation of cytoplasmic membranes by ultracentrifugation were performed as before [3, 13].

Artificial induction of transmembrane pH gradients

Artificial transmembrane pH gradients of 3.5–4.0 pH units were induced by the addition of 50 μl of 0.1 M HCl to 10 ml of 3.8–4.0 mg (dry wt.) ml^{-1} starved cell suspension incubated in 10 mM phosphate buffer at pH 6.8.

Analytical methods

Growth yields (*Y*), specific growth rate (μ), specific glucose uptake rate (*q*), and intracellular ATP concentration in all strains were calculated from the data of exponential growth phase. Cell concentration was determined as OD550, and dry cell mass of the suspensions was calculated by reference to a calibration curve. Glucose concentration was measured by HPLC (Agilent 1100 series), using a Biorad Aminex HPX-87H column. Samples for ATP determination were quenched in ice-cold 10% trichloroacetic acid and assayed by the standard luciferin-luciferase method using LKB Wallac 1251 Luminometer [21]. Concentration of dissolved oxygen was monitored by a Radiometer Clark-type oxygen electrode in a thermostatted electrode cell (30 °C). Protein concentration in cell-free extracts and membrane samples was determined according to Markwell *et al.* [22]. All results are means of at least three replicates.

Results

Effects of DCCD on the batch growth and glycolysis under aerobic conditions

To analyze the contribution of H^+-dependent ATPase to aerobic growth of *Z. mobilis* wild-type and respiratory mutant strains, we studied effects of DCCD on the key aerobic batch growth parameters. Series of aerobic batch cultivations of wild-type strain Zm6 and respiratory mutants revealed positive correlation between the growth yield and the added DCCD concentration (Table 2). Presence of DCCD in the growth medium had negligible effect on the intracellular ATP concentration and the specific growth rate μ, yet greatly provoked decrease of the specific glucose uptake rate (*q*). For the wild-type strain, negative correlation between the specific glucose uptake rate and the added DCCD concentration was apparent. In both respiratory mutant cultures, specific glucose consumption rate showed higher sensitivity to 50 μM than 100 μl DCCD concentration, yet, the overall effect of DCCD was similar to that in Zm6. Although at present it is difficult to explain these strain-specific differences, in general increase of DCCD concentration in the media had a pronounced negative effect on *q* in all strains.

Use of DCCD for establishing the direction of the H^+-dependent ATPase reaction

To establish the direction of the H^+-dependent ATPase reaction, we monitored the change of intracellular ATP level immediately after addition of DCCD. The time course of the intracellular ATP concentration after the addition of 50 μM DCCD revealed that all *Z. mobilis* strains responded similarly to DCCD (Fig. 1). Its addition caused a

Table 2. Aerobic growth parameters of *Z. mobilis* wild-type strain Zm6 and respiratory mutants Zm6-cytB and Zm6-cydB, in the presence of various DCCD concentrations growth yield *Y* (g dry wt. mol^{-1}), specific glucose uptake rate *q* (g g^{-1} h^{-1}), specific growth rate μ (h^{-1}), and average intracellular ATP (mM) levels are presented for exponential growth phase.

		DCCD concentration (μM)			
Strain	Parameter	–	50	100	200
Zm6	Y	15.01 ± 0.2	20.58 ± 1.93	22.16 ± 5.06	25.52 ± 7.23
	q	4.36 ± 0.6	3.23 ± 0.56	3.09 ± 0.87	2.80 ± 1.05
	μ	0.37 ± 0.01	0.36 ± 0.04	0.37 ± 0.02	0.38 ± 0.10
	ATP	1.21 ± 0.04	1.8 ± 0.13	1.59 ± 0.15	1.65 ± 0.16
Zm6-cytB	Y	13.01 ± 1.7	18.24 ± 4.20	18.13 ± 7.7	19.27 ± 3.52
	q	4.97 ± 0.2	3.47 ± 0.65	3.84 ± 1.6	3.24 ± 0.32
	μ	0.36 ± 0.03	0.34 ± 0.02	0.35 ± 0.01	0.31 ± 0.02
	ATP	1.33 ± 0.12	1.76 ± 0.09	1.30 ± 0.16	1.50 ± 0.14
Zm6-cydB	Y	13.55 ± 0.4	18.98 ± 0.57	18.09 ± 2.7	19.81 ± 1.3
	q	4.12 ± 0.6	2.82 ± 0.57	3.22 ± 0.8	2.39 ± 0.1
	μ	0.31 ± 0.04	0.27 ± 0.03	0.32 ± 0.03	0.26 ± 0.02
	ATP	1.07 ± 0.09	1.42 ± 0.06	1.20 ± 0.18	0.950 ± 0.07

Results are means of three replicates.

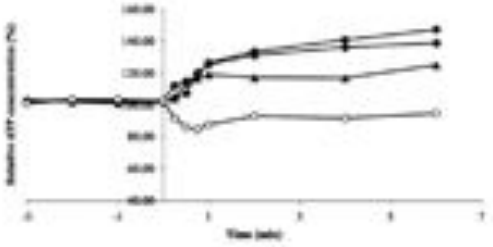

Figure 1. Effect of 50 μM DCCD on the relative intracellular ATP levels of *Z. mobilis* wild-type strain Zm6, respiratory mutants Zm6-cyt8, Zm6-cyd8, and *E. coli* JM109. DCCD was added at zero time (zero time refers to the moment of DCCD addition). Results are means of three replicates. Symbols: ● Zm6-cyt8, ▲ Zm6-cyd8, ◆ Zm6, and ○ *E. coli* JM109.

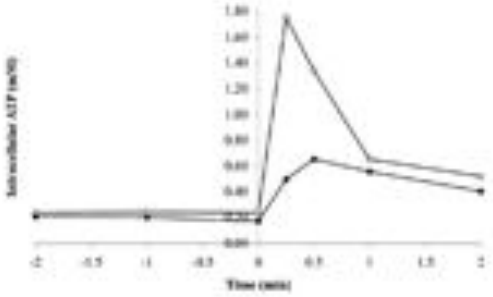

Figure 2. Effect of 50 μM DCCD on the intracellular ATP levels after acidification of the external medium. DCCD was added 5 min before acid pulses. Results are means of three independent experiments. Symbols: ◇ Zm6 and ◆ Zm6 + 0.05 mM DCCD.

pronounced increase of the ATP intracellular concentration. These results indicated that the hydrolyzing activity of the H^+-dependent ATPase is taking place in *Z. mobilis* also under aerobic conditions. This finding was directly opposite to what we obtained with *E. coli*. DCCD addition to aerobically growing *E. coli* culture, caused a decrease of ATP intracellular concentration (Fig. 1) in complete agreement with the expected operation of its ATPase in the direction of ATP synthesis.

To make sure that DCCD indeed inhibits *Z. mobilis* H^+-dependent ATPase, we carried out a series of experiments, where we monitored intracellular ATP levels after acidification of the external medium with and without addition of DCCD to starved cells. Transient increase of the intracellular ATP levels after acid pulses directly showed the ability of H^+-dependent ATPase to carry out ATP synthesis in the wild-type strain (Fig. 2), as well as in the respiratory mutants (data not shown), which is consistent with earlier reports [13]. DCCD addition at 50 μM concentration caused a significant decrease of ATP synthesis, in response to acid pulse (Fig. 2).

To confirm that the observed increase of the ATP concentration in *Z. mobilis* strains was not caused by yet unknown non-specific DCCD interaction with respiratory chain of this bacterium we performed experiments in membrane vesicles by monitoring oxygen consumption rate with 0.1 mM NADH in the presence of various DCCD concentrations. The results clearly indicated that sub-millimolar concentrations of DCCD did not stimulate respiration, but instead, inhibited it. Even the lowest concentration, 50 μM DCCD, caused an 4% decay of oxygen consumption rate, and more pronounced effects were observed after addition of 100 and 200 μM DCCD (Fig. 3).

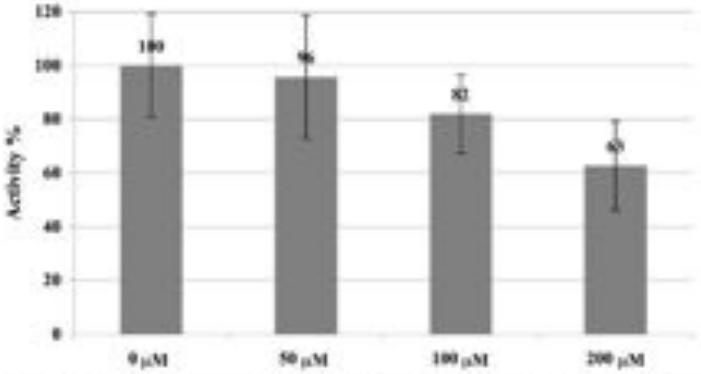

Figure 3. Relative effect of DCCD addition on the wild-type Zm6 membrane vesicle respiration rate. DCCD was added 5 min before experiments. Average values of three independent experiments are presented for control and each DCCD concentration.

ATP synthesis in *Z. mobilis* wild type and respiratory mutants

Since cultivation results (Table 2) indicated that none of the *Z. mobilis* respiratory branches, when operating as the sole electron transport route under fermenting conditions (Fig. 5), gave rise to any increase of the aerobic growth yield, we compared the ability of all strains to carry out oxidative phosphorylation under non-fermenting conditions by ethanol addition to non-growing cell suspensions. The time course of ATP intracellular concentration immediately after addition of 2% (v/v) ethanol showed closely similar ATP synthesis in all strains, within the range of measurement error (Fig. 4). Thus, the ability of both *Z. mobilis* respiratory branches to carry out oxidative phosphorylation under non-fermenting conditions proved to be comparable.

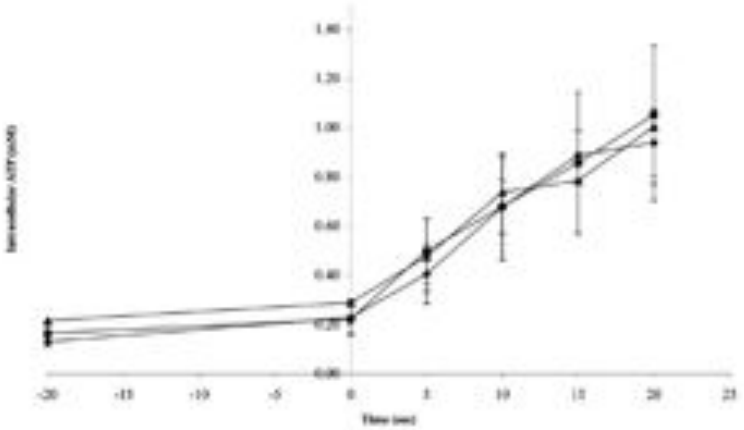

Figure 4. ATP levels of *Z. mobilis* wild-type strain Zm6, respiratory mutants Zm6-cydB, and Zm6-cydB after addition of 2% (v/v) ethanol at zero time (zero time refers to the moment of ethanol addition). Symbols: ◆ Zm6, ● Zm6-cydB, and ▲ Zm6-cydB.

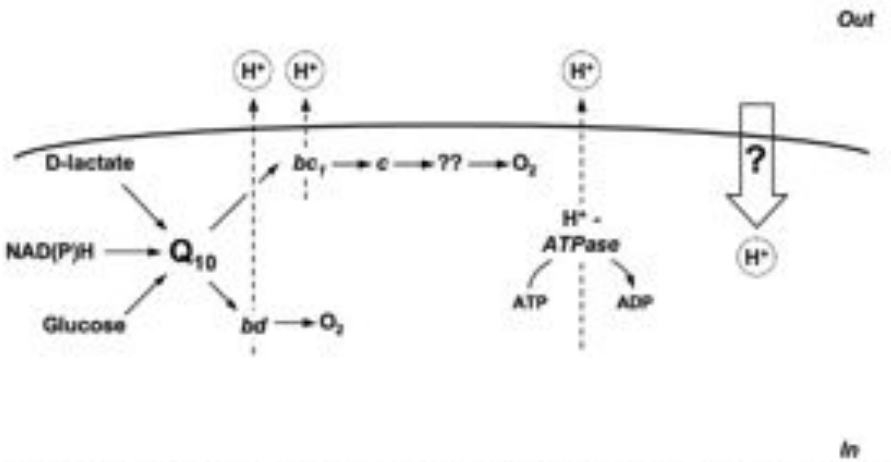

Figure 5. Electron transport chain and H^+-dependent ATPase of *Z. mobilis*. Energy-coupling sites are shown with dashed arrows. Hypothetical transmembrane flux, causing dissipation of the proton-motive force, shown with solid arrow.

Discussion

The energetically inefficient aerobic metabolism of *Z. mobilis* is quite unique, being one of the least well understood among facultatively anaerobic microorganisms. All evidence accumulated for bacteria so far, indicated that respiration should give considerable increase of aerobic growth, as, for example, shown for lactic acid bacteria with electron transport components similar to those of *Z. mobilis* [23]. The results of the present study confirm that *Z. mobilis* respiratory system does not facilitate the aerobic growth, and thus, does not appear to participate in ATP synthesis under fermenting conditions. This untypical physiology for facultatively anaerobic microbe might be either related to the properties of *Z. mobilis* H^+-dependent ATPase, or energetic (in)efficiency of its electron transport chain. The reported increase of the intracellular ATP level after ethanol addition to starved cells under aerobic conditions, as well as the induced ATP synthesis by acidification of the external medium in this study, proved the ability of H^+-dependent ATPase to carry out ATP synthesis under non-fermenting conditions. Also, *Z. mobilis* genome contains necessary genes to encode all catalytic and H^+-translocating subunits of typical F_0F_1-type H^+-dependent ATPase [24]. Their protein sequence alignment with obligatory aerobic bacterium *Gluconobacter oxydans* H24 [25] possessing oxidative phosphorylation [26] revealed significant genetic similarity (Supplementary Table S1). Taken together, in complete agreement with previous reports [13, 27], our results confirm that *Z. mobilis* H^+-dependent ATPase appears to be a quite ordinary bacterial H^+-dependent ATPase, capable of reversible transformation of energy. Therefore, not the H^+-dependent ATPase by itself, but rather the *Z. mobilis* respiratory system as a whole might be responsible for the lack of oxidative phosphorylation under fermenting conditions.

Although our earlier reports showed comparable oxygen consumption rate of the *Z. mobilis* wild-type and respiratory mutants *cyt*B, *cyd*B [18], one of these electron transport pathway branches might be poorly coupled to proton translocation, thus resulting in a lower ATP outcome and decrease of the aerobic growth yields. However, the obtained results in this study clearly indicated that none of *Z. mobilis* respiratory branches, when operating as the sole electron transport route, gave rise to any deviation from the aerobic growth yield of the wild-type strain. Apparently inactivation of cytochrome *bd* or cytochrome bc_1 complex in the alternative branches of *Z. mobilis* respiratory chain did not affect aerobical growth properties, suggesting that both pathways might also be comparable in terms of the proton translocation and generation of the proton-motive force (Δp).

Due to the low permeability of *Z. mobilis* outer membrane for the probes of transmembrane electric potential ($\Delta\Psi$) direct quantitative study of the Δp has proven to be complicated [17, 28]. By monitoring the time-course of intracellular ATP shortly after DCCD addition, we were able to judge if the level of generated Δp had been sufficient to turn H^+-dependent ATPase toward oxidative phosphorylation prior to its inhibition. DCCD, binds covalently to a DCCD-sensitive carboxyl group of a c-subunit in F_0 complex, and thereby inhibits the activity of H^+-dependent ATPase [29]. Increase of the intracellular ATP levels in response to DCCD in *Z. mobilis* under aerobic conditions indicated, that the H^+-dependent ATPase had functioned in the direction of hydrolysis and hence, that generated Δp might not be sufficient for ATP synthesis. Notably, instead of non-specific stimulation, DCCD caused a partial inhibition of glucose consumption and, much like for mitochondria of yeasts [30], also inhibited membrane vesicle respiration. These findings confirm that DCCD interaction with the H^+-dependent ATPase is the only feasible explanation for the observed rise of intracellular ATP concentration in response to its addition during the aerobic growth. We therefore conclude that the hydrolyzing activity of the H^+-dependent ATPase is taking place in *Z. mobilis* also under aerobic growth conditions.

This novel finding, so far not reported for *Z. mobilis*, elucidates why DCCD addition caused significant increase of the aerobic growth yields observed within this study. Apparently in *Z. mobilis*, the H^+-dependent ATPase competes for ATP with biosynthesis both under anaerobic and aerobic conditions. This is very much different from what has been reported for other facultatively anaerobic bacteria. For example, even 10–100 μM DCCD concentrations are inhibitory to the aerobic growth of *E. coli* [31]. At the same time, under anaerobic conditions similar ATP spilling mechanism was suggested earlier also for obligately fermentative *Streptococcus bovis* – another example of the "uncoupled growth" among bacteria [32]. It has been shown that in *S. bovis*, H^+-dependent ATPase is the major free energy-spilling reaction under conditions of excess glucose [33].

Futhermore, in a good agreement with previous reports [34], the observed decrease of glycolytic flux in the presence of DCCD accompanying the slight increase of the intracellular ATP concentration, indicated that ATP consuming reactions might exert significant control over the flux in E–D pathway. That is in a good agreement with our recently published studies of the E–D pathway kinetics, showing that ATP-consuming reactions largely

control the glucose consumption rate when it attains its maximum, with flux control coefficients C_i^J reaching 71% [35]. Therefore, H^+-dependent ATPase, in combination with biosynthetic reactions, controls the glucose consumption rate also during the aerobic growth of *Z. mobilis*. By rapidly supplying ADP for glycolysis, H^+-dependent ATPase contributes to the high glycolytic flux observed in the E–D pathway that at the same time generates too high phosphorylation potential for the weakly coupled respiratory system, to shift the H^+-dependent ATPase toward ATP synthesis. Therefore, we can state that "uncoupled growth" is not just an intrinsic property of anaerobically cultivated *Z. mobilis*, but can also be used to describe the inefficient aerobic growth of this very untypical facultatiwly anaerobic microoeganism.

A scheme of the putative *Z. mobilis* respiratory chain and its relation to H^+-dependent ATPase is presented in Fig. 5. Hydrolyzing activity of the H^+-dependent ATPase should inevitably lead to an increase of Δp, which raises the question of its dissipation mechanisms. Despite the fact that it is not possible at present to point out the specific reaction or mechanism responsible for dissipation, the leakage of cytoplasmic membrane most likely would not be sufficient for futile spilling of the generated transmembrane Δp. Most probably, an active pathway for Δp dissipation should be involved to support continuous ATP hydrolysis by H^+-dependent ATPase. However, such a pathway so far remains undiscovered.

Acknowledgments

This work was funded by Grant 09.1306 of Latvian Council of Science and by Latvian ESF project 2009/0138/1DP/1.1.2.1.2/09/IPIA/VIAA/004.

References

[1] Strohdeicher, M., Neuß, B., Bringer-Meyer, S., Sahm, H., 1990. Electron transport chain of *Zymomonas mobilis*. Interaction with the membrane-bound glucose dehydrogenase and identification of ubiquinone 10. *Arch. Microbiol.*, **154**, 536–543.

[2] Reyes, L., Scopes, R.K., 1991. ATPase from *Zymomonas mobilis*: purification and characterization. *Biochim. Biophys. Acta*, **1068**, 174–178.

[3] Kalnenieks, U., Galinina, N., Bringer-Meyer, S, Poole, R.K., 1998. Membrane D-lactate oxidase in *Zymomonas mobilis*: evidence for a branched respiratory chain. *FEMS Microbiol. Lett.*, **168**, 91–97.

[4] Sootsuwan, K., Lertwattanasakul, N., Thanonkeo, P., Matsushita, K. et al., 2008. Analysis of the respiratory chain in ethanologenic *Zymomonas mobilis* with a cyanide-resistant bd-type ubiquinol oxidase as the only terminal oxidase and its possible physiological roles. *J. Mol. Microbiol. Biotechnol.*, **14**(4), 163–175.

[5] Charoensuk, K., Irie, A., Lertwattanasakul, N., Sootsuwan, K. et al., 2011. Physiological importance of cytochrome *c* peroxidase in ethanologenic thermotolerant *Zymomonas mobilis*. *J. Mol. Microbiol. Biotechnol.*, **20**(2), 70–82.

[6] Hayashi, T., Kato, T., Furukawa, K., 2012. Respiratory chain analysis of *Zymomonas mobilis* mutants producing high levels of ethanol. *Appl. Environ. Microbiol.*, **78**(16), 5622–5629.

[7] Belaich, J.P., Senez, J.C., 1965. Influence of aeration and pantothenate on growth yields of *Zymomonas mobilis*. *J. Bacteriol.*, **89**, 1195–1200.

[8] Bringer, S., Finn, R.K., Sahm, H., 1984. Effect of oxygen on the metabolism of *Zymomonas mobilis*. *Arch. Microbiol.*, **139**, 376–381.

[9] Hayashi, T., Furutta, Y., Furukawa, K., 2011. Respiration-deficient mutants of *Zymomonas mobilis* show improved growth and ethanol fermentation under aerobic and high temperature conditions. *J. Biosci. Bioeng.*, **111**, 414–419.

[10] Viikari, L., 1986. By-product formation in ethanol fermentation by *Zymomonas mobilis*. Technical Research Centre of Finland. Publication 27.

[11] Viikari, L., 1988. Carbohydrate metabolism in *Zymomonas*. *CRC Crit. Rev. Biotechnol.*, **7**, 237–261.

[12] Kalnenieks, U., Galinina, N., Strazdina, I., Kravale, Z. et al., 2008. NADH dehydrogenase deficiency results in low respiration rate and improved aerobic growth of *Zymomonas mobilis*. *Microbiology*, **154**, 989–994.

[13] Kalnenieks, U., De Graaf, A.A., Bringer-Meyer, S., Sahm., H., 1993. Oxidative phosphorylation in *Zymomonas mobilis*. *Arch. Microbiol.*, **160**, 74–79.

[14] Rogers, P.L., Lee, K.J., Skotnicki, M.L., Tribe, D.E., 1982. Ethanol Production by *Zymomonas mobilis*. *Adv. Biochem. Eng.*, **23**, 37–84.

[15] Jones, C.W., Doelle, H.W., 1991. Kinetic control of ethanol production by *Zymomonas mobilis*. *Appl. Microbiol. Biotechnol.*, **35**, 4–9.

[16] Arfman, N., Worrell, V., Ingram, L.O., 1992. Use of the tac promoter and lacIq for the controlled expression of *Zymomonas mobilis* fermentative genes in *Escherichia coli* and *Zymomonas mobilis*. *J. Bacteriol.*, **174**, 7370–7378.

[17] Kalnenieks, U., Pankova, L.M., Slovinka J.E., 1987. Proton motive force in *Zymomonas mobilis*. *Biokhimiya (USSR)*, **52**, 720–723.

[18] Strazdina, I., Kravale, Z., Galinina, N., Rutkis, R. et al., 2012. Electron transport and oxidative stress in *Zymomonas mobilis* respiratory mutants. *Arch. Microbiol.*, **194**, 461–471.

[19] Osman, Y.A., Ingram, L.O., 1985. Mechanism of ethanol inhibition of fermentation in *Zymomonas mobilis* CP4. *J. Bacteriol.*, **164**, 173–180.

[20] Osman, Y.A., Conway, T., Bonetti, S.J., Ingram, L.O., 1987. Glycolytic flux in *Zymomonas mobilis*: enzyme and metabolite levels during batch fermentation. *J. Bacteriol.*, **169**, 3726–3736.

[21] Anderson, R.F., Patel, K.B., Evans, M.D., 1985. Changes in the survival curve shape of *E. coli* cells following irradiation in the presence of uncouplers of oxidative phosphorylation. *Int. J. Radiat. Biol.*, **48**, 495–504.

[22] Markwell, M., Haas S.M., Bieber L.L., Talbert N.E., 1978. A modification of the Lowry procedure to simplify protein

determination in membrane and lipoprotein samples. Anal. Biochem., **87**, 206–210.

[23] Brooijmans, R.J.W., Poolman, B., Schuurman-Wolters, G.K., De Vos, W.M. et al., 2007. Generation of a membrane potential by *Lactococcus lactis* through aerobic electron transport. J. Bacteriol., **189**(14), 5203–5209.

[24] Seo, J.S., Chong, H., Park, H.S., Yoon, K.O. et al., 2005. The genome sequence of the ethanologenic bacterium *Zymomonas mobilis* ZM4. Nat. Biotechnol., **23**, 63–68.

[25] Ge, X., Zhao, Y., Hou, W., Zhang, W. et al., 2013. Complete genome sequence of the industrial strain *Gluconobacter oxydans* H24. Genome Announc., **1**(1), e00003–13. doi: 10.1128/genomeA.00003-13

[26] Richhardt, J., Luchterhand, B., Bringer, S., Büchs, J. et al., 2013. Evidence for a key role of cytochrome bo_3 oxidase in respiratory energy metabolism of *Gluconobacter oxydans*. J. Bacteriol., **195**(18), 4210–4220.

[27] Dawes, E.A., Large, P.J., 1970. Effect of starvation on the viability and cellular constituents of *Zymomonas anaerobia* and *Zymomonas mobilis*. J. Gen. Microbiol., **60**, 31–62.

[28] Ruhrmann, J., Krämer, R., 1992. Mechanism of glutamate uptake in *Zymomonas mobilis*. J. Bacteriol., **174**, 7579–7584.

[29] Steffens, K., Schneider, E., Herkenhoff, B., Schmid, R., Altendorf, K., 1984. Chemical modification of the F_0 part of the ATP synthase (F_1F_0) from *Escherichia coli*, effects on proton conduction and F_1 binding. Eur. J. Biochem., **138**, 617–622.

[30] Mauro, D.E., Lenaz, G., 1985. A clarification of the effects of DCCD on the electron transfer and antimycin binding of the mitochondrial bc_1 complex. J. Bioenerg. Biomembr., **17**(2), 109–121.

[31] Singh, A.P., Bragg, P.D., 1974. Effect of dicyclohexylcarbodiimide on growth and membrane-mediated processes in wild type and heptose-deficient mutants of *Escherichia coli* K-12. J. Bacteriol., **119**(1), 129–137.

[32] Russell, J.B., Strobel, H.J., 1990. ATPase-dependent energy spilling by the ruminal bacterium, *Streptococcus bovis*. Arch. Microbiol., **153**, 378–383.

[33] Russell, J.B., Cook, G.M., 1995. Energetics of bacterial growth: balance of anabolic and catabolic reactions. Microbiol. Rev., **59**, 48–62.

[34] Ugurbil, K., Rottenberg, H., Glynn, P., Shulman, R.G., 1978. ^{31}P nuclear magnetic resonance studies of bioenergetics and glycolysis in anaerobic *Escherichia coli* cells. Proc. Natl. Acad. Sci. USA, **75**(5), 2244–2248.

[35] Rutkis, R., Kalnenieks, U., Stalidzans, E., Fell, D.A., 2013. Kinetic modeling of *Zymomonas mobilis* Entner–Doudoroff pathway: insights into control and functionality. Microbiology, **159**, 2674–2689.

3.5 Kinetic modeling of Zymomonas mobilis Entner-Doudoroff pathway: insights into control and functionality

Microbiology (2013), 159, 2674–2689 DOI 10.1099/mic.0.071340-0

Kinetic modelling of the *Zymomonas mobilis* Entner–Doudoroff pathway: insights into control and functionality

Reinis Rutkis,[1] Uldis Kalnenieks,[1] Egils Stalidzans[2] and David A. Fell[3]

[1]Institute of Microbiology and Biotechnology, University of Latvia, Kronvalda Boulv. 4, Riga LV-1586, Latvia

[2]Biosystems Group, Department of Computer Systems, Latvia University of Agriculture, Liela Iela 2, Jelgava LV-3001, Latvia

[3]Department of Biological and Medical Sciences, Oxford Brookes University, Headington, Oxford OX3 0BP, UK

Correspondence
Reinis Rutkis
reinisrutkis@gmail.com

Received 16 July 2013
Accepted 30 September 2013

Zymomonas mobilis, an ethanol-producing bacterium, possesses the Entner–Doudoroff (E-D) pathway, pyruvate decarboxylase and two alcohol dehydrogenase isoenzymes for the fermentative production of ethanol and carbon dioxide from glucose. Using available kinetic parameters, we have developed a kinetic model that incorporates the enzymic reactions of the E-D pathway, both alcohol dehydrogenases, transport reactions and reactions related to ATP metabolism. After optimizing the reaction parameters within likely physiological limits, the resulting kinetic model was capable of simulating glycolysis *in vivo* and in cell-free extracts with good agreement with the fluxes and steady-state intermediate concentrations reported in previous experimental studies. In addition, the model is shown to be consistent with experimental results for the coupled response of ATP concentration and glycolytic flux to ATPase inhibition. Metabolic control analysis of the model revealed that the majority of flux control resides not inside, but outside the E-D pathway itself, predominantly in ATP consumption, demonstrating why past attempts to increase the glycolytic flux through overexpression of glycolytic enzymes have been unsuccessful. Co-response analysis indicates how homeostasis of ATP concentrations starts to deteriorate markedly at the highest glycolytic rates. This kinetic model has potential for application in *Z. mobilis* metabolic engineering and, since there are currently no E-D pathway models available in public databases, it can serve as a basis for the development of models for other micro-organisms possessing this type of glycolytic pathway.

INTRODUCTION

Zymomonas mobilis is a facultatively anaerobic, ethanol-producing bacterium that possesses the Entner–Doudoroff (E-D) pathway, which differs in several respects from glycolysis and the pentose phosphate pathway typical of other organisms. The intrinsically rapid carbohydrate metabolism of *Z. mobilis* has been studied in great detail during the past decades (Barrow *et al.*, 1984; Osman *et al.*, 1987; De Graaf *et al.*, 1999) and all the enzymes of the E-D pathway have been purified and characterized kinetically (Scopes, 1983, 1984, 1985; Scopes *et al.*, 1985; Scopes & Griffiths Smith, 1984, 1986; Kinoshita *et al.*, 1985; Pawlik *et al.*, 1986). Complete genome sequences for various *Z. mobilis* strains have been reported in recent years, providing the opportunity to compare currently uncharacterized *Z. mobilis* enzymes with those from different databases (Seo *et al.*, 2005; Kouvelis *et al.*, 2009; Pappas *et al.*, 2011; Desiniotis *et al.*, 2012). In spite of these diverse studies, this accumulated knowledge has scarcely yet been exploited as the basis for building a comprehensive kinetic model of this key component of *Z. mobilis* central metabolism. The only recent attempt focused on the aspects of interaction between the engineered non-oxidative part of the pentose phosphate pathway and the native *Z. mobilis* E-D glycolysis for xylose fermentation,

Abbreviations: ADH, alcohol dehydrogenase; AK, adenylate kinase; E-D pathway, Entner–Doudoroff pathway; ENO, enolase; GAPD, glyceraldehyde-3-phosphate dehydrogenase; GF, glucose facilitator; GK, glucokinase; GPD, glucose-6-phosphate dehydrogenase; KDPGA, 2-keto-3-deoxy-6-phosphogluconate aldolase; MCA, metabolic control analysis; PDC, pyruvate decarboxylase; PEP, phosphoenolpyruvate; PGD, 6-phosphogluconate dehydratase; PGK, 3-phosphoglycerate kinase; PGL, 6-phosphogluconolactonase; PGM, phosphoglycerate mutase; PYK, pyruvate kinase.

Supplementary material is available with the online version of this paper.

assuming constant intracellular concentrations of the essential metabolic cofactors ADP, ATP, $NAD(P)^+$ and NAD(P)H (Altintas *et al.*, 2006). Whilst such a simplification certainly reduces model complexity, since the E-D pathway itself is a major component of ATP and NAD(P)(H) turnover, this assumption of their constant concentrations significantly limits applicability of the model. In order to investigate interactions between the various ATP consumption reactions and the E-D pathway, a generalized ATP-consuming reaction has been introduced into the E-D

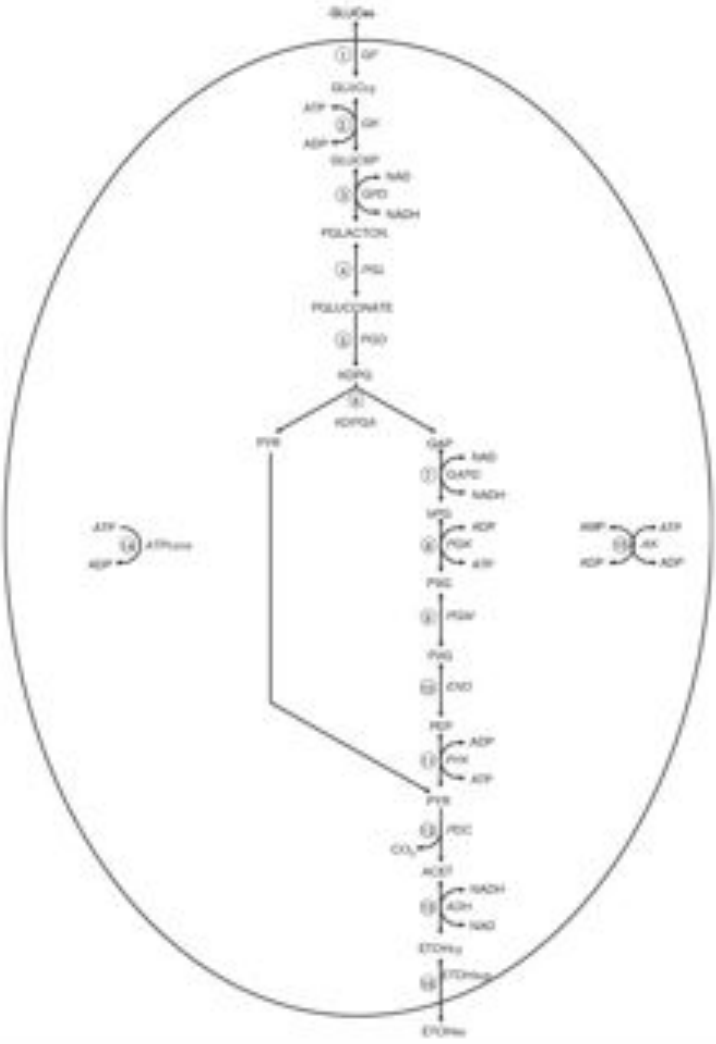

Fig. 1. Reactions included in the model of the E-D glucose utilization pathway. The numbered enzymes in these pathways are: (1) glucose facilitator (GF); (2) glucokinase (GK); (3) glucose-6-phosphate dehydrogenase (GPD); (4) 6-phosphogluconolactonase (PGL); (5) 6-phosphogluconate dehydratase (PGD); (6) 2-keto-3-decoy-6-phosphogluconate aldolase (KDPGA); (7) glyceraldehyde-3-phosphate dehydrogenase (GAPD); (8) 3-phosphoglycerate kinase (PGK); (9) phosphoglycerate mutase (PGM); (10) enolase (ENO); (11) pyruvate kinase (PYK); (12) pyruvate decarboxylase (PDC); (13) alcohol dehydrogenase (ADH); (14) ATP-consuming reactions (ATPcons); (15) adenylate kinase (AK); (16) ethanol export (ETOHexp). Other abbreviations are defined in Table S1.

Table 1. Rate equations used in this study

The reaction numbers correspond to those depicted in Fig. 1.

No.	Reaction	Rate equation
1	v_{PGI}	$\frac{\frac{V_f}{K_{m,GLUC_6P}}\cdot\left(GLUC_6P-\frac{FRU6P}{K_{eq}}\right)}{1+\frac{GLUC_6P}{K_{m,GLUC_6P}}+\frac{FRU6P}{K_{m,FRU6P}}}$
2	v_{PFK}	$\frac{\frac{V_f}{K_{m,FRU6P}\cdot K_{cat}\cdot\left(1+\frac{FRU6P}{K_{m,FRU6P}}\right)}\cdot\left(FRU6P\cdot ATP-\frac{FDP\cdot ADP}{K_{eq}}\right)}{1+\frac{GLUC_6P}{K_{m,GLUC_6P}}+\frac{FRU6P}{K_{m,FRU6P}}+\left(1+\frac{ATP}{K_{m,ATP}\cdot\left(1+\frac{FRU6P}{K_{m,FRU6P}}\right)}\right)+\frac{ADP}{K_{m,ADP}}}$
3	v_{GPD}	$\frac{V_f\cdot\frac{GLUC6P}{K_{m,GLUC6P}}\cdot\frac{NAD}{K_{m,NAD}\cdot\left(1+\frac{ATP}{K_{i,ATP}}\right)}\cdot\left(1-\frac{PGLACTON\cdot NADH}{GLUC6P\cdot NAD\cdot K_{eq}}\right)}{\left(\frac{1+\left(\frac{PEP}{K_{a,PEP}}\right)^4}{1+\alpha^4\cdot\left(\frac{PEP}{K_{a,PEP}}\right)^4}+\frac{1+\alpha^4\cdot\left(\frac{PEP}{K_{i,PEP}}\right)^4}{1+\alpha^4\cdot\left(\frac{PEP}{K_{i,PEP}}\right)^4}\right)\cdot\left(\left(\frac{GLUC6P}{K_{m,GLUC6P}}+\frac{PGLACTON}{K_{m,PGLACTON}}\right)^4+\left(\frac{GLUC6P}{K_{m,GLUC6P}}+\frac{PGLACTON}{K_{m,PGLACTON}}\right)^4\cdot\left(\frac{NAD}{K_{m,NAD}\cdot\left(1+\frac{ATP}{K_{i,ATP}}\right)}+\frac{NADH}{K_{m,NADH}}\right)^4\right)}{\left(\frac{NAD}{K_{m,NAD}\cdot\left(1+\frac{ATP}{K_{i,ATP}}\right)}+\frac{NADH}{K_{m,NADH}}\right)^4+\left(\frac{GLUC6P}{K_{m,GLUC6P}}+\frac{PGLACTON}{K_{m,PGLACTON}}\right)^4\cdot\left(\frac{NAD}{K_{m,NAD}\cdot\left(1+\frac{ATP}{K_{i,ATP}}\right)}+\frac{NADH}{K_{m,NADH}}\right)^4}$
4	v_{PGL}	$\frac{\frac{V_f}{K_{m,PGLACTON}\cdot\left(1+\frac{GLUC6P}{K_{i,GLUC6P}}\right)}\cdot\left(PGLACTON-\frac{PGLUCONATE}{K_{eq}}\right)}{1+\frac{PGLACTON}{K_{m,PGLACTON}\cdot\left(1+\frac{GLUC6P}{K_{i,GLUC6P}}\right)}+\frac{PGLUCONATE}{K_{m,PGLUCONATE}}}$
5	v_{PGD}	$\frac{V_f\cdot\frac{PGLUCONATE}{K_{m,PGLUCONATE}\cdot\left(1+\frac{PYR}{K_{i,PYR}}\right)}}{1+\frac{PGLUCONATE}{K_{m,PGLUCONATE}\cdot\left(1+\frac{PYR}{K_{i,PYR}}\right)}}$
6	v_{EDPGA}	$\frac{V_f\cdot KDPG-\frac{V_r\cdot GAP\cdot PYR}{K_{eq}\cdot K_{m,GAP}}}{1+\frac{KDPG}{K_{m,KDPG}}+\frac{PYR}{K_{m,PYR}}+\frac{GAP}{K_{m,GAP}}+\frac{KDPG\cdot GAP}{K_{m,KDPG}\cdot K_{i,GAP}}+\frac{PYR\cdot GAP}{K_{m,PYR}\cdot K_{i,GAP}}}$
7	v_{GAPD}	$\frac{\frac{V_f}{K_{m,GAP}\cdot K_{m,NAD}}\cdot\left(GAP\cdot NAD-\frac{APG\cdot NADH}{K_{eq}}\right)}{\left(1+\frac{GAP}{K_{m,GAP}}+\frac{APG}{K_{m,APG}}\right)\cdot\left(1+\frac{NAD}{K_{m,NAD}}+\frac{NADH}{K_{m,NADH}}\right)}$
8	v_{PGK}	$\frac{\frac{V_f}{K_{m,APG}\cdot K_{m,ADP}}\cdot\left(APG\cdot ADP-\frac{PSG\cdot ATP}{K_{eq}}\right)}{\left(1+\frac{APG}{K_{m,APG}}+\frac{PSG}{K_{m,PSG}}\right)\cdot\left(1+\frac{ADP}{K_{m,ADP}}+\frac{ATP}{K_{m,ATP}}\right)}$

Table 1. cont.

No.	Reaction	Rate equation
9	v_{PGIM}	$\frac{\frac{V_{f,...}}{K_{...}}\cdot\left(PGI-\frac{F6C}{K_{...}}\right)}{1+\frac{PGI}{K_{...}}+\frac{F6C}{K_{...}}}$
10	v_{ENO}	$\frac{\frac{V_{f,...}}{K_{...}}\cdot\left(P2G-\frac{PEP}{K_{...}}\right)}{1+\frac{P2G}{K_{...}}+\frac{PEP}{K_{...}}}$
11	v_{PYK}	$\frac{\frac{V_f}{K_{...}\cdot K_{...}}\cdot\left(PEP\cdot ADP-\frac{PYR\cdot ATP}{K_{eq}}\right)}{\left(1+\frac{PEP}{K_{...}}+\frac{PYR}{K_{...}}\right)\cdot\left(1+\frac{ADP}{K_{...}}+\frac{ATP}{K_{...}}\right)}$
12	v_{PDC}	$\frac{V_f\cdot\frac{PYR}{K_{...}}}{1+\frac{PYR}{K_{...}}}$
13	v_{ADH}	$\frac{\frac{V_f\cdot NADH\cdot ACET}{K_{...}\cdot K_{...}}-\frac{V_r\cdot K_{...}\cdot NAD\cdot ETOH}{K_{eq}\cdot K_{...}\cdot K_{...}\cdot K_{...}}}{1+\frac{NADH}{K_{...}}+\frac{K_{...}\cdot ACET}{K_{...}\cdot K_{...}}+\frac{NADH\cdot ACET}{K_{...}\cdot K_{...}}+\frac{NAD}{K_{...}}+\frac{K_{...}\cdot ETOH}{K_{...}\cdot K_{...}}+\frac{ETOH\cdot NAD}{K_{...}\cdot K_{...}}}$
14	$v_{ATPConst}$	$\frac{V_f\cdot ATP}{K_{...}+ATP}$
15	v_{AK}	$\frac{\frac{V_f}{K_{...}}\cdot\left(ADP^2-\frac{ATP\cdot AMP}{K_{eq}}\right)}{\left(1+\frac{ADP}{K_{...}}+\frac{ATP}{K_{...}}\right)\cdot\left(1+\frac{ADP}{K_{...}}+\frac{AMP}{K_{...}}\right)}$
16	$V_{ETOHtransp}$	$k\cdot(ETOH_o-ETOH_i)$

model described here. It has previously been proposed that the constitutively high catabolic rate that makes *Z. mobilis* an outstanding ethanol producer must be complemented by an intrinsic growth-independent, ATP-wasting reaction. This latter might be responsible for the 'uncoupled growth' phenomenon in this bacterium (Jones & Doelle, 1991). Incorporating adenylate and nicotinamide nucleotide metabolism into a computer model also offers the potential to inform the debate about the details of the role of the organism's respiratory system in aerobic metabolism (Kalnenieks *et al.*, 1993, 2008; Strazdina *et al.*, 2012).

There is good reason to expect that kinetic modelling of the *Z. mobilis* E-D pathway could also find application in metabolic engineering of this bacterium. A recently published stoichiometric analysis of *Z. mobilis* central metabolism revealed several metabolic engineering strategies to obtain high-value products, such as glycerate, succinate and glutamate, and also suggested the possibility of glycerol conversion to ethanol (Pentjuss *et al.*, 2013). However, analysis of the stoichiometric matrix just uncovers these possibilities, and further in-depth studies of the dynamics and regulation of *Z. mobilis* central metabolism are required to proceed with metabolic engineering. Indeed, in spite of the recent progress in the molecular biology of *Z. mobilis*, attempts to optimize metabolic processes by overexpression of intuitively chosen enzymes that are thought to be important for the rate of ethanol formation have led to counterintuitive results, such as a decrease of glycolytic flux (Snoep *et al.*, 1995). Such reports underline the need for quantitative metabolic control analysis before selection of enzymes that might exert flux control in *Z. mobilis*; this can be directly achieved by means of kinetic modelling.

Currently, there are also no kinetic models of the E-D pathway in public databases for any other micro-organisms possessing this form of glycolysis. Therefore, our present attempt to use accumulated experimental knowledge for kinetic modelling of the *Z. mobilis* E-D pathway might be useful for broader applications in microbial metabolic engineering.

METHODS

Modelling

Characteristics of the system, simplifying assumptions and moiety conservation. The model includes all the enzymes of the E-D pathway, glucose facilitator (GF), alcohol dehydrogenases (ADHs) and a reaction simulating ethanol export (Fig. 1). As in other glycolytic models, we have lumped all ATP hydrolysing reactions into one general ATP-consuming reaction, whose initial properties are set according to experimental data, taking into account that the membrane-bound F_0F_1-type ATPase is responsible for a significant part of ATP turnover in *Z. mobilis* (Reyes & Scopes, 1991). We have added the adenylate kinase (AK) reaction to equilibrate the AMP, ADP and ATP pools according to experimental observations.

Glucose-6-phosphate dehydrogenase (GPD) of *Z. mobilis* acts on both NAD and NADP, but has a higher specific activity with the former (Scopes, 1997). Since both ADHs (Kinoshita *et al.*, 1985) are specific to NAD(H) rather than NADP(H), we assume that the E-D pathway is turning over NAD rather than NADP. Any activity of GPD with NADP is likely to be coupled with the biosynthetic demands of growth, but this represents only 2 % of the glucose consumption (Swings & De Ley, 1977; Rogers *et al.*, 1982).

Two moiety-conservation relationships can be computed from the stoichiometry matrix of this set of reactions: one attributable to adenine nucleotides and the other to the nicotinamide nucleotide pool. The moiety-conserved sum is assigned on the basis of experimental observations. According to earlier reports, the ATP content of the cell, depending on the growth medium used, is maintained between 900 and 3600 μM, and it remains constant during the exponential phase in the range 1200–1500 μM (Lazdunski & Belaich, 1972). These values are in good agreement with data obtained later, where maximal concentrations of AMP, ADP and ATP were estimated to be 1500–2000 μM, with the ATP/ADP ratio near 1, by the 18th hour of fermentation (Osman *et al.*, 1987). Therefore we have assumed the following total adenylate moiety:

$$ATP + ADP + AMP = 3500\ \mu M \quad (1)$$

Adenylate charge (Atkinson, 1968) is calculated as (ATP + ½ ADP)/3500 and is used for comparison of the adenine nucleotide status with experiments where the total adenylate concentration may have been different.

In the case of the nicotinamide conservation, we have assumed that NAD(H) makes up most of the 4500 μM intracellular NAD(P)(H) pool, detected in *Z. mobilis* by NMR, without taking into account NADP(H) (De Graaf *et al.* 1999). Hence:

$$NAD^+ + NADH = 4500\ \mu M \quad (2)$$

For steady state modelling, we maintained constant extracellular glucose and ethanol concentrations with respective values of 140 000 μM and 1000 μM. In time-course simulations, glucose and ethanol were variables of the model, simulated as a closed system.

Enzyme kinetics. The rate equations for the individual enzymic reactions are presented together with the transport reactions in Table 1. The numbers of these equations correspond with those depicted in Fig. 1. All the equations were modelled according to the available literature data on *Z. mobilis* enzyme kinetics using generic, reversible rate equations (see Appendix), with the exception of GPD, where we directly fitted experimental observations (Scopes, 1997) to the universal rate equation for systems biology (Rohwer *et al.*, 2007). The source of the initial parameter values and more detailed derivations of the enzymic rate equations are given in the supplementary material (available in *Microbiology* Online). Enzyme rate units were all converted to micromoles per second per litre cell volume ($\mu mol\ l^{-1}\ s^{-1}$).

The model was built by entering these rate equations into the COPASI biochemical simulation software package, v. 4.8 (Hoops *et al.*, 2006), which assembles the set of ordinary differential equations automatically.

Glucose uptake fluxes in micromoles per second reported by COPASI were converted to grams of glucose per gram dry weight per hour ($g\ g^{-1}\ h^{-1}$) for comparison with experimentally reported measurements. For calculations we assumed that 1 mg dry weight of biomass corresponds to 2.2 μl of intracellular volume on average (Strohhäcker *et al.*, 1993).

Parameter optimization. Since the *in vitro* kinetic parameters were assembled from a variety of sources, in order to combine them into a coherent kinetic model, the maximum velocities of all reactions were optimized according to experimentally obtained steady-state intermediate concentrations. In order to have mutually compatible values for as many E-D intermediate concentrations as possible, and to avoid incompatibility of data coming from different analytical methods, we have used metabolite concentrations obtained by ^{31}P NMR in bacterial cells harvested at late exponential growth phase (Barrow *et al.*, 1984; Osman *et al.*, 1987). Metabolite concentrations were determined from spectra of extracts prepared 3–4 min after addition of glucose to cell suspensions, which correspond to quasi steady-state concentrations (Strohhäcker *et al.*, 1995). Initial values of the maximum velocities (V_i) were derived from the data of the 18th hour of batch fermentation (Osman *et al.*, 1987). This was chosen to ensure that the intermediate concentrations and V_i values used correspond roughly to the same physiological condition of the cells, where, according to ^{31}P NMR studies, specific glucose uptake rate slightly exceeds 5 $g\ g^{-1}\ h^{-1}$ (De Graaf *et al.*, 1999), which we used as the target value of glycolytic flux for parameter optimization. This value is also in good agreement with earlier reports, where *Z. mobilis* was likewise grown in ^{31}P NMR experiments on 10 % glucose anaerobically (Rogers *et al.*, 1979).

According to previous reports, most of the enzymes from the E-D pathway change their activity up to fivefold during batch fermentation; therefore, the upper and lower boundaries of V_i values that we set for each reaction during parameter optimization was a factor of five above and below the initial value (Osman *et al.*, 1987). $Km(s)$ values, which have been assumed or obtained from other databases attributable to other micro-organisms, were optimized within a factor of three above and below the initial value. Parameter optimization was also carried out using COPASI software using various optimization algorithms.

Quantifying the flux control. The control of a particular enzyme, i, on a glycolytic flux under steady-state conditions is defined by flux control coefficient C_i^J expressed as a percentage:

$$C_i^J = \frac{\partial J}{\partial v_i} \cdot \frac{v_i}{J} \cdot 100\% = \frac{\partial \ln J}{\partial \ln v_i} \cdot 100\% \quad (3)$$

in which v_i is the rate of enzyme i, J is a steady-state pathway flux (Kacser & Burns, 1973; Fell, 1992). The flux control coefficients of enzymes and transporters were calculated by COPASI and the results obtained always obeyed the summation theorem (Kacser & Burns, 1973):

$$\sum_{i=1\ldots n} C_i^J = 100\% \quad (4)$$

in which the summation is over all n enzymes in the model.

The effect of changing the activity (amount) of a single enzyme on the pathway flux was determined according to Small & Kacser (1993):

$$f = \frac{1}{1-\left[\frac{r-1}{r+100}\right]C_i^J} \quad (5)$$

in which f is the fold flux increase value and r is the fold increase of the enzyme activity.

Quantifying ATP homeostasis. Changes in an enzyme activity affect metabolite concentrations as well as fluxes and the concentration control coefficient quantifies the magnitude of this effect on a metabolite. It is defined in the same way as for the flux control coefficient. Thus, for metabolite S_j, the concentration control coefficient with respect to enzyme i is:

$$C_i^{S_j} = \frac{\partial S_j}{\partial v_i}\cdot\frac{v_i}{S_j}\cdot 100\,\% = \frac{\partial \ln S_j}{\partial \ln v_i}\cdot 100\,\% \quad (6)$$

The extent to which metabolite concentrations can be maintained relatively constant as fluxes change is a measure of metabolic homeostasis (Hofmeyr *et al.*, 1995; Cornish-Bowden & Hofmeyr, 1994; Thomas & Fell, 1996, 1998). This can be quantified by the ratio of the metabolite's concentration control coefficient to the flux control coefficient of the same enzyme, which has been defined as the co-response coefficient (Hofmeyr *et al.*, 1995; Cornish-Bowden & Hofmeyr, 1994). Thus, for metabolite S_j, flux J and enzyme i as defined in equations 3 and 6:

$$\Omega_i^{S_j/J} = \frac{C_i^{S_j}}{C_i^J} = \frac{\partial \ln S_j}{\partial \ln f} \quad (7)$$

The final term in the above equation results from the terms $\partial \ln v_i$ and the scaling factor 100 cancelling from the equation. This is useful since it is not necessary to know the change in enzyme activity used to perturb the system in order to calculate the co-response coefficient from simultaneous measurements of metabolite concentration and flux, provided that the perturbation is produced by modulation of a single enzyme, i. This contrasts with experimental determinations of flux and concentration control coefficients, which *do* require a measure of the enzyme activity change involved. Hence the co-response coefficient may be obtained from the slope of a log–log graph of concentration against flux. Alternatively, for a small enough perturbation, the co-response coefficient may be approximated from the difference between adjacent points as:

$$\Omega_i^{S_j/J} \approx \frac{\Delta S_j}{\Delta J} \quad (8)$$

In this paper, we determine the ATP: $J_{glycolysis}$ co-response coefficient with respect to ATPase, i.e. $\Omega_{ATPase}^{ATP,\,J_{glycolysis}}$ in this way.

Experimental

Bacterial strains. Bacterial strains *Z. mobilis* ATCC 29191 (Zm6) and its mutant derivatives Zm6-cyt8 and Zm6-cyt9 used in the present study were maintained and cultivated as described previously (Strandins *et al.*, 2012).

Preparation of non-growing cell suspensions. For the preparation of non-growing cell suspension, cells were harvested at late exponential phase, sedimented, washed and resuspended in 100 mM potassium phosphate buffer (pH 6.9), containing 2 mM magnesium sulfate, to a biomass concentration of 6.8–7.0 g (dry weight) l^{-1}.

Biochemical analyses. Samples for ATP determination were quenched in ice-cold 10 % trichloroacetic acid and assayed by the standard luciferin–luciferase method using an LKB Wallac 1251 Luminometer. Glucose concentration was measured by HPLC (Agilent 1100 series), using a Bio-Rad Aminex HPX–87H column.

RESULTS AND DISCUSSION

Initial model validation

In order to evaluate the model, the first question we addressed was whether the optimized E-D model is capable of reproducing glycolytic fluxes comparable to those reported earlier for *Z. mobilis*. The final version of our optimized model (hereafter – the optimized model) gave a specific glucose uptake rate of 4.9 g g^{-1} h^{-1}, close to our target. Evaluation of the difference between initial (Osman *et al.*, 1987) and optimized V_f values (Table 2) revealed that, for the majority of enzymes, these remained within a factor of three of the starting estimate and lie within the range of values reported across batch fermentation. V_f initial values used for parameter optimization for the majority of enzymes rose during optimization and came closer to values in French-press extracts reported earlier (Algar & Scopes, 1985). The calculated intermediate metabolite concentrations under steady conditions (Table 3), apart from phosphoenolpyruvate (PEP), were close to the NMR values within a factor of 1.5. The low PEP concentration predicted by the model is consistent with earlier reports that also suggest very low PEP intracellular levels (Algar & Scopes, 1985). Also the adenylate charge obtained (0.65) was consistent with experimental observations by Algar & Scopes (1985).

Simulation of glycolysis in cell-free extracts

To investigate whether the resulting model is able to simulate experiments other than those used for acquisition of initial parameters, we have carried out *in silico* simulation of earlier analyses of glycolysis in *Z. mobilis* (Algar & Scopes, 1985). First of all, by inserting reported E-D pathway enzyme activities in French-press extracts into the optimized model, we aimed to reproduce glycolysis *in situ*. Since Algar & Scopes did not report the activity for 6-phosphogluconolactonase, we have used our optimized value for this reaction. Also, phosphoglycerate kinase was assayed in the reverse direction and therefore the physiological activity for this reaction was calculated by using the Haldane relationship for multi-substrate reactions (Bisswanger, 2002). With these new enzyme activities, the model also reached steady state with a glycolytic flux in the model corresponding to an *in situ* rate of 5.2 g g^{-1} h^{-1}. This is in the range of the optimized model and earlier observations, where *Z. mobilis* was grown on different initial glucose concentrations with reported specific glucose uptake rates slightly below 5.5 g g^{-1} h^{-1} (Rogers *et al.*, 1979).

Table 2. Initial and optimized kinetic parameters of the model reactions

Units for each parameter are: V_f, μmol l^{-1} s^{-1}; K_{eq}, K_m, μmol l^{-1}; k, l s^{-1}; Keq dimensionless, except reaction No.6, Keq, μmol.

No.	Reaction	Kinetic parameter	Value		Ratio	Reference
			Initial	Optimized	Optimized/initial	
1	Glucose facilitator (GF)	V_f	7000	7000	1.00	DiMarco & Romano (1985)
		K_{eq}	1			Assumed
		$K_{MGLUCOSE}$	5000			DiMarco & Romano (1985)
		$K_{MATPGLUCOSE}$	5000			DiMarco & Romano (1985)
2	Glucokinase (GK)	V_f	6000	6263	1.04	Chenau et al. (1987)
		K_{eq}	450			Rubbiès & Boyer (1957)
		$K_{MGLUCOSE}$	220			Scopes et al. (1983)
		K_{MATP}	800			Scopes et al. (1983)
		$K_{MGLUCOSE6P}$	15000			Scopes et al. (1983)
		$K_{MGLUCOSE6P}$	1000	2608	2.61	Assumed
		K_{MATP}	1000	2458	2.46	Assumed
3	Glucose-6-phosphate dehydrogenase (G6PD)	V_f	8500	17484	3.00	Chenau et al. (1987)
		K_{eq}	1.4			Wamser et al. (1970), Glaser & Brown (1955)
		K_{MG6P6P}	232.7			Calculated from Scopes (1997)
		K_{MNADP}	231.8			Calculated from Scopes (1997)
		K_{MNADPH}	1000	2994	2.99	Assumed
		K_{MATP}	1400			Scopes (1983)
		K_{MNADPH}	1000	2998	3.00	Assumed
		K_{IATP}	14.1			Calculated from Scopes (1997)
		A	1.75			Calculated from Scopes (1997)
		σ	0.5			Calculated from Scopes (1997)
4	Phosphogluconolactonase (PGL)	V_f	2000	7848	3.92	Chenau et al. (1987)

Table 2. cont.

No.	Reaction	Kinetic parameter	Value		Ratio	Reference
			Initial	Optimized	Optimized/initial	
		K_{eq}	6400			Assumed from Goldberg *et al.* (2004)
		$K_{6PGLUCONATE}$	25			Scopes (1985)
		$K_{6PGLUCONATE}$	1000	351	0.35	Assumed
		K_{NADP+}	300			Scopes (1985)
5	6-Phosphogluconate dehydratase (PGD)	V_f	2000	4925	2.46	Osman *et al.* (1987)
		$K_{6PGLUCONATE}$	50			Scopes & Griffiths-Smith (1984)
		K_{PYR}	2000			Scopes & Griffiths-Smith (1984)
6	KDPG aldolase (KDPGA)	V_f	2000	7629	3.81	Osman *et al.* (1987)
		K_{eq}	1300			Assumed from Goldberg *et al.* (2004)
		K_{KDPG}	250			Scopes (1984)
		K_{GAP3P}	1000	2994	2.99	Assumed
		K_{PYR}	1000	369	0.37	Assumed
		K_{ATP}	1000	2996	3.00	Assumed
7	Glyceraldehyde-3-phosphate dehydrogenase (GAPD)	V_f	70000	30000	0.76	Osman *et al.* (1987)
		K_{eq}	0.04			Assumed from Goldberg *et al.* (2004)
		K_{GAP}	210	282	1.59	Teusink *et al.* (2000)
		K_{NAD}	90	133	1.48	Teusink *et al.* (2000)
		K_{NADH}	60	107	1.78	Teusink *et al.* (2000)
		K_{BPG}	10	9	0.90	Teusink *et al.* (2000)
8	3-Phosphoglycerate kinase (PGK)	V_f	9000	44990	5.00	Osman *et al.* (1987)
		K_{eq}	3000			Teusink *et al.* (2000), Krietsch & Bücher (1970)
		K_{BPG}	3	5	1.50	Teusink *et al.* (2000)
		K_{ADP}	200	517	2.59	Teusink *et al.* (2000)
		K_{3PG}	1300			Pawlak *et al.* (1986)
		K_{ATP}	1300			Pawlak *et al.* (1986)
9	Phosphoglycerate mutase (PGM)	V_f	45000	27454	0.61	Osman *et al.* (1987)

Table 2. cont.

No.	Reaction	Kinetic parameter	Value		Ratio	Reference
			Initial	Optimized	Optimized/initial	
		K_{GPDH}	62			Teusink *et al.* (2000)
		K_{GPD1}	1100			Pawlak *et al.* (1986)
		K_{GPD2}	80	28	0.35	Teusink *et al.* (2000)
10	Enolase (ENO1)	V_f	25600	5457	0.22	Otsman *et al.* (1987)
		K_{eq}	4			Wold & Ballou (1957)
		K_{ENO1}	80			Pawlak *et al.* (1986)
		K_{ENO2}	300	167	0.55	Teusink *et al.* (2000)
11	Pyruvate kinase (PYK)	V_f	70000	88774	1.27	Otsman *et al.* (1987)
		K_{eq}	5000			Assumed from Goldberg *et al.* (2004)
		K_{PYK1}	80			Pawlak *et al.* (1986)
		K_{ACT1P}	170			Pawlak *et al.* (1986)
		K_{FDP1}	210	78	0.37	Teusink *et al.* (2000)
		K_{ATP2}	1500	502	0.33	Teusink *et al.* (2000)
12	Pyruvate decarboxylase (PDC)	V_f	7500	9731	1.30	Otsman *et al.* (1987)
		K_{PDC6}	400			Bringer-Meyer *et al.* (1986)
13	Alcohol dehydrogenase (ADH 1)	V_f	10000	2033	0.20	Kinoshita *et al.* (1985)
		K_{eq}	10000			Assumed from Goldberg *et al.* (2004)
		K_{ADH1}	86			Kinoshita *et al.* (1985)
		K_{ADH2}	73			Kinoshita *et al.* (1985)
		$K_{ADH3/4/5}$	27			Kinoshita *et al.* (1985)
		K_{ADH7}	34			Kinoshita *et al.* (1985)
		K_{ACDH1}	6800			Kinoshita *et al.* (1985)
		K_{ACDH2}	76			Kinoshita *et al.* (1985)
14	Alcohol dehydrogenase (ADH II)	V_f	37500	184732	4.93	Kinoshita *et al.* (1985)

Table 2. cont.

No.	Reaction	Kinetic parameter	Value		Ratio	Reference
			Initial	Optimized	Optimized/initial	
		K_{eq}	10000			Assumed from Goldberg *et al.* (2004)
		K_{ADGLY}	1300			Kinoshita *et al.* (1985)
		K_{ADGLU}	110			Kinoshita *et al.* (1985)
		K_{ADGNT}	12			Kinoshita *et al.* (1985)
		K_{ADGI}	140			Kinoshita *et al.* (1985)
		K_{ADTRH}	27000			Kinoshita *et al.* (1985)
		K_{ADGM}	18			Kinoshita *et al.* (1985)
14	ATP consumption (ATPcons)	V_f	6000	4439	0.74	Reyes & Scopes (1991)
		K_{ADTP}	500			Reyes & Scopes (1991), Lardinoski & Bolnick (1972)
15	Adenylate kinase (AK)	V_f	1100	856	0.74	Zhinunis *et al.* (2001)
		K_{ADDP}	92	247	2.68	Saint Girons *et al.* (1987)
		K_{eq}	0.5			Goldberg *et al.* (2004)
		K_{ADTP}	66	195	2.95	Saint Girons *et al.* (1987)
		K_{ADAP}	38	27	0.71	Saint Girons *et al.* (1987)
16	Ethanol export (ETOHexp)	k	4	1		Assumed

Table 3. Comparison of the initial steady-state intermediate concentrations derived by ^{31}P NMR studies (Barrow *et al.*, 1984) and model predictions after parameter optimization with specific glucose uptake rate 4.9 g g^{-1} h^{-1} (grams glucose per gram dry weight per hour)

	Concentration (μM)		Ratio
Intermediate	**^{31}P NMR**	**Model**	**Model/^{31}P NMR**
Glucose 6-phosphate	1748	1815	1.04
6-Phosphogluconate	280	268	0.96
6-Phosphoglucono-lactone		259	
2-Keto-3-deoxy-6-phosphogluconate	630	920	1.46
Glyceraldehyde 3-phosphate	240	354	1.48
1,3-Bisphosphoglycerate		4	
3-Phosphoglycerate	2688	2774	1.03
2-Phosphoglycerate	212	230	1.08
Phosphoenolpyruvate	189	66	0.35
Pyruvate		955	
Acetaldehyde		48	
NAD		1518	
NADH		2982	
ATP*	1500	1671	1.11
ADP*	1500	1313	0.88
AMP*	500	516	1.03

*ATP, ADP and AMP concentrations are assumed according to AUXP moiety conservation.

Since specific glucose uptake and ATP consumption rates of the cells from which the extracts were obtained were not reported by Algar & Scopes (1985), and our assumed values may slightly differ from those present *in situ*, further model validation was necessary in order to use it for any predictions. Therefore, we undertook a more detailed examination of the optimized model by simulating consumption of 1 M glucose in cell-free extracts reported in the same study (Algar & Scopes, 1985). As in the *in vitro* experiments, we set the initial glucokinase (GK) activity to between 250 and 330 μmol l^{-1} s^{-1} (300 μmol l^{-1} s^{-1}) and proportionally estimated activities for all other enzymes on the basis of previous assumptions and values reported in French-press extracts (Table S2). The total activity of the ADH reaction given by Algar & Scopes (1985) was proportionally distributed between both ADH isoenzymes according to the optimized model. ATP consumption activity was set to that used in the cell-free extracts as externally added enzyme – 200 μmol l^{-1} s^{-1} (Algar & Scopes, 1985). In order to simulate cell-free conditions, both transport reactions were eliminated from the model, and lastly, since initial concentrations for E-D pathway metabolites were not reported by Algar & Scopes (1985), we assumed those according to steady-state concentrations reported for the optimized model (Table 3). Remarkably, the glycolytic flux obtained *in silico* was very similar to that in the *in vitro* experiment (Table 4) and the main difference was the lack of intermediate accumulation which occurred to substantial levels in the experiments. Since metabolite concentrations are much more sensitive to changes in enzyme activity than fluxes, a plausible explanation for the accumulation of intermediates in the *in vitro* experiments might be enzyme denaturation during the time-course resulting in a 'drift' in the steady state, whereas the model simulations assume the enzymes are stable and all remain at their initial levels.

Most importantly, in our *in silico* simulation, the intermediate concentrations obtained were reasonably close to those reported in ^{31}P NMR studies, indicating that computational simulations of the E-D pathway in cell-free extracts reliably simulate the situation *in situ* (Barrow *et al.*, 1984). Therefore, one can speculate that there is no specific 'metabolite tunelling' required for the E-D pathway to proceed, and rather that *Z. mobilis*, in respect to its central glycolytic pathway, can be adequately described as a 'bag of enzymes'.

As demonstrated in other experiments with *Z. mobilis* cell-free extracts, ATPase activity should match closely glucose consumption, and insufficient ATP consumption leads to accumulation of intermediates such as glucose 6-phosphate (Algar & Scopes, 1985). To examine whether this feature can be observed *in silico*, we undertook a series of simulations where, on varying the rate of ATP consumption, we monitored the concentration of glucose 6-phosphate. Indeed, reduction of generalized ATPase activity in the model by 25 % caused accumulation of glucose 6-phosphate to 27 mM and decline of the glycolytic flux by 12 % 60 min after glucose addition. Apart from the fact that this qualitatively resembles the observations in the *in vitro* experiments (Algar & Scopes, 1985), it indicates the control of the glycolytic flux by ATP consumption. To examine this hypothesis in greater detail,

Table 4. Time-course of metabolite levels (in mM) in cell-free extracts after addition of 1.0 M glucose

◆ Data from cell-free experiments by Algar & Scopes (1985); ◇ model simulation. For definitions of intermediates, see Table S1.

Intermediate		Time (min)						
		0	1.5	5	15	30	45	60
GLUC	◆		0.98	0.95	0.89	0.75	0.60	**0.48**
	◇	1.00	0.98	0.95	0.86	0.72	0.59	**0.47**
GLUC6P	◆		3.00	2.60	2.80	1.30	0.80	**0.50**
	◇	1.82	4.04	4.64	4.86	3.77	2.35	**1.50**
PGLUCONATE	◆		0.40	0.90	2.00	2.30	1.30	**0.50**
	◇	0.27	0.03	0.03	0.03	0.02	0.02	**0.02**
KDPG	◆		1.30	1.80	3.70	4.80	6.10	**7.00**
	◇	0.92	0.17	0.19	0.21	0.24	0.25	**0.24**
PYR	◆		0.30	0.80	1.00	2.10	7.00	**14.20**
	◇	0.94	0.25	0.24	0.23	0.22	0.21	**0.20**
ACET	◆		0.10	0.80	0.70	1.10	2.00	**3.00**
	◇	0.05	2.07	2.45	3.03	3.56	3.92	**4.20**
ETOH	◆		0.03	0.08	0.23	0.45	0.73	**1.04**
	◇	0.00	0.03	0.10	0.28	0.55	0.82	**1.07**
NAD^+	◆		0.27	0.53	1.00	1.30	1.38	**1.32**
	◇	1.52	3.08	2.75	2.27	1.93	1.73	**1.64**
ATP	◆		0.50	0.10	1.80	2.30	2.00	**1.50**
	◇	1.67	1.91	1.84	1.69	1.50	1.35	**1.19**
Adenylate charge	◆		0.25	0.05	0.69	0.68	0.43	**0.38**
	◇	0.66	0.60	0.59	0.56	0.52	0.49	**0.46**

we carried out a metabolic control analysis investigation using both the initial model and the model simulating glycolysis in cell-free extracts.

Control of glycolytic flux under steady-state conditions

We carried out metabolic control analysis (MCA) for both the optimized model and the model simulating glycolysis in cell-free extracts. The generalized ATP-consuming reaction exerted a major control over glycolytic flux with C_J^J values of 36 and 71 % for the optimized and cell-free extract models, respectively. To extend this finding, we also included in the MCA an optimized model with the activity of the generalized ATP-consuming reaction reduced by 15 % (Table 5). As in the experimental cell-free extracts (Algar & Scopes, 1985), a decrease of generalized ATPase activity resulted in an increase of glucose 6-phosphate steady-state concentration to 16 mM and further reduction of glycolytic flux by almost 10 % (Table 5). In general, the MCA suggested that the ATP-consuming reaction exerts major control over glycolytic flux and, counterintuitively, revealed a negative flux control coefficient for the GK reaction. This result strongly resembles previous experimental observations with *Escherichia coli*, suggesting that the majority of flux control (>75 %) resides not inside but outside the glycolytic pathway, i.e. with the enzymes that hydrolyse ATP (Koebmann *et al.*, 2002). This allowed us to speculate that anabolic reactions, in combination with ATP dissipation by F_0F_1-ATPase, control the glycolytic flux also during the 'uncoupled growth' of *Z. mobilis* when glycolytic flux attains its maximum. [Note that Reyes & Scopes (1991) calculate that F_0F_1-ATPase may contribute over 20 % of the total intracellular ATP turnover.] This is indirectly supported by experiments showing that inhibition of H^+-dependent ATPase results in decline of glycolytic flux and increase of *Z. mobilis* growth yields, suggesting the competition between anabolic and ATP-dissipating reactions (Rutkis and others, unpublished). Flamholz *et al.* (2013) proposed that generally the E-D pathway is favoured by microbes that rely largely on other sources of ATP, so that its lower yield relative to the EMP is insignificant compared with the saving in protein investment in enzymes that they propose arises because of the greater thermodynamic driving force per step. They noted, however, that *Z. mobilis* is an exception as it does not have an additional major source of ATP.

Metabolic control analysis also demonstrates why attempts in the past to increase the glycolytic flux in *Z. mobilis* through overexpression of glycolytic enzymes have been unsuccessful. Negligible flux control coefficients for the majority of the E-D pathway reactions (Table 5) partly explain why overexpression of a few intuitively chosen enzymes has not resulted in the increase of glycolytic flux (Arfman *et al.*, 1992; Snoep *et al.*, 1995). According to MCA, only the pyruvate decarboxylase (PDC) reaction exerts substantial control with C_J^J values reaching 27 % in the optimized model. Based on the flux control coefficients we

Table 5. Scaled flux control coefficients C_i^J of the glycolytic flux in the E-D pathway

Control coefficients above 5% are shown in bold type.

Reaction	Specific glucose uptake rate (q_s)		
	4.5*	4.9†	0.197‡
1 GF – glucose facilitator	0	0	–
2 GK – glucokinase	**−8**	**−8**	**−6**
3 GPD – glucose-6-phosphate dehydrogenase	0	1	7
4 PGL – 6-phosphogluconolactonase	4	1	5
5 PGD – 6-phosphogluconate dehydratase	3	3	0
6 KDPGA – 2-keto-3-deoxy-6-phosphogluconate aldolase	2	3	0
7 GAPD – glyceraldehyde-3-phosphate dehydrogenase	1	1	0
8 PGK – 3-phosphoglycerate kinase	1	1	0
9 PGM – phosphoglycerate mutase	3	**6**	1
10 ENO – enolase	**11**	**23**	2
11 PYK – pyruvate kinase	2	5	**8**
12 PDC – pyruvate decarboxylase	**11**	**27**	**8**
13 ADH I – alcohol dehydrogenase I	0	0	0
13 ADH II – alcohol dehydrogenase II	0	0	**6**
14 ATPcons – ATP consuming reactions	**70**	**36**	**71**
15 AK – adenylate kinase	0	0	0
16 ETOHexp – ethanol transport	0	0	–

*Optimized model with reduced activity of the generalized ATP-consuming reaction by 15% – 4400 μmol l^{-1} s^{-1} to 3800 μmol l^{-1} s^{-1}.
†Optimized model.
‡Simulation of the cell-free experiment by Algar & Scopes (1985).

obtain, and earlier reported enzyme activities in recombinant strains (Snoep *et al.*, 1995), we have used equation 5 to calculate the anticipated effects of glyceraldehyde-3-phosphate dehydrogenase (GAPD), 3-phosphoglycerate kinase (PGK), phosphoglycerate mutase (PGM), ADH I, ADH II and PDC overexpression on glycolytic flux in the E-D pathway and compared this to values calculated from experimental data (Table 6). As was observed experimentally, for all enzymes with the exception of PDC, the calculations suggested little or no increase of glycolytic flux in recombinant strains without addition of IPTG, when enzyme activity was increased just a few times. The significantly higher flux control coefficient for the PDC reaction suggested that overexpression of this enzyme more than threefold may lead to an increase of glycolytic flux of almost 23%. However, such an increase was not observed experimentally; further, experimental observations revealed that a more than 10-fold increase of enzyme activity after addition of 2 mM IPTG slowed down glycolysis by up to 25%. Given our calculations, this indirectly confirms earlier suggestions that the protein burden effect indeed might be a serious side effect of overexpression of enzymes possessing little or no control over the flux in the E-D pathway. However, in *Z. mobilis*, enzymes involved in fermentation compose as much as 50% of total protein (Algar & Scopes, 1985), so the protein burden effect might not be as pronounced in other micro-organisms where wild-type levels of E-D pathway enzymes are not so great. Nevertheless, according to equation 3, simultaneous overexpression of PDC, enolase (ENO) and PGM below the protein burden threshold has the potential to increase the glycolytic flux up to 25% (6.6 g g^{-1} h^{-1}). This clearly demonstrates that the optimized model could serve to develop efficient metabolic engineering strategies for *Z. mobilis* in spite of the protein burden effect. Note also that the EMP pathway (Embden Meyerhof Parnas pathway) could not generate an equivalent glycolytic flux in *Z. mobilis* according to the calculations of Flamholz *et al.* (2013), which suggest that the EMP pathway would need not less than 3.5 times the protein investment for the same flux, which would be infeasible given the 50% of cell protein already devoted to the E-D pathway.

Co-response analysis and experimental validation

We have recently made measurements of the response of ATP concentration and glycolytic flux to inhibition of ATPase by dicyclohexylcarbodiimide in wild-type *Z. mobilis* and two respiratory chain mutants, *cytB* and *cydB* (Rutkis and others, unpublished). The measurements have been used in neither the construction of the model nor parameter estimation. They allow calculation of the ATP:glycolytic flux co-response coefficient with respect to ATPase using equation 8, as shown in Table S3. The same co-response coefficient can be calculated from the model by simulating it with different levels of ATPase

Table 6. Calculated flux increase values (δ) for model simulation and experimental data

Reaction	Flux increase value (δ)			
	Model simulation		Experimental values*	
	0 mM IPTG	2 mM IPTG	0 mM IPTG	2 mM IPTG
GAPD – glyceraldehyde 3-phosphate dehydrogenase	1.006	1.009	0.985	0.748
PGK – 3-phosphoglycerate kinase	1.004	1.009	0.956	0.655
PGM – phosphoglycerate mutase	1.012	1.029	1.005	0.995
PDC – pyruvate decarboxylase	1.229		0.903	
ADH I – alcohol dehydrogenase I	1.000	1.000	0.985	0.767
ADH II – alcohol dehydrogenase II	1.000	1.000	0.981	0.885

*According to Snoep *et al.* (1995).

activity. The experimental and simulated values are shown in Fig. 2, plotted against the glycolytic flux.

The results show that the model correctly captures the relationship between ATP concentration and glycolytic flux for both wild-type and respiratory mutant strains, and also implies that the respiratory deletions have not affected the regulatory pattern of the E-D pathway and catabolic ATP yield per unit of consumed glucose. At the highest glycolytic flux considered (about 4.6 g g^{-1} h^{-1}, ln value 1.53), the co-response coefficient is approximately −4.0. This shows that at this point, ATP homeostasis is poor, since a 1% increase in glycolytic flux would be associated with a 4% decrease in ATP concentration. At a flux of about 3.9 g g^{-1} h^{-1}, the co-response coefficient is smaller in magnitude, close to −1.0, where a 1% increase in glycolytic flux is linked to a 1% decrease in ATP concentration. At the lowest glycolytic flux obtained with the lowest ATPase activities (3.0 g g^{-1} h^{-1}, ln value 1.1), the co-response coefficient is about −0.23, so that ATP homeostasis is much improved in that it takes a 4% change in glycolytic flux to produce a 1% change in ATP concentration in the opposite direction.

CONCLUSIONS

In this study, by using available kinetic parameters, we have developed an *in silico* model of the *Z. mobilis* E-D pathway that also incorporates both ADHs, transport reactions and reactions related to ATP metabolism. Even though parameters of the rate equations were optimized with respect to a single set of conditions, the resulting kinetic model was able to achieve good agreement with previous experimental studies both *in situ* and *in vitro*. The analysis suggests that

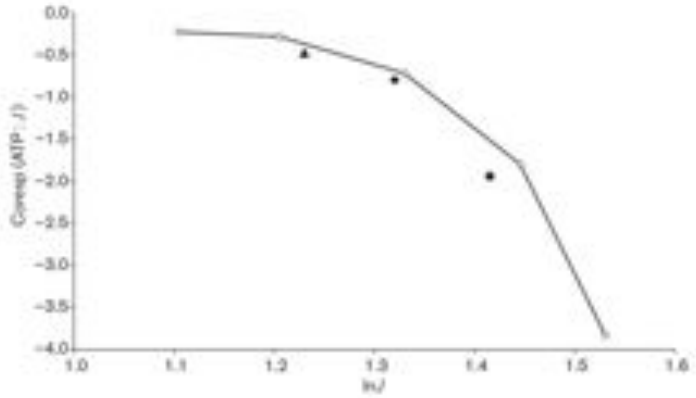

Fig. 2. Experimental and simulated co-response coefficients. ATP and glycolytic flux measurements were made in the absence and presence of 50 μM dicyclohexylcarbodiimide on wild-type and two mutant strains. Co-response coefficients [Coresp (ATP : *J*)] were calculated as in equation 8. The log of the glycolytic flux (ln *J*) in the uninhibited bacteria averaged 1.5; inhibition of the ATPase lowered the flux and increased the ATP levels. The experimental points are plotted as the mean log value of the flux for the pair of values used for the calculation of the co-response. ◆, Zm6; ●, Zm6-cytB; ▲, Zm6-cytB; □, model simulation.

the central glycolytic pathway of *Z. mobilis* can be adequately described as a 'bag of enzymes' and there is no a priori need to invoke 'metabolite channelling' to explain its properties.

MCA analysis revealed that the majority of flux control resides not inside, but outside the E-D pathway. That strongly suggests the need to look for more complex solutions to increasing the glycolytic flux than overexpression of certain E-D pathway enzyme(s). Since the ATP-consuming reactions exerted a major control over the flux in the E-D pathway, their increase, within physiological capacity, making growth more uncoupled, might serve as the appropriate strategy to increase the glycolytic flux in *Z. mobilis*. However, the co-response analysis indicates that cellular ATP homeostasis declines to a critical degree.

On a broader perspective, many other bacteria use the E-D pathway, and this new model may act as a template for simulating their metabolism.

ACKNOWLEDGEMENTS

This work was funded by Latvian European Social Fund projects 2009/0271/1DP/1.1.1.2.0/09/APIA/VIAA/128 and 2009/0138/1DP/1.1.2.1.2/09/IPIA/VIAA/004.

REFERENCES

Algar, E. M. & Scopes, R. K. (1985). Studies on cell-free metabolism: ethanol production by extracts of *Zymomonas mobilis*. *J Biotechnol* **2**, 275–287.

Altintas, M. M., Eddy, C. K., Zhang, M., McMillan, J. D. & Kompala, D. S. (2006). Kinetic modeling to optimize pentose fermentation in *Zymomonas mobilis*. *Biotechnol Bioeng* **94**, 273–295.

Atkinson, D. E. (1968). The energy charge of the adenylate pool as a regulatory parameter. Interaction with feedback modifiers. *Biochemistry* **7**, 4030–4034.

Arfman, N., Worrell, V. & Ingram, L. O. (1992). Use of the *tac* promoter and *lacI*^{q} for the controlled expression of *Zymomonas mobilis* fermentative genes in *Escherichia coli* and *Zymomonas mobilis*. *J Bacteriol* **174**, 7570–7578.

Barrow, K. D., Collins, J. G., Norton, R. S., Rogers, P. L. & Smith, G. M. (1984). ^{31}P nuclear magnetic resonance studies of the fermentation of glucose to ethanol by *Zymomonas mobilis*. *J Biol Chem* **259**, 5711–5716.

Bisswanger, H. (2002). *Enzyme Kinetics – Principles and Methods*. Weinheim: Wiley.

Bringer-Meyer, S., Schimz, K. L. & Sahm, H. (1986). Pyruvate decarboxylase from *Zymomonas mobilis*: isolation and partial characterization. *Arch Microbiol* **146**, 105–110.

Cornish-Bowden, A. & Hofmeyr, J.-H. S. (1994). Determination of control coefficients in intact metabolic systems. *Biochem J* **298**, 367–375.

De Graaf, A. A., Striegel, K., Wittig, R. M., Laufer, B., Schmitz, G., Wiechert, W., Sprenger, G. A. & Sahm, H. (1999). Metabolic state of *Zymomonas mobilis* in glucose-, fructose-, and xylose-fed continuous cultures as analysed by ^{13}C- and ^{31}P-NMR spectroscopy. *Arch Microbiol* **171**, 371–385.

Desiniotis, A., Kouvelis, V. N., Davenport, K., Bruce, D., Detter, C., Tapia, R., Han, C., Goodwin, L. A., Woyke, T. & other authors (2012). Complete genome sequence of the ethanol-producing *Zymomonas mobilis* subsp. *mobilis* centrotype ATCC 29191. *J Bacteriol* **194**, 5966–5967.

DiMarco, A. A. & Romano, A. H. (1985). D-Glucose transport system of *Zymomonas mobilis*. *Appl Environ Microbiol* **49**, 151–157.

Doelle, H. W. (1982). Kinetic characteristics and regulatory mechanisms of glucokinase and fructokinase from *Zymomonas mobilis*. *European J Appl Microbiol Biotechnol* **14**, 241–246.

Fell, D. A. (1992). Metabolic control analysis: a survey of its theoretical and experimental development. *Biochem J* **286**, 313–330.

Flamholz, A., Noor, E., Bar-Even, A., Liebermeister, W. & Milo, R. (2013). Glycolytic strategy as a tradeoff between energy yield and protein cost. *Proc Natl Acad Sci U S A* **110**, 10039–10044.

Glaser, L. & Brown, D. H. (1955). Purification and properties of D-glucose-6-phosphate dehydrogenase. *J Biol Chem* **216**, 67–79.

Goldberg, R. N., Tewari, Y. B. & Bhat, T. N. (2004). Thermodynamics of enzyme-catalyzed reactions – a database for quantitative biochemistry. *Bioinformatics* **20**, 2874–2877.

Hofmeyr, J.-H. S., Cornish-Bowden, A. & Rohwer, J. M. (1995). Taking enzyme kinetics out of control; putting control into regulation. *Eur J Biochem* **232**, 833–837.

Hoops, S., Sahle, S., Gauges, R., Lee, C., Pahle, J., Simus, N., Singhal, M., Xu, L., Mendes, P. & Kummer, U. (2006). COPASI – a COmplex PAthway Simulator. *Bioinformatics* **22**, 3067–3074.

Hoppner, T. C. & Doelle, H. W. (1983). Purification and kinetic characteristics of pyruvate decarboxylase and ethanol dehydrogenase from *Zymomonas mobilis* in relation to ethanol production. *Eur J Appl Microbiol Biotechnol* **17**, 152–157.

Jones, C. W. & Doelle, H. W. (1991). Kinetic control of ethanol production by *Zymomonas mobilis*. *Appl Microbiol Biotechnol* **35**, 4–9.

Kacser, H. & Burns, J. A. (1979). Molecular democracy: who shares the controls? *Biochem Soc Trans* **7**(5), 1149–1160.

Kalnenieks, U., De Graaf, A. A., Bringer-Meyer, S. & Sahm, H. (1993). Oxidative phosphorylation in *Zymomonas mobilis*. *Arch Microbiol* **160**, 74–79.

Kalnenieks, U., Galinina, N., Strazdina, I., Kravale, Z., Pickford, J. L., Rutkis, R. & Poole, R. K. (2008). NADH dehydrogenase deficiency results in low respiration rate and improved aerobic growth of *Zymomonas mobilis*. *Microbiology* **154**, 989–994.

Kinoshita, S., Kakizono, T., Kadota, K., Das, K. & Taguchi, H. (1985). Purification of two alcohol dehydrogenases from *Zymomonas mobilis* and their properties. *Appl Microbiol Biotechnol* **22**, 249–254.

Koebmann, B. J., Westerhoff, H. V., Snoep, J. L., Nilsson, D. & Jensen, P. R. (2002). The glycolytic flux in *Escherichia coli* is controlled by the demand for ATP. *J Bacteriol* **184**, 3909–3916.

Kouvelis, V. N., Davenport, K. W., Brettin, T. S., Bruce, D., Detter, C., Han, C. S., Nolan, M., Tapia, R., Damoulaki, A. & other authors (2011). Genome sequence of the ethanol-producing *Zymomonas mobilis* subsp. *pomaceae* lectotype strain ATCC 29192. *J Bacteriol* **193**, 5089–5090.

Kouvelis, V. N., Saunders, E., Brettin, T. S., Bruce, D., Detter, C., Han, C., Tapas, M. A. & Pappas, K. M. (2009). Complete genome sequence of the ethanol producer *Zymomonas mobilis* NCIMB 11163. *J Bacteriol* **191**, 7140–7141.

Krietsch, W. K. G. & Bücher, T. (1970). 3-Phosphoglycerate kinase from rabbit skeletal muscle and yeast. *Eur J Biochem* **17**, 568–580.

Lazdunski, A. & Belaich, J. P. (1972). Uncoupling in bacterial growth: ATP pool variation in *Zymomonas mobilis* cells in relation to different uncoupling conditions of growth. *J Gen Microbiol* **70**, 187–197.

Lee, K. J., Skotnicki, M. L., Tribe, D. E. & Rogers, P. L. (1980). Kinetic studies on a highly productive strain of *Zymomonas mobilis*. *Biotechnol Lett* **2**, 339–344.

Neale, A. D., Scopes, R. K., Kelly, J. M. & Wettenhall, R. E. (1986). The two alcohol dehydrogenases of *Zymomonas mobilis*. Purification by differential dye ligand chromatography, molecular characterisation and physiological roles. *Eur J Biochem* **154**, 119–124.

Osman, Y. A., Conway, T., Bonetti, S. J. & Ingram, L. O. (1987). Glycolytic flux in *Zymomonas mobilis*: enzyme and metabolite levels during batch fermentation. *J Bacteriol* **169**, 3726–3736.

Pappas, K. M., Kouvelis, V. N., Saunders, E., Brettin, T. S., Bruce, D., Detter, C., Balakireva, M., Han, C. S., Savvakis, G. & other authors (2011). Genome sequence of the ethanol-producing *Zymomonas mobilis* subsp. *mobilis* lectotype strain ATCC 10988. *J Bacteriol* **193**, 5051–5052.

Parker, C., Peekhaus, N., Zhang, X. & Conway, T. (1997). Kinetics of sugar transport and phosphorylation influence glucose and fructose co-metabolism by *Zymomonas mobilis*. *Appl Environ Microbiol* **63**, 3519–3525.

Pawluk, A., Scopes, R. K. & Griffiths-Smith, K. (1986). Isolation and properties of the glycolytic enzymes from *Zymomonas mobilis*. The five enzymes from glyceraldehyde-3-phosphate dehydrogenase through to pyruvate kinase. *Biochem J* **238**, 275–281.

Pentjuss, A., Odzina, I., Kostromins, A., Fell, D. A., Stalidzans, E. & Kalnenieks, U. (2013). Biotechnological potential of respiring *Zymomonas mobilis*: a stoichiometric analysis of its central metabolism. *J Biotechnol* **165**, 1–10.

Reyes, L. & Scopes, R. K. (1991). Membrane-associated ATPase from *Zymomonas mobilis*: purification and characterization. *Biochim Biophys Acta* **1068**, 174–178.

Robbins, E. A. & Boyer, P. D. (1957). Determination of the equilibrium of the hexokinase reaction and the free energy of hydrolysis of adenosine triphosphate. *J Biol Chem* **224**, 121–135.

Rogers, P. L., Lee, K. J. & Tribe, D. E. (1979). Kinetics of alcohol production by *Zymomonas mobilis* at high sugar concentrations. *Biotechnol Lett* **1**, 165–170.

Rogers, P. L., Lee, K. J., Skotnicki, M. L. & Tribe, D. E. (1982). Ethanol production by *Zymomonas mobilis*. *Adv Biochem Eng* **23**, 37–84.

Rohwer, J. M., Hanekom, A. J., Hendrik, S. & Hofmeyr, J.-H. S. (2007). A universal rate equation for systems biology. *Proceed 2nd Intern ESCEC Symp*, pp. 175–187.

Saint Girons, I., Gilles, A. M., Margarita, D., Michelson, S., Monnot, M., Fermandjian, S., Danchin, A. & Bârzu, O. (1987). Structural and catalytic characteristics of *Escherichia coli* adenylate kinase. *J Biol Chem* **262**, 622–629.

Schoberth, S. M., Chapman, B. E., Kuchel, P. W., Willig, R. M., Grotendorst, J., Jansen, P. & DeGraff, A. A. (1996). Ethanol transport in *Zymomonas mobilis* measured by using in vivo nuclear magnetic resonance spin transfer. *J Bacteriol* **178**, 1756–1761.

Scopes, R. K. (1983). An iron-activated alcohol dehydrogenase. *FEBS Lett* **156**, 303–306.

Scopes, R. K. (1984). Use of differential dye-ligand chromatography with affinity elution for enzyme purification: 2-keto-3-deoxy-6-phosphogluconate aldolase from *Zymomonas mobilis*. *Anal Biochem* **136**, 525–529.

Scopes, R. K. (1985). 6-Phosphogluconolactonase from *Zymomonas mobilis*. *FEBS Lett* **193**, 185–188.

Scopes, R. K. (1997). Allosteric control of *Zymomonas mobilis* glucose-6-phosphate dehydrogenase by phosphoenolpyruvate. *Biochem J* **326**, 733–735.

Scopes, R. K. & Griffiths-Smith, K. (1984). Use of differential dye-ligand chromatography with affinity elution for enzyme purification: 6-phosphogluconate dehydratase from *Zymomonas mobilis*. *Anal Biochem* **136**, 530–534.

Scopes, R. K. & Griffiths-Smith, K. (1986). Fermentation capabilities of *Zymomonas mobilis* glycolytic enzymes. *Biotechnol Lett* **8**, 653–656.

Scopes, R. K., Testolin, V., Stoter, A., Griffiths-Smith, K. & Algar, E. M. (1985). Simultaneous purification and characterization of glucokinase, fructokinase and glucose-6-phosphate dehydrogenase from *Zymomonas mobilis*. *Biochem J* **228**, 627–634.

Seo, J. S., Chong, H., Park, H. S., Yoon, K. O., Jung, C., Kim, J. J., Hong, J. H., Kim, H., Kim, J. H. & other authors (2005). The genome sequence of the ethanologenic bacterium *Zymomonas mobilis* ZM4. *Nat Biotechnol* **23**, 63–68.

Small, J. R. & Kacser, H. (1993). Responses of metabolic systems to large changes in enzyme activities and effectors. 1. The linear treatment of unbranched chains. *Eur J Biochem* **213**, 613–624.

Snoep, J. L., Yomano, L. P., Westerhoff, H. V. & Ingram, L. O. (1995). Protein burden in *Zymomonas mobilis*: negative flux and growth control due to overproduction of glycolytic enzymes. *Microbiology* **141**, 2329–2337.

Strazdina, I., Kravale, Z., Galinina, N., Rutkis, R., Poole, R. K. & Kalnenieks, U. (2012). Electron transport and oxidative stress in *Zymomonas mobilis* respiratory mutants. *Arch Microbiol* **194**, 461–471.

Strohhäcker, J., De Graaf, A. A., Schoberth, S. M., Willig, R. M. & Sahm, H. (1993). ^{31}P Nuclear magnetic resonance studies of ethanol inhibition in *Zymomonas mobilis*. *Arch Microbiol* **159**, 484–490.

Swings, J. & De Ley, J. (1977). The biology of *Zymomonas*. *Bacteriol Rev* **41**, 1–46.

Teusink, B., Passarge, J., Reijenga, C. A., Esgalhado, E., van der Weijden, C. C., Schepper, M., Walsh, M. C., Bakker, B. M., van Dam, K. & other authors (2000). Can yeast glycolysis be understood in terms of in vitro kinetics of the constituent enzymes? Testing biochemistry. *Eur J Biochem* **267**, 5313–5329.

Thomas, S. & Fell, D. A. (1998). Design of metabolic control for large flux changes. *J Theor Biol* **192**, 285–298.

Thomas, S. & Fell, D. A. (1998). A control analysis exploration of the role of ATP utilisation in glycolytic flux control and glycolytic-metabolite-concentration regulation. *Eur J Biochem* **258**, 956–967.

Thomas, T. M. & Scopes, R. K. (1998). The effects of temperature on the kinetics and stability of mesophilic and thermophilic 3-phosphoglycerate kinases. *Biochem J* **330**, 1087–1095.

Vinogradov, A. D. (2000). Steady-state and pre-steady-state kinetics of the mitochondrial H(+)(H) ATPase: is ATP synthase a reversible molecular machine? *J Exp Biol* **203**, 41–49.

Vogel, G. & Steinhart, R. (1976). ATPase of *Escherichia coli*: purification, dissociation, and reconstitution of the active complex from the isolated subunits. *Biochemistry* **15**, 208–216.

Weisser, P., Krämer, R., Sahm, H. & Sprenger, G. A. (1995). Functional expression of the glucose transporter of *Zymomonas mobilis* leads to restoration of glucose and fructose uptake in *Escherichia coli* mutants and provides evidence for its facilitator action. *J Bacteriol* **177**, 3351–3354.

Wills, C., Kretsfil, P., Londo, D. & Martin, T. (1981). Characterization of the two alcohol dehydrogenases of *Zymomonas mobilis*. *Arch Biochem Biophys* **210**, 775–785.

Wold, F. & Ballou, C. E. (1957). Studies on the enzyme enolase. I. Equilibrium studies. *J Biol Chem* **227**, 301–312.

Wurster, B. & Hess, B. (1970). Kinetic analysis of the glucosephosphate isomerase-glucose-6-phosphate dehydrogenase system from yeast in vitro. *Hoppe Seylers Z Physiol Chem* **351**, 1537–1544.

Zikmanis, P., Kruce, R. & Auzina, L. (2001). Interrelationships between growth yield, ATPase and adenylate kinase activities in *Zymomonas mobilis*. *Acta Biotechnol* **21**, 171–178.

Edited by: G. Thomas

4 DISCUSSION

The results of the studies in this thesis present the comprehensive research of the mechanistic reasons for *Zymomonas mobilis* uncoupled metabolism both under aerobic and anaerobic conditions.

4.1 Structure and function of the respiratory chain

The question why *Z. mobilis* does not use oxidative phosphorylation to stimulate aerobic growth is partly attributable to the structure of the respiratory chain and energy coupling in particular. One of main tasks of the present thesis was to find out, whether some putative branche of its respiratory chain with low degree of energy-coupling is not dominating the electron transport. The genome sequence of *Z. mobilis* (Seo *et al*., 2005) reveals genes encoding several NAD(P)H dehydrogenases, as well as electron-transport dehydrogenases for D- lactate and glucose. Also the previous physiologycal studies supports the presence of more than one NAD(P)H dehydrogenase in its electron-transport chain revealing two components with different Km values for NADH (Kalnenieks *et al*., 1996). The apparent Km for the activity that prevails in anaerobically grown cells was found to be close to 7 μM, as for the energy-coupling NADH dehydrogenase complex I in *E. coli*, encoded by the *nuo* operon (Matsushita *et al*., 1987; Leif *et al*., 1995). However, since *Z. mobilis* genome does not contain any sequences homologous to *nuo* operon, the presence of 'nuo-like' (or the low-Km) energy-coupling NADH dehydrogenase seems obscure. The apparent Km of the other component, prevailing in aerobically grown cells, was around 60 μM (Kim *et al*., 1995; Kalnenieks *et al*., 1996). This is a typical value for the energy non-generating type II NADH dehydrogenase, encoded by *ndh* (Yagi, 1991). Evidence that inactivation of *ndh* gene by insertion of the chloramphenicol-resistance determinant resulted in a total loss of NADH and NADPH oxidase activities in the mutant *Z. mobilis ndh* cell membranes (see Chapter 3.1), clearly shows that the *ndh* gene product is the sole functional respiratory NAD(P)H dehydrogenase in *Z. mobilis*. Therefore, lack of energy coupling NADH dehydrogenese may greatly lower the proton-motive force generation in *Z. mobilis* respiratory chain. Apart from *ndh*, the *Z. mobilis* genome (Seo *et al*., 2005) contains a gene homologous to *mda*B of *E. coli*, encoding an NADPH-specific quinone reductase. Homologues of the *MdaB* protein

are known to act as antioxidant factors in many pathogenic bacteria, helping to cope with the oxidative stress accompanying inflammation processes (Wang & Maier, 2004). The putative function of the *MdaB* homologue in *Z. mobilis* has not been investigated so far. Also, at present the physiological role of some other respiratory chain components remains uncertain.

Inactivation of NAD(P)H dehydrogenase in the *Z. mobilis ndh* mutant cell membranes resulted in overexpression of D-lactate oxidase that appeared to be the dominant oxidase in this mutant strain (Fig. 1b, c; see section 3.1 in Chapter 3.1). It is suggested that the elevated D- lactate oxidase in aerated cells has some physiological importance for the aerobic metabolism of *Z. mobilis ndh* mutant. Some-what similar as it was reported for a *Corynebacterium glutamicum* type II NADH dehydrogenase-deficient strain, D-lactate dehydrogenase might serve to compensate for the lack of respiratory NAD(P)H oxidation (Nantapong *et al*., 2004). D-lactate in *Z. mobilis* might be produced from pyruvate and NADH by the cytoplasmic lactate dehydrogenase, and then reoxidized by the respiratory D-lactate dehydrogenase. That it may form a kind of 'lactate shunt' for NADH reoxidation. However, very low rate of the oxygen uptake in the mutant strain suggests low activity of such a putative shunt. Furthermore importance of lactate shunt is also questioned by NADH reoxidation in the respiratory chain since it competes with highly active alcohol dehydrogenase reaction. Therefore it is tempting to think that increased D-lactate oxidase activity in the mutant strain under aerobic conditions, might have some other, so far unknown function that most likely have a loose conection to oxidative phosphorylation.

Despite only one functional respiratory NAD(P)H dehydrogenase, downstream of quinones *Z. mobilis* apparently has a branched electron transport chain. The known *Z. mobilis* genome sequences contain genes encoding a cytochrome bc_1 complex and cytochrome *c* (Seo *et al*., 2005; Yang *et al*., 2009; Kouvelis *et al*., 2011), yet lack sequences homologous to any known bacterial cytochrome *c* oxidase genes. At the same time, the ability of both aerobically cultivated mutants, Zm6- *cytB* and Zm6-*cydB*, to consume oxygen, as well as the difference seen in the antimycin sensitivity of their respiration, and in the kinetics of the cytochrome *d* reduction with NADH, indicates the presence of at least two branches of electron transport in the *Z. mobilis* respiratory chain. The results of this study are discussed in Chapter 3.2. The effects of the *cydB* mutation clearly demonstrate that cytochrome *bd* is involved in electron

transport. Yet, the apparent lack of genes for other terminal oxidases raises the intriguing problem of what could be the nature of the oxidase activity manifested in the Zm6-*cydB* strain, and apparently terminating the bc_1 branch. Speculation that the cytochrome c peroxidase gene product might function instead of alternative oxidase is plausible. Yet it was not possible to demonstrate any relation of the cytochrome bc_1 branch to the hydrogen peroxide resistance of the *Z. mobilis* cells. However, recent study by Charoensuk *et al*. (2011), reported an electron transport chain-linked NADH-dependent peroxidase activity in a thermotolerant *Z. mobilis* strain. Therefore, it may be concluded that the cytochrome *c* peroxidase activity might largely depend on the strain and culture conditions.

It is possible that the rapid, yet energetically inefficient respiratory chain in *Z. mobilis* helps to prevent oxidative stress in aerobically growing culture. This hypothesis is in a good agreement with studies by FT-IR spectroscopy discussed in Chaper 3.3. Macromolecular components, analyzed by FT-IR spectroscopy, like cell membrane lipids, proteins, and nucleic acids, are the primary molecular targets of reactive oxygen species during oxidative stress (Avery, 2011). In all analyzed *Z. mobilis* strains, lipid concentrations were higher under aerobic growth conditions - for example the content of lipids in *Z. mobilis* parent strain Zm-6 was 4% and 2% dry weight (DW) under aerobic and anaerobic growth conditions respectively. It is known that the increase of lipid content is one of cells responses to stress. Thus, there is a good reasson to assume that *Z. mobilis* respiratory chain may help to prevent oxidative stress under aerobic conditions.

4.2 Aerobic growth of the respiratory mutant strains

Opposite to what may be expected, *ndh* deficiency resulted in slight increase of *Z. mobilis* biomass yield, i.e. $Y_{X/S}$, cell yield normalized with respect to glucose consumption, and dramatic stimulation of aerobic growth. The mutant strain Zm6-*ndh* grew substantially faster than Zm6, at the end of the exponential phase typically reaching a threefold higher biomass concentration (Fig. 2, Chapter 3.1). However, the downshift of pO_2 that occurred during the growth of Zm6 was much larger than that seen in the mutant, indicating a higher respiration rate of the parent culture. Accordingly, the mutant culture showed an increased aerobic ethanol yield ($Y_{P/S}$, Table 2, Chapter 3.1), because more reducing equivalents were diverted towards ethanol synthesis due to very low oxygen uptake rate. In general, the aerobic growth of the *ndh*-deficient mutant strain resembled that of Zm6 in the presence of cyanide (Kalnenieks *et al*., 2000, 2003). Cyanide typically caused the growth stimulation of Zm6 after a prolonged lag phase, when, following an initial period of complete inhibition, the re-emerging respiration reached 30–50 % of the respiration rate in the control culture (Kalnenieks *et al*., 2000). Our present results with the Zm6-*ndh* strain tend to support the hypothesis that the stimulating effect result simply from inhibition of the bulk oxygen consumption, since the oxygen uptake in the *ndh* mutant strain is too low for any measurable impact of oxidative phosphorylation. We therefore suggest that the observed elevation of the aerobic growth rate and moderate rise of biomass yield ($Y_{X/S}$) of *Z. mobilis* does not result from extra ATP generation by oxidative phosphorylation, but occurs whenever the NADH flux is redirected from respiration to ethanol synthesis, so that less acetaldehyde, the toxic precursor of ethanol (Wecker & Zall, 1987), is accumulated in the culture. The role of acetaldehyde is futher discussed in Chapter 4.3.

Despite the similar respiration capacity of aerobically cultivated *Z. mobilis* cytochrome *bd* or cytochrome bc_1 mutant strains, hypothetically one of these electron transport pathway branches might be poorly coupled to proton translocation, thus resulting in lower ATP outcome and decrease of the aerobic growth yields. However, as it is discussed in Chapter 3.4 a series of aerobic batch cultivations did not support such a hypothesis. Calculated aerobic growth yields of wild-type strain, cytochrome *bd* and cytochrome bc_1 respiratory mutants revealed very similar Yx/s values around 13-15 $g*mol^{-1}$ in all strains. Apparently *Z. mobilis* aerobic growth could not be

improved by knocking out any particular respiratory branch. These results do not support existence of one major, energetically inefficient electron transport branch that might cause the observed poor aerobic growth and lack of oxidative phosphorylation in growing *Z. mobilis* culture.

4.3 The physiological role of acetaldehyde

Previous suggestion that the observed elevation of the aerobic growth rate and biomass yield ($Y_{X/S}$) of *Z. mobilis ndh* mutant occurs because less acetaldehyde is accumulated in the culture was reinforced by the finding that also vigorous aeration of of Zm6 cultures improved the aerobic growth rate. As described in Capter 3.1, under strictly anaerobic conditions, the growth curves of Zm6 and *ndh* mutant strain were identical, but the aerobic behavior of the two strains differed substantially. In shaken flasks without hyperventilation Zm6 at the early stationary phase accumulated acetaldehyde 33 mM and grew much slower than the mutant strain. In the mutant strain, due to its low respiration rate, accumulation of acetaldehyde was negligible; its concentration at the end of the batch cultivation did not exceed 0.6 mM. In addition hyperventilation of the shaken flask cultures barely affected the growth of *ndh* mutant yet greatly improved that of Zm6. Similarly low acetaldehyde concentration in both hyperventilated cultures suggest that either a low rate of acetaldehyde generation (as in Zm6-*ndh* mutant) or an efficient removal of acetaldehyde (as in the hyperventilated Zm6) is of prime importance for aerobic growth stimulation in *Z. mobilis.*

Notably, the aerobic growth stimulation of Zm6 never extended beyond the limits imposed by its fermentative catabolism. Therefore experiments with the hyperventilation of the shaken flask cultures once again demonstrated that, even at very low acetaldehyde concentrations, the respiratory chain did not contribute to the aerobic batch growth of *Z. mobilis.* Thus, acetaldehyde acting as a potent inhibitor of growth is not the key factor that causes the deficiency of oxidative phosphorylation in growing *Z. mobilis*.

4.4 The physiological role of Z. mobilis H^+-dependent ATPase

Long-lasting question why, *Z. mobilis* respiratory system does not appear to participate in ATP synthesis during aerobic growth might be related to an impaired aerobic ATP turnover: either the H^+-dependent ATPase for some reasons is unable to turn to ATP synthesis, or the newly synthesized ATP gets rapidly hydrolysed by other reactions. Apparently, the rate of the excess ATP hydrolysis must be equal to the difference between ATP production by catabolic reactions and its utilization by anabolic processes. *Z. mobilis* possess several ATP-hydrolysing enzymes: periplasmic nucleotidase(s), acid and alkaline phosphatases, and the membrane H^+-dependent ATPase (Reyes & Scopes, 1991). The H^+-dependent ATPase contributes up to 20% of the overall ATP turnover in *Z. mobilis* cells and has been considered as partly responsible for the uncoupled growth (Reyes & Scopes, 1991). The previously reported increase of *Z. mobilis* anaerobic growth yield in the presence of the H^+-dependent inhibitor DCCD (Kalnenieks *et al*., 1987) indicates that H^+-dependent ATPase hydrolysing activity may be competing with the biosynthetic ATP demand in anaerobically growing culture. However such a competition for ATP under aerobic conditions is quite an opposite to what have been reported for other facultatively anaerobic bacteria. For example, even 10-100 micromolar DCCD concentrations are inhibitory to the aerobic growth of *E.coli,* a typical representative of a facultatively anaerobic microorganism that posseses oxidative phosphorylation (Singh & Bragg, 1974). Our results, where we monitored the time course of the intracellular ATP concentration after the addition of 50 micromolar DCCD (Chapter 3.4., Fig. 2), show that DCCD addition caused a pronounced increase of the ATP intracellular concentration in all *Z. mobilis* strains. These results strongly indicate that the hydrolysing activity of the H^+-dependent ATPase is taking place in *Z. mobilis* also under aerobic conditions. This surprising finding, yet not reported for *Z. mobilis*, was dramatically different to what we obtained with *E.coli.* DCCD addition to aerobically growing *E. coli* culture*,* caused a transient decrease of ATP intracellular concentration in complete agreement with the expected operation of its ATPase in the direction of ATP synthesis. So far, under anaerobic conditions a similar ATP dissipating mechanism was suggested earlier also for obligately fermentative *Streptococcus bovis* - another example of uncoupled growth among bacteria (Russel & Strobel, 1990). It has been shown that in *S. bovis*, H^+-dependent ATPase is the major free energy-spilling reaction under conditions of excess glucose (Russel & Cook, 1995).

The observed rise of growth yield in *Z. mobilis* (Chapter 3.4) was both due to increase of specific growth rate and a simultaneous decrease of glucose consumption caused by addition of DCCD. That is in a good agreement with previous reports (Ugurbil *et al*., 1978). DCCD caused a partial inhibition of glucose consumption, therefore interaction with the H^+-dependent ATPase remains as the only feasible explanation for the increase of ATP level, shown in Fig. 1 (Chapter 3.4). Apparently, by rapidly supplying ADP for glycolysis, H^+-dependent ATPase also contributes to the high glycolytic flux observed in the E-D pathway. During aerobic growth on glucose, the rapidly operating E-D pathway presumably generates too high phosphorylation potential for the weakly coupled respiratory system to shift the H^+-dependent ATPase towards ATP synthesis, by this preventing oxidative phosphorylation. At the same time, by supplying the large amounts of ADP, H^+-dependent ATPase facilitates the rapid operation of the E-D pathway. Therefore, uncoupled growth is not just an intrinsic property of anaerobically cultivated *Z. mobilis*, but can also be used to describe the inefficient aerobic growth of this very untypical facultatively anaerobic microorganism.

4.5 Kinetic modeling of the E-D pathway

Increase of the intracellular ATP concentration accompanying the decrease of glycolytic flux observed in Chapter 3.4, indicated that energy-dissipating reactions (ATP consumption) might control glycolytic flux in the E-D pathway. In order to examine this hypothesis one should use a kinetic model of the E-D pathway to quantitatively estimate the impact of ATP consuming reaction rate on glycolytic flux *via* metabolic control analysis (MCA). The only existing kinetic model of E-D pathway published so far was focused on the aspects of interaction between the engineered nonoxidative part of the pentose phosphate pathway for xylose utilization and the native *Z. mobilis* E-D glycolysis, assuming constant intracellular concentrations of the essential metabolic cofactors ADP, ATP, $NAD(P)^+$ and NAD(P)H (Altintas *et al.,* 2006). Such an assumption significantly limits general applicability of the model and in particular to study *Z. mobilis* uncoupled metabolism. Thus it was necessary to create kinetic model of the E-D pathway *de novo* by incorporating adenylate and nicotinamide nucleotide metabolism. Moreover, unlike in previous attempts (see Altintas *et al.,* 2006), the equilibrium constants were

introduced in all enzyme rate equations to obey the thermodynamic constraints of the Haldane relationship, during parameter optimisation.

The final version of our optimized model (hereafter – the optimized model) gave a specific glucose uptake rate of 4.9 g g^{-1} h^{-1}, that was close to experimentally observed values. Evaluation of the difference between the initially assumed (Osman *et al*., 1987) and optimized *Vf* values (Table 2, in chapter 3.5) revealed that, for the majority of enzymes, these remained within a factor of three of the starting estimate and lie within the range of values reported across batch fermentation in several works (Osman *et al.,* 1987, De Graaf *et al*., 1999). For the majority of enzymes, the initially assumed values for *Vf* rose during optimization and approached the values seen in French-press extracts reported earlier (Algar & Scopes, 1985). To evaluate the created model after parameter optimisation, glycolytic fluxes of the optimized E-D model was compared to those reported earlier for *Z. mobilis* in various experimental studies.

First of all, the kinetics of glycolysis *in situ* was reproduced by inserting the E-D pathway enzyme activities in French-press extracts reported by Algar & Scopes (1985) into the optimized model. With these new enzyme activities, the model also reached steady state with a glycolytic flux corresponding to an *in situ* rate of 5.2 g g^{-1} h^{-1}. This was in the range of the optimized model and earlier observations, where *Z. mobilis* was grown on different initial glucose concentrations, with the reported specific glucose uptake rates slightly below 5.5 g g^{-1} h^{-1} (Rogers *et al*., 1979). More detailed examination of the optimized model by simulating consumption of 1 M glucose in cell-free extracts reported by Algar & Scopes (1985), revealed that glycolytic flux obtained *in silico* was very similar to that in the *in vitro* experiment (detailed description of these results is available in Chapter 3.5). Remerkably, the intermediate concentrations obtained by *in silico* simulation, were reasonably close to those reported in ^{31}P NMR studies, indicating that computational simulations of the E-D pathway in cell-free extracts reliably simulate the situation *in situ* (Barrow *et al*., 1984). Therefore, there seems to be no specific „metabolite tunelling“ required for the E-D pathway to proceed, and instead *Z. mobilis*, with respect to its central glycolytic pathway, can be adequately described as a „bag of enzymes“.

It is important to mention, that since there are currently no E-D pathway models available in public databases, the developed kinetic model has potential not only for application in *Z. mobilis* metabolic studies and engineering, but can also

serve as a basis for the development of models for other microorganisms possessing this type of glycolytic pathway.

4.6 Do energy-dissipating reactions control glycolytic flux in E-D pathway?

Model analysis primarily was focused to reveal if energy-dissipating reactions (ATP consumption) controls glycolytic flux in E-D pathway. By using metabolic control analysis of the E-D pathway this assumption was confirmed revealing that generalized ATP consuming reaction exert a major control over glycolytic flux with C_i^J values 36% and 71% for the optimized and the cell free extract model respectively (results discussed in Chapter 3.5). This result strongly resembles previous experimental observations with growing *E. coli*, suggesting that the majority of flux control (>75%) resides not inside but outside the glycolytic pathway, i.e., with the enzymes that hydrolyze ATP (Koebmann *et al.,* 2002). This allows to speculate that anabolic reactions, in combination with ATP dissipation, control the glycolysis also during the uncoupled growth of *Z. mobilis*.

The results in Chapter 3.5 show that the relationship between ATP concentration and glycolytic flux is not affected by the respiratory deletions. Their regulatory pattern of the E-D pathway and catabolic ATP yield per unit of consumed glucose is the same. The extent to which metabolite concentrations can be maintained relatively constant as fluxes change is a measure of metabolic homoeostasis that is quantified by co-response coefficient (Hofmeyr *et al,* 1993; Cornish-Bowden & Hofmeyr, 1994; Thomas & Fell, 1996, 1998). Obtained results reveal that at the highest glycolytic flux considered (about 4.6 g/g/h, log value 1.53), the co-response coefficient is approximately -4.0. This shows that at this point, ATP homeostasis is poor, since a 1% increase in glycolytic flux, due to rise of the ATP-dissipating activity would be associated with a 4% decrease in ATP concentration. At a flux of about 3.9 g/g/h, the co-response coefficient is smaller in magnitude, close to -1.0, where a 1% increase in glycolytic flux is linked to a 1% decrease in ATP concentration. At the lowest glycolytic flux obtained with the lowest ATPase activities (3.0 g/g/h, log value 1,1), the co-response coefficient is about -0.23, so that ATP homeostasis is much improved in that it takes a 4% change in glycolytic flux to produce a 1% change in ATP concentration in the opposite direction.

4.7 Putative energy dissipating mechanisms

Finding the key role of the H^+-dependent ATPase does not solve completely the problem of energy dissipation during uncopled growth. It is clear that H^+-dependent ATPase does not dissipate energy but, instead, converts it into the form of transmembrane proton-motive force (Δp). Therefore, hydrolysing activity of the H^+-dependent ATPase should inevitably lead to an increase of Δp, which subsequently raises the question of its dissipation mechanisms. Taking into account the similarity of metabolic behaviour, as well as the akin role of H^+-dependent ATPase for the energy dissipation pathway in between *Z. mobilis* and *S. bovis*, the presence of a futile proton cycle in *Z. mobilis* a priori seems realistic, and deserves further examination. Perhaps, high proton leakage with impaired maintenance of the proton-motive force contributes to the lack of the oxidative phosphorylation in aerobically growing *Z. mobilis* cultures. Studies of membrane permeability, in *Z. mobilis* so far have focussed mainly on the non-specific, membrane-disrupting effects of ethanol that may also facilitate discussed proton leakage. The detrimental action of ethanol at high concentrations on the permeability of *Z. mobilis* plasma membrane was extensively studied in the 1980s (Osman & Ingram, 1985; Osman *et al*., 1987). It was shown that ethanol causes an increase in the rate of leakage of small molecules and ions, including protons. The accumulation of ethanol during fermentation may be responsible for the gradual collapse in ΔpH seen in batch cultures grown on media with high (20%) glucose concentration during the stationary growth phase (Osman *et al*., 1987). Apparently, ethanol decreases the barrier function and resistance of the plasma membrane, and thus probably adds to the energetic uncoupling at some stages of growth. However, since the energy dissipation in *Z. mobilis* occurs also at very low concentration of ethanol under aerobic conditions, it still cannot be regarded as the clue to the uncoupled growth phenomenon. Therefore the leakage of cytoplasmic membrane most likely would not be sufficient for futile spilling of the generated transmembrane Δp.

Paradoxically, however, the possible Δp-dissipating effect of carbon dioxide, the second major end product of *Z. mobilis* catabolism, has not been analysed. Several papers about the effect of CO_2 on fermentation performance of *Z. mobilis* (see e.g., Nipkow *et al*., 1985; Veeramallu & Agrawal, 1986), as well as on that of yeast, *E. coli* and some other bacteria (Janda & Kotyk, 1985; Lacoursiere *et al*., 1986) were

published in the 1980s. They describe complex inhibitory and uncoupling effects of carbon dioxide on the culture growth and product synthesis, yet do not consider the putative mechanisms at the membrane level. *Z. mobilis* is one of the most rapid producers of CO_2 among microorganisms. Apparently, the major part of CO_2 leaves the cell by passive diffusion in the form of a neutral molecule. Measurements with erythrocytes suggest that the lipid bilayer of the cell membrane does not represent a serious diffusion barrier for CO_2 (Forster *et al*., 1998). At the same time, part of the generated CO_2 in the cytoplasm might undergo hydration in the reaction, catalysed by carbonic anhydrase (Merlin *et al*., 2003), with subsequent dissociation of carbonic acid into a proton and bicarbonate anion. Knowing the respective equilibrium constants (Mills & Urey, 1940; Merlin *et al*., 2003), and taking 6.4 for the intracellular pH, we can estimate that, under equilibrium conditions, approximately 10% of carbon dioxide in *Z. mobilis* should be present in the form of bicarbonate anion. Export of bicarbonate anions from the cell would represent an efficient pathway of Δp dissipation, equivalent to import of protons: a unit negative charge would be translocated into the external medium, decreasing $\Delta\psi$, while a proton would be left behind in the cytoplasm, diminishing the transmembrane pH gradient. However futher experimental studies are needed to confirm this hypothesis.

4.8 Approaches to increase the glycolytic flux in Z. mobilis E-D pathway

Besides the importance of H^+-dependent ATPase in *Z, mobilis* metabolism metabolic control analysis carried out with the kinetic model also demonstrates, why attempts in the past to increase the glycolytic flux through over-expression of various E-D pathway enzymes have been unsuccessful. Negligible flux control coefficients for the majority of the E-D pathway reactions (Chapter 3.5), partly explain why over-expression of a few intuitively chosen enzymes have not resulted in the increase of glycolytic flux (Arfman *et al.,* 1992; Snoep *et al.,* 1995). According to MCA, only the PDC reaction exerts substantial control with C_i^J values reaching 27% in the optimized model. Calculated effects of GAPD, PGK, PGM, ADHI, ADHII and PDC over-expression on glycolytic flux in the E-D pathway and comparison to values calculated from experimental data revealed little or no increase of glycolytic flux in almost all recombinant strains without addition of IPTG. The significantly higher flux control coefficient for the PDC reaction suggested that over-expression of this enzyme more

than 3-fold, may lead to an increase of glycolytic flux of almost 23%. However such an increase was not observed experimentally; furthermore, experimental observations revealed that more than 10 fold increase of enzyme activity after addition of 2mM IPTG slowed down glycolysis by up to 25%. Given our calculations, this indirectly confirms earlier suggestions that the protein burden effect indeed might be a serious side effect of over-expression of enzymes possessing little or no control over the flux in E-D pathway. In *Z. mobilis* enzymes involved in fermentation comprise as much as 50% of total protein (Algar & Scopes, 1985), so the protein burden effect might be even more pronounced than in other microorganisms where wild-type levels of catabolic enzymes are not so great. Nevertheless, according to calculations from model data, simultaneous overexpression of PDC, ENO, PGM below the protein burden threshold has the potential to increase the glycolytic flux up to 25 % (6.6 g/g/h). Moreover, since ATP disipating reactions possess major control over glycolytic flux and at the same time are responsible for ATP dissipation under uncoupled growth conditions, overexpression of H^+-dependent ATPase within physiological capacity, making growth more uncoupled, might serve as the appropriate strategy to increase the glycolytic flux in *Z. mobilis*.

This clearly demonstrates that *in silico* metabolic analysis could serve not only to understand better *Z. mobilis* physiology but also to develop efficient metabolic engineering strategies avoiding the protein burden effect.

Accordingly, the latest results of *Z. mobilis* modeling achieved at different scales, by combining stoichiometric, thermodynamic and kinetic models of central metabolism illustrate the relevance of *in silico* analysis for microorganisms producing biorenewables (Please see the review article in Appendix).

5 CONCLUSIONS

1. The respiratory chain of *Z. mobilis* contains only one functional NAD(P)H dehydrogenase, product of the *ndh* gene.

2. The electron transport chain in *Z. mobilis* contains at least two electron pathways to oxygen that are simmilar to the respect of low-efficiency of energy-coupling.

3. Inhibition of respiration stimulates *Z. mobilis* aerobic growth partly due to reduction of toxic acetaldehyde in the media.

4. The absence of oxidative phosphorylation activity in aerobically growing *Z. mobilis* primarilly results from insufficient degree of energy coupling between the proton-motive force and the F_0F_1 type H^+-dependent ATPase.

5. By using available kinetic parameters and incorporating reactions related to ATP and NADH metabolism, for the first time the kinetic model of E-D pathway was built and deposited in bio-model database.

6. The developed *in silico* kinetic model of the *Z. mobilis* E-D pathway was able to achieve good agreement with previous experimental studies both *in situ* and *in vitro* conditions, therefore having the potential to serve as a basis for the development of models for other microorganisms possessing this type of glycolytic pathway.

7. MCA revealed that the majority of flux control resides outside the E-D pathway, suggesting that glycolytic flux in *Z. mobilis* during the uncoupled growth is largely controled by ATP consuming reactions.

8. The model identifies set of enzymatic reactions overexpression of wich might increase the glycolytic flux in *Z. mobilis*.

6 MAIN THESIS FOR DEFENCE

1. The absence of oxidative phosphorylation activity in aerobically growing *Z. mobilis* primarily results from insufficient degree of energy coupling between the proton-motive force and the F_0F_1 type H^+-dependent ATPase, preventing its switching from ATP hydrolysis to ATP synthesis under conditions, when a rapid substrate-level production of ATP takes place in the E-D pathway.

2. There is no specific „metabolite tunelling“ required for the E-D pathway to proceed, and *Z. mobilis*, in respect to its central glycolytic pathway, can be adequately described as a „bag of enzymes“.

3. Major control of the rapid *Z. mobilis* catabolism resides outside the E-D pathway. The pathway is largely controled by ATP consuming reactions and F_0F_1 type H^+-dependent ATPase in particular.

7 LIST OF ORIGINAL PUBLICATIONS

1. *M.M. Toma, J. Raipulis, I. Kalnina and R. Rutkis (2005) Does Probiotic Yeast Act as Antigenotoxin?* ***Food Technol. Biotechnol.*** *43 (3) 301-305.*
2. *U. Kalnenieks, N. Galinina, M.M. Toma, J.L. Pickford, R. Rutkis, R.K. Poole (2006) Respiratory behaviour of a Zymomonas mobilis adhB::kanr mutant supports the hypothesis of two alcohol dehydrogenase isoenzymes catalysing opposite reactions.* ***FEBS Letters*** *580: 5084-5088.*
3. *U. Kalnenieks, R. Rutkis, Z. Kravale, I. Strazdina, N. Galinina (2007) High aerobic growth with low respiratory rate: The ndh-deficient Zymomonas mobilis.* ***Journal of Biotechnology*** *131(2S), S264.*
4. *U. Kalnenieks, N. Galinina, I. Strazdina, Z. Kravale, J.L. Pickford, R. Rutkis, R.K. Poole (2008) NADH dehydrogenase deficiency results in low respiration rate and improved aerobic growth of Zymomonas mobilis.* ***Microbiology*** *154: 989-994.*
5. *N. Galinina, Z. Lasa, I. Strazdina, R. Rutkis, U. Kalnenieks (2012) Effect of ADH II deficiency on the intracellular redox homeostasis in Zymomonas mobilis.* ***The Scientific World Journal****,Volume 2012, Article ID 742610,1-6.*
6. *I. Strazdina, Z. Kravale, N. Galinina, R. Rutkis, R. K. Poole, U. Kalnenieks (2012) Electron transport and oxidative stress in Zymomonas mobilis respiratory mutants.* ***Archives of Microbiology,*** *194: 461–471.*
7. *M. Grube, R. Rutkis, M. Gavare, Z. Lasa, I. Strazdina, N. Galinina, and U. Kalnenieks (2012) Application of FT-IR Spectroscopy for Fingerprinting of Zymomonas mobilis Respiratory Mutants.* ***Spectroscopy: An International Journal,*** *27 (5-6): 581 – 585. DOI:10.1155/2012/163712.*
8. *Odzina I., Rubina T., Rutkis R., Kalnenieks U., Stalidzans E., (2010) Structural model of biochemical network of Zymomonas mobilis adaptation for glycerol conversion into bioethanol.* ***Applied Information and Communication Technologies****, Proceedings, of the 4-th International Scientific Conference Applied information and communication technologies. Jelgava, Latvija, 22-23. April, 2010, 50 – 54.*
9. *Rutkis R., Kalnenieks U, Stalidzans E.,. Fell D.A.I (2013) Kinetic modeling of Zymomonas mobilis Entner-Doudoroff pathway: insights into control and functionality.* ***Microbiology,*** *159: 2674–2689. DOI 10.1099/mic.0.071340-0*
10. *Kalnenieks U, Pentjuss A, Rutkis R, Stalidzans E, Fell D.A. (2014) Modeling of Zymomonas mobilis central metabolism for novel metabolic engineering strategies.* ***Frontiers of microbiology,*** *5:1-7. DOI: 10.3389/fmicb.2014.00042.*
11. *Rutkis R., Galinina N., Strazdina I., Kalnenieks U. (2014) The inefficient aerobic energetics of Zymomonas mobilis: identifying the bottleneck.* ***Journal of Basic Microbiology****, In Press. DOI 10.1002/jobm.201300859.*

8 APPROBATION OF THE RESEARCH

8.1 International

1. Meeting on Microbial Respiratory Chains. „**How is the respiratory chain of *Zymomonas mobilis* supplied with NADH?“** (R. Rutkis, Ņ. Galinina, U. Kalnenieks), March, 19-22 2006, Tomar, Portugal.
2. 13th European Congress on Biotechnology. „**High aerobic growth with low respiratory rate: The ndh-deficient *Zymomonas mobilis.“* (**Reinis Rutkis, Uldis Kalnenieks, Inese Strazdina, Zane Kravale un Nina Galinina). September 16-19, 2007, Barcelona, Spain.
3. The 9th International Conference on Systems Biology. „**The regulatory function of metabolic chanelling: ethanol cycle in *Zymomonas mobilis.“*** (U. Kalnenieks, R. Rutkis, Ņ. Galiņina, Toma, Malda Maija), August 22-28, 2008, Goteborg, Sweden.
4. The 11th international conference on Systems Biology. **„Oxidative stress response in several respiratory mutants of *Zymomonas mobilis.“*** (Inese Strazdina, Zane Kravale, Nina Galinina, Reinis Rutkis un Uldis Kalnenieks), October 10-15, 2010, Edinburgh, Scotland.
5. 30th European Congress on Molecular Spectroscopy. **„Use of FT-IR spectroscopy data for systems analysis of *Zymomonas mobilis* metabolism.“ (**M. Grube, M. Gavare, R. Rutkis, U. Kalnenieks, N. Mironova-Ulmane). 29th of August– 3rd September 3, 2010, Florence Italy.
6. 7th European conference on bacterial respiratory chains. „**The unresolved respiratory chain of *Zymomonas mobilis.“* (**Zane Lasa, Inese Strazdina, Reinis Rutkis, Nina Galinina, Robert K. Poole and Uldis Kalnenieks), May 11-14, 2011 Lund, Sweden.
7. FEMS, The 4th Congress of European Microbiologists. **„Aerobic energy metabolism in *Zymomonas mobilis* respiratory knock-out mutants.“** (M. Grube, R. Rutkis, M. Gavare, Z. Lasa, I. Strazdina, N. Galinina and U. Kalnenieks) June 26-30, 2011, Geneve, Switcerland.
8. 14th European Conference on the Spectroscopy of Biological Molecules. **„FT-IR spectroscopy analysis of continuously cultivated *Z. mobilis* respiratory mutants.“ (**M. Grube, R. Rutkis, M. Gavare, Z. Lasa, I. Strazdina, N. Galinina, U. Kalnenieks), 28th August – 3rd September, 2011, Koimbra, Portual.
9. Microbial stress: from molecules to systems. **„Aerobic growth and electron transport in *Zymomonas mobilis*: the role of cytochrome *c* peroxidase.“** (I. Strazdina, N. Galinina, R. Rutkis, and U. Kalnenieks), May 10-13, 2012 Belgirate, Italy.

8.1 National

1. R. Rutkis, N. Galinina and U. Kalnenieks. **Alternative electron transfer pathways in bacteria: *Z. mobilis* example**. 64th Scientific Conference of the University of Latvia, February, 2006. Riga, Latvia.

2. R. Rutkis, N. Galinina and U. Kalnenieks. **Physyological properties of *Z. mobilis* respiratory chain mutant**. 65th Scientific Conference of the University of Latvia, February, 2007. Riga, Latvia.

3. R. Rutkis. **Microbial biofuels – inovations and alternatives**. 66th Scientific Conference of the University of Latvia, February, 2008. Riga, Latvia.

4. R. Rutkis, I. Strazdina, Z. Kravale, N. Galinina and U. Kalnenieks. **Oxidative stress in *Zymomonas mobilis***. 68th Scientific Conference of the University of Latvia, February, 2010. Riga, Latvia.

5. R. Rutkis, I. Strazdina, N. Galinina and U. Kalnenieks. ***Zymomonas mobilis* uncoupled growth under aerobic conditions.** 71th Scientific Conference of the University of Latvia, February, 2013. Riga, Latvia. Riga, Latvia.

9 ACKNOWLEDGEMENTS

This work was funded by Latvian ESF projects 2009/027/1DP/1.1.1.2.0/09/APIA/VIAA/128 and 2009/0138/1DP/1.1.2.1.2/09/IPIA/VIAA/004.

I acknowledge Prof. David Fell for a great support in mathematical modeling of *Z. mobilis* biochemical networks and specially my supervisor Prof. Uldis Kalnenieks for his assistance in the entire reearch process.

10 REFERENCES

Algar, E. M. and Scopes, R. K. (1985) Studies on cell-free metabolism: Ethanol production by extracts of *Zymomonas mobilis*. J Biotechnol, 2, 275–287.

Altintas, M. M., Eddy, C. K., Zhang, M., JMcMillan, J. D. and Kompala, D. S. (2006) Kinetic Modeling to Optimize Pentose Fermentation in *Zymomonas mobilis*. Biotechn and Bioengg, 94, 273–295.

An, H., Scopes, R.K., Rodriguez, M., Keshav, K.F. and Ingram, L.O. (1991) Gel electrophoretic analysis of *Zymomonas mobilis* glycolytic and fermentative enzymes: identification of alcohol dehydrogenase II as a stress protein. J Bacteriol. 173, 5975–5982.

Anderson R.F., Patel K.B., Evans M.D .(1985) Int J Radiat Biol, 48, 495-504.

Arfman N., Worrell V. and Ingram L. O. (1992) Use of the *tac* promoter and *lacP* for the controlled expression of *Zymomonas mobilis* fermentative genes in *Escherichia coli* and *Zymomonas mobilis*. J Bacteriol, 174, 7370-7378.

Atkinson, D. E. (1968) The Energy Charge of the Adenylate Pool as a Regulatory Parameter. Interaction with Feedback Modifiers. Biochem, 7, 4030–4034.

Avery S. V. (2011) Molecular targets of oxidative stress. Biochem J, 434, 201— 210.

Barrow, K. D., Collins, G. J., Norton R. S., Rogers P. L., and Smith G. M. (1984) ^{31}P Nuclear magnetic resonance studies of the fermentation of glucose to ethanol by *Zymomonas mobilis*. J biol chem 259, 5711–5716.

Belaich, J.P. and Senez, J.C. (1965) J Bacteriol, 89, 1195–1200.

Bergmeyer, H. U., Gawehn, K., Grassl, M. (1974) Glutathione reductase. Bergmeyer HU (ed) Methods of enzymatic analysis, vol 1. Academic Press, New York, 465–466.

Bisswanger, K. (2002) Enzyme kinetics – principles and methods. Wiley-VCH Verlag GmbH, Weinheim (Federal Republic of Germany).

Bringer-Meyer, S. and Sahm, H. (1989) Junctions of catabolic and anabolic pathways *in Zymomonas mobilis*: phosphoenolpyruvate carboxylase and malic enzyme. Appl Microbiol Biotechnol, 31, 529–536.

Bringer-Meyer, S., Schimz, K. L., Sahm, H. (1986) Pyruvate decarboxylase from *Zymomonas mobilis*: Isolation and partial characterization. Arch Microbiol, 146, 105–110.

Casazza, J.P. and Veech, R. L. (1986) The interdependence of glycolytic and pentose cycle intermediates in ad libitum fed rats. J Biol Chem 261(2), 690–698.

Charoensuk, K., Irie, A., Lertwattanasakul, N., Sootsuwan, K., Thanonkeo, P., Yamada, M. (2011) Physiological importance of cytochrome *c* peroxidase in ethanologenic thermotolerant *Zymomonas mobilis*. J Mol Microbiol Biotechnol, 20, 70–82.

Cornish-Bowden, A. and Hofmeyr, J-H.S. (1994) Determination of control coefficients in intact metabolic systems. Biochem J, 298, 367–375.

Dawes, E. A., Medgley, M. and Ishaq, M. (1970) The endogenous metabolism of anaerobic bacteria. Final technical report for Contract no. DAJA 37-67-C-0567. European research office, U S Army, 60, 31–62.

Dawes, E. A., Ribbons, D. W. and Large, P. J. (1966) The route of ethanol formation in *Zymomonas mobilis*. Biochem J, 98, 795–803.

De Graaf, A. A., Striegel, K., Wittig, R. M., Laufer, B., Schmitz, G., Wiechert, W., Sprenger, G. A., Sahm, H. (1999) Metabolic state of *Zymomonas mobilis* in glucose-, fructose-, and xylose-fed continuous cultures as analysed by ^{13}C- and ^{31}P-NMR spectroscopy. Arch Microbiol, 171, 371–385.

Desiniotis, A., Kouvelis, V. N., Davenport, K., Bruce, D., Detter, C., Tapia, R., Han, C., Goodwin, L. A., Woyke, T. and other authors (2012) Complete genome sequence of the ethanol-producing *Zymomonas mobilis* subsp. mobilis centrotype ATCC 29191. J Bacteriol, 194, 5966-7.

Di Marco, A. A. and Romano A. H. (1985) D-Glucose transport system of *Zymomonas mobilis*. Appl Environ Microbiol, 49, 151–157.

Dien, B. S., Cotta, M. A. and Jeffries, T. W. (2003) Bacteria engineered for fuel ethanol production: current status. Appl Microbiol Biotechnol, 63, 258–266.

Doelle, H. W. (1982) Kinetic Characteristics and Regulatory Mechanisms of Glucokinase and Fructokinase from *Zymomonas mobilis*. European J Appl Microbiol Biotechnol, 14, 241–246.

Ellfolk, N. and Soininen, R. (1970) *Pseudomona*s cytochrome *c* peroxidase. Acta Chem Scand, 24, 2126–2136.

Flamholz, A., Noor E., Bar-Even A., Liebermeister W., Milo R. (2013) Glycolytic strategy as a tradeoff between energy yield and protein cost. Proc Natl Acad Sci USA, 110, 10039–10044.

Forster, R. E., Gros, G., Lim, L., Ono, Y. and Wunder, M. (1998) The effect of 4,40-diisothiocyanato-stilbene-2,20-disulfonate on CO2 permeability of the red blood cell membrane. Proc Natl Acad Sci USA, 95, 15815–15820.

Fuhrer, T., Fischer, E. and Sauer, U. (2005) Experimental identification and quantification of glucose metabolism in seven bacterial species. J Bacteriol, 187, 1581–1590.

Gibss, M. and DeMoss, R. D. (1954) Anaerobic dissimilation of ^{14}C-labelled glucose and fructose by *Pseudomonas lindneri*. J Biol Chem, 207, 689–694.

Gonzalez-Flecha, B. and Demple, B. (1994) Intracellular generation of superoxide as a by-product of *Vibrio harveyi* luciferase expressed in *Escherichia coli*. J Bacteriol, 176, 2293–2299.

Gonzalez-Flecha, B. and Demple, B. (1995) Metabolic sources of hydrogen peroxide in aerobically growing *Escherichia coli*. J Biol Chem, 270, 13681–13687.

Grube, M., Bekers, M., Upite D., and Kaminska, E. (2002) IR-spectroscopic studies of *Zymomonas mobilis* and levan precipitate. Vibrat Spectrosc, 28, 277—285.

Hofmeyr, J-H. S., Cornish-Bowden, A., Rohwrer, J. M. (1993) Taking enzyme kinetics out of control: putting control into regulation. Eur J Biochem, 212, 833–837.

Hoops, S., Sahle, S., Gauges, R., Lee, C., Pahle, J., Simus, N., Singhal, M., Xu, L., Mendes, P. and Kummer, U. (2006) COPASI — a COmplex PAthway SImulator. Bioinf, 22, 3067–74.

Janda, S. and Kotyk, A. (1985) Effects of suspension density on microbial metabolic processes. Folia Microbiol, 30, 465–473.

Jones, C. W., and Doelle, H. W. (1991) Kinetic control of ethanol production by *Zymomonas mobilis*. Appl Microbiol Biotechnol, 35, 4–9.

Kalnenieks, U. (2006) Physiology of *Zymomonas mobilis*: some unanswered questions. Adv In Microb Physiol, 51, 73-117.

Kalnenieks, U., De Graaf, A. A., Bringer-Meyer, S., Sahm. H. (1993) Oxidative phosphorylation in *Zymomonas mobilis*. Arch Microbiol, 160, 74–79.

Kalnenieks, U., Galinina, N., Bringer-Meyer, S. and Poole, R. K. (1998) Membrane D-lactate oxidase in *Zymomonas mobilis*: evidence for a branched respiratory chain. FEMS Microbiol Lett, 168, 91–97.

Kalnenieks, U., Galinina, N., Toma, M. M. and Poole, R. K. (2000) Cyanide inhibits respiration yet stimulates aerobic growth of *Zymomonas mobilis*. Microbiol, 146, 1259–1266.

Kalnenieks, U., Galinina, N., Toma, M. M. and Skards, I. (1996) Electron transport chain in aerobically cultivated *Zymomonas mobilis*. FEMS Microbiol Lett, 143, 185–189.

Kalnenieks, U., Toma, M. M., Galinina, N. and Poole, R. K. (2003) The paradoxical cyanide-stimulated respiration of *Zymomonas mobilis*: cyanide sensitivity of alcohol dehydrogenase (ADH II). Microbiol, 149, 1739–1744.

Kalnenieks, U. Z., Pankova, L. M. and Shvinka, J. E. (1987) Proton motive force in *Zymomonas mobilis*. Biokhimiya (USSR), 52, 720–723.

Kelly, M. J., Poole, R. K., Yates, M. G. and Kennedy, C. (1990) Cloning and mutagenesis of genes encoding the cytochrome bd terminal oxidase complex *Azotobacter vinelandii*: mutants deficient in the cytochrome d complex are unable to fix nitrogen in air. J Bacteriol, 172, 6010–6019.

Kim, I. S., Barrow, K. D. and Rogers, P. L. (2000) Kinetic and nuclear magnetic resonance studies of xylose metabolism by recombinant *Zymomonas mobilis* ZM4(pZB5). Appl Environ Microbiol, 66, 186–193.

Kim, Y. J., Song, K. -B. and Rhee, S. K. (1995) A novel aerobic respiratory chain-linked NADH oxidase system in *Zymomonas mobilis*. J Bacteriol, 177, 5176–5178.

Kinoshita, S., Kakizono, T., Kadota, K., Das, K., Taguchi, H. (1985) Purification of two alcohol dehydrogenases from *Zymomonas mobilis* and their properties. Appl Microbiol Biotechnol, 22, 249–254.

Koebman, B. J., Westerhoff, H. V., Snoep, J. L., Nilsson, D., Jensen P. R. (2002) The glycolytic flux in *Escherichia coli* is controlled by the demand for ATP. J Bacteriol, 184, 3909–3916.

Korshunov, S., Imlay, J.A. (2010) Two sources of endogenous hydrogen peroxide in *Escherichia coli*. Mol Microbiol, 75, 1389–1401.

Kosako, Y., Yabuuchi, E., Naka, T., Fujiwara, N. and Kobayashi, K. (2000) Proposal of *Sphingomonadaceae* fam. nov., consisting of *Sphingomonas Yabuuchi* et al. 1990, *Erythrobacter* Shiba and Shimidu 1982, *Erythromicrobium* Yurkov et al. 1994, *Porphyrobacter* Fuerst et al. 1993, *Zymomonas* Kluyver and van Niel 1936, and *Sandaracinobacter* Yurkov et al. 1997, with the type genus *Sphingomonas* Yabuuchi et al. 1990. Microbiol Immunol, 44, 563–575.

Kouvelis, V. N., Davenport, K. W., Brettin, T. S., Bruce, D., Detter, C., Han, C. S., Nolan, M., Tapia, R., Damoulaki, A. and other authors (2011) Genome sequence of the ethanol-producing *Zymomonas mobilis* subsp. pomaceae lectotype strain ATCC 29192. J Bacteriol, 193, 5050–5051.

Lacoursiere, A., Thompson, B. G., Kole, M. M., Ward, D. and Gerson, D. F. (1986) Effects of carbon dioxide concentration on anaerobic fermentations of *Escherichia coli.* Appl Microbiol Biotechnol, 23, 404–406.

Lau, M .W., Gunawan, C., Balan, V., Dale, B. E., (2010). Comparing the fermentationperformance of *Escherichia coli* KO11, *Saccharomyces cerevisiae* 424A(LNH-ST) and *Zymomonas mobilis* AX101 for cellulosic ethanol production. Biotechnol for Biof, 3, 11.

Lawford, H. G. and Rousseau, J. D. (2000) Comparative energetics of glucose and xylose metabolism in recombinant *Zymomonas mobilis*. Appl Biochem Biotechnol, 84-86, 277–293.

Lawford, H. G. and Stevnsborg, N. (1986) Pantothenate limitation does not induce uncoupled growth of *Zymomonas* in chemostat culture. Biotechnol Lett, 8, 345–350.

Leif, H., Sled, V. D., Ohnishi, T., Weiss, H. and Friedrich, T. (1995) Isolation and characterization of the proton-translocating NADH : ubiquinone oxidoreductase from *Escherichia coli*. Eur J Biochem, 230, 538–548.

Liang, C. C., Lee, W. C. (1998) Characteristics and transformation of *Zymomonas mobilis* with plasmid pKT230 by electroporation. Bioprocess Eng, 19, 81–85.

Markwell, M. A. K., Haas, S. M., Bieber, L. L. and Talbert, N. E. (1978) A modification of the Lowry procedure to simplify protein determination in membrane and lipoprotein samples. Anal Biochem, 87, 206–210.

Matsushita, K., Ohnishi, T. and Kaback, R. H. (1987) NADH-ubiquinone oxidoreductases of the *Escherichia coli* aerobic respiratory chain. Biochem, 26, 7732–7737.

Merlin, C., Masters, M., McAteer, S. and Coulson, A. (2003) Why is carbonic anhydrase essential to *Escherichia coli*? J Bacteriol, 185, 6415–6424.

Mills, G.A. and Urey, H.C. (1940) The kinetics of isotopic exchange between carbon dioxide, bicarbonate ion, carbonate ion and water. J Am Chem Soc, 62, 1019–1026.

Nantapong, N., Kugimiya, Y., Toyama, H., Adachi, O. and Matsushita, K. (2004) Effect of NADH dehydrogenase-disruption and over-expression on respiration-related metabolism in *Corynebacterium glutamicum* KY 9714. Appl Microbiol Biotechnol, 66, 187–193.

Neveling, U., Klasen, R., Bringer-Meyer, S. and Sahm, H. (1998) Purification of the pyruvate dehydrogenase multienzyme complex of *Zymomonas mobilis* and identification and sequence analysis of the corresponding genes. J Bacteriol, 180, 1540–1548.

Nipkow, A., Sonnleitner, B. and Fiechter, A. (1985) Effect of carbon dioxide on growth of *Zymomonas mobilis* in continuous culture. Appl Microbiol Biotechnol, 21, 287–291.

Osman, Y. A. and Ingram, L. O. (1985) Mechanism of ethanol inhibition of fermentation in *Zymomonas mobilis* CP4. J Bacteriol, 164, 173–180.

Osman, Y. A., Conway, T., Bonetti, S.J., Ingram, L.O. (1987) Glycolytic flux in *Zymomonas mobilis*: Enzyme and metabolite levels during batch fermentation. J Bacteriol, 169, 3726–3736.

Pankova, L. M., Shvinka, Y. E., Beker, M. E. and Slava, E. E. (1985) Effect of aeration on *Zymomonas mobilis* metabolism. Mikrobiologiya (USSR), 54, 141–145.

Pappas, K. M., Kouvelis, V. N., Saunders, E., Brettin, T. S., Bruce, D., Detter, C., Balakireva, M., Han, C. S., Savvakis, G. and other authors (2011) Genome sequence of the ethanol-producing *Zymomonas mobilis* subsp. mobilis *lectotype* strain ATCC 10988. J Bacteriol, 193, 5051– 5052.

Pawluk, A., Scopes, R. K., Griffiths-Smith K. (1986) Isolation and properties of the glycolytic enzymes from *Zymomonas mobilis*: The five enzymes from glyceraldehyde-3-phosphate dehydrogenase through pyruvate kinase. Biochem J, 238, 275–281.

Pentjuss, A., Odzina, I., Kostromins, A., Fell, D., Stalidzans, E., Kalnenieks, U. (2013) Biotechnological potential of respiring *Zymomonas mobilis*: A stoichiometric analysis of its central metabolism. J Biotechnol, 165, 1-10.

Poole, R. K. and Cook, G.M. (2000) Redundancy of aerobic respiratory chains in bacteria? Routes, reasons and regulation. Adv Microb Physiol, 43, 165–224.

Reyes, L., Scopes, R. K. (1991) Membrane-associated ATPase from *Zymomonas mobilis*: Purification and characterization. Biochim Biophys Acta, 1068, 174–178.

Rogers, P. L., Lee, K. J., Skotnicki, M. L. and Tribe, D.E. (1982) Ethanol production by *Zymomonas mobilis*. Adv Biochem Eng, 23, 37–84.

Rohwer, J. M., Hanekom, A. J., Hendrik, S., Hofmeyr, J. H. S. (2006) A universal rate equation for systems biology. Proceed 2nd Intern ESCEC Symp, 175–187.

Russell, J. B. and Cook, G. M. (1995) Energetics of bacterial growth: balance of anabolic and catabolic reactions. Microbiol Rev, 59, 48–62.

Russell, J. B. and Strobel, H. J. (1990) ATPase-dependent energy spilling by the ruminal bacterium, *Streptococcus bovis*. Arch Microbiol, 153, 378–383.

Sahm, H. and Bringer-Meyer, S. (1987) Continuous ethanol production by *Zymomonas mobilis* on an industrial scale. Acta Biotechnol, 7, 307–313.

Sahm, H., Bringer-Meyer, S. and Sprenger, G. (1992) The genus *Zymomonas*. In: The Prokaryotes, 3, 2287–2301.

Saint Girons I, Gilles, A. M., Margarita, D., Michelsonlf, S., Monnot, M., Fermandjianl, S., Danchin, A. and Bârzu, O. (1987) Structural and catalytic characteristics of *Escherichia coli* adenylate kinase. J biol chem, 262, 622–629.

Sambrook, J., Fritsch, E. F., Maniatis, T. (1989) Molecular cloning: a laboratory manual, 2nd edn. Cold Spring Harbor Laboratory, Cold Spring Harbor.

Scopes, R. K. (1983) An iron-activated alcohol deyhdrogenase. FEBS Lett, 156, 303–306.

Scopes, R. K. (1984) Use of differential dye-ligand chromatography with affinity elution for enzyme purification: 2-Keto-3-deoxy-6-phosphogluconate aldolase from *Zymomonas mobilis*. Anal Biochem, 136, 525–529.

Scopes, R. K. (1985) 6-Phosphogluconolactonase from *Zymomonas mobilis*. FEBS Lett, 193, 185–188.

Scopes, R. K. (1997) Allosteric control of *Zymomonas mobilis* glucose-6-phosphate dehydrogenase by phosphoenolpyruvate. Biochem J, 326, 731–735.

Scopes, R. K. and Griffiths-Smith K. (1984) Use of differential dye-ligand chromatography with affinity elution for enzyme purification: 6-Phosphogluconate dehydratase from *Zymomonas mobilis*. Anal Biochem, 136, 530–534.

Scopes, R. K. and Griffiths-Smith, K. (1986) Fermentation capabilities of Zymomonas *mobilis* glycolytic enzymes. Biotechnol Lett, 8, 653–656.

Scopes, R. K., Testolin, V., Stoter A, Griffiths-Smith, K., Algar, E.M. (1985) Simultaneous purification and characterization of glucokinase, fructokinase and glucose 6-phosphate dehydrogenase from *Zymomonas mobilis*. Biochem J, 228, 627–634.

Seo, J. S., Chong, H., Park, H. S., Yoon, K. O., Jung, C., Kim, J. J., Hong, J. H., Kim, H., Kim, J, H. and other authors (2005) The genome sequence of the ethanologenic bacterium *Zymomonas mobilis* ZM4. Nat Biotechnol, 23, 63–68.

Singh, A. P. and Bragg, P. D. (1974) Effect of dicyclohexylcarbodiimide on growth and membrane-mediated processes in wild type and heptose-deficient mutants of *Escherichia coli* K-12. J Bacteriol, 119, 129-137.

Small, L. J. and Kascer, H. (1993) Responses of metabolic systems to large changes in enzyme activities and effectors. Eur J Biochem, 213, 613–624.

Snoep, J. L., Arfman, N., Yomano, L. P., Fliege, R. K., Conway, T. and Ingram, L. O. (1994) Reconstitution of glucose uptake and phosphorylation in a glucose-negative mutant of *Escherichia coli* by using *Zymomonas mobilis* genes encoding the glucose facilitator protein and glucokinase. J Bacteriol, 176, 2133–2135.

Snoep, J. L., Arfman, N., Yomano, L. P., Westerhoff, H. V., Conway, T. and Ingram, L. O. (1996) Control of glycolytic flux in *Zymomonas mobilis* by glucose 6-phosphate dehydrogenase activity. Biotechnol Bioeng, 51, 190–197.

Snoep, J. L., Yomano, L, P., Westerhoff, H, V., Ingram. L. O. (1995) Protein burden in *Zymomonas mobilis*: negative flux and growth control due to overproduction of glycolytic enzymes. Microbiol 141, 2329–2337.

Sootsuwan, K., Lertwattanasakul, N., Thanonkeo, P., Matsushita, K., Yamada, M. (2008) Analysis of the respiratory chain in ethanologenic *Zymomonas mobilis* with a cyanide-resistant bd-type ubiquinol oxidase as the only terminal oxidase and its possible physiological roles. J Mol Microbiol Biotechnol, 14:163–175.

Sprenger, G. (1996) Carbohydrate metabolism in *Zymomonas mobilis*: a catabolic highway with some scenic routes. FEMS Microbiol Lett, 145, 301–307.

Strohdeicher, M., Neuß, B., Bringer-Meyer, S., Sahm, H. (1990) Electron transport chain of *Zymomonas mobilis*. Interaction with the membrane-bound glucose dehydrogenase and identification of ubiquinone 10. Arch Microbiol, 154, 536–543.

Strohhäcker, J., De Graaf, A.A., Schoberth, S. M., Wittig, R. M. and Sahm, H. (1993) ^{31}P Nuclear magnetic resonance studies of ethanol inhibition in *Zymomonas mobilis*. Arch Microbiol, 159, 484–490.

Swings, J. and De Ley, J. (1977) The biology of *Zymomonas*. Bacteriol Rev, 41, 1–46.

Thomas, S. and Fell, D. A. (1998) A control analysis exploration of the role of ATP utilisation in glycolytic-flux control and glycolytic-metabolite-concentration regulation. Eur J Biochem, 258, 956–967.

Thomas, S. and Fell., D. A. (1996) Design of metabolic control for large flux changes. J Theor Biol, 182, 285–298.

Ugurbil, K., Rottenberg, H., Glynn, P., and Shulman, R. G. (1978) ^{31}P nuclear magnetic resonance studies of bioenergetics and glycolysis in anaerobic *Escherichia coli* cells. Proc Nati Acad Sci USA, 75, 2244-2248.

Veeramallu, U. K. and Agrawal, P. (1986) The effect of CO_2 ventilation on kinetics and yields of cell-mass and ethanol in batch cultures of *Zymomonas mobilis.* Biotechnol Lett, 8, 811–816.

Viikari, L. (1986) By-product formation in ethanol fermentation by *Zymomonas mobilis*. Technical Research Centre of Finland, Publication 27.

Viikari, L. (1988) Carbohydrate metabolism in *Zymomonas*. CRC Crit Rev Biotechnol, 7, 237–261.

Viikari, L. and Berry, D. R. (1988) Carbohydrate metabolism in *Zymomonas*. Crit Rev Biotechnol, 7, 237–261.

Wang, G. and Maier, R. J. (2004) An NADPH quinone reductase of *Helicobacter pylori* plays an important role in oxidative stress resistence and host colonization. Infect Immun, 72, 1391–1396.

Wecker, M. S. A. and Zall, R. R. (1987) Production of acetaldehyde by *Zymomonas mobilis*. Appl Environ Microbiol, 53, 2815–2820.

Weisser, P., Kramer, R., Sahm, H. and Sprenger, G. A. (1995) Functional expression of the glucose transporter of *Zymomonas mobilis* leads to restoration of glucose and fructose uptake in *Escherichia coli* mutants and provides evidence for its facilitator action. J Bacteriol, 177, 3351–3354.

White, D. C., Sutton, S. D. and Ringelberg, D. B. (1996) The genus *Sphingomonas*: physiology and ecology. Curr Opin Biotechnol, 7, 301–306.

Yagi, T. (1991) Bacterial NADH-quinone oxidoreductases. J Bioenerg Biomembr, 23, 211–225.

Yang, S., Pappas, K. M., Hauser, L. J. L. and M. L, Chen, G. L., Hurst, G. B., Pan, C., Kouvelis, V. N., Typas, M. A., Pelletier, D. A., Klingeman, D. L., Chang, Y. J., Samatova, N. F., Brown, S. D. (2009) Improved genome annotation for *Zymomonas mobilis*. Nat Biotechnol 27:893–894.

11 APPENDIX

frontiers in
MICROBIOLOGY

PERSPECTIVE ARTICLE
published: 05 February 2014
doi: 10.3389/fmicb.2014.00042

Modeling of *Zymomonas mobilis* central metabolism for novel metabolic engineering strategies

Uldis Kalnenieks[1]*, Agris Pentjuss[2], Reinis Rutkis[3], Egils Stalidzans[2,3] and David A. Fell[4]

[1] Institute of Microbiology and Biotechnology, University of Latvia, Riga, Latvia
[2] Department of Computer Systems, Latvia University of Agriculture, Jelgava, Latvia
[3] SIA TSI-IT, Jelgava, Latvia
[4] Department of Biological and Medical Sciences, Oxford Brookes University, Oxford, UK

Edited by:
Katherine M. Pappas, University of Athens, Greece

Reviewed by:
Jason Warren Cooley, University of Missouri, USA
Patrick Hallenbeck, University of Montreal, Canada

***Correspondence:**
Uldis Kalnenieks, Institute of Microbiology and Biotechnology, University of Latvia, Kronvalda boulevard 4, Riga, LV-1586, Latvia
e-mail: kalnen@lanet.lv

Mathematical modeling of metabolism is essential for rational metabolic engineering. The present work focuses on several types of modeling approach to quantitative understanding of central metabolic network and energetics in the bioethanol-producing bacterium *Zymomonas mobilis*. Combined use of Flux Balance, Elementary Flux Mode, and thermodynamic analysis of its central metabolism, together with dynamic modeling of the core catabolic pathways, can help to design novel substrate and product pathways by systematically analyzing the solution space for metabolic engineering, and yields insights into the function of metabolic network, hardly achievable without applying modeling tools.

Keywords: stoichiometric modeling, elementary flux modes, kinetic modeling, systems biology, metabolic engineering, Entner-Doudoroff pathway, central metabolism, *Zymomonas mobilis*

INTRODUCTION

Zymomonas mobilis, a member of the family of *Sphingomonadaceae*, is an unusual facultatively anaerobic Gram-negative bacterium, which has a very efficient homoethanol fermentation pathway. High ethanol yields, outstanding ethanol productivity (exceeding by 3–5 fold that of yeast; see Rogers et al., 1982), and tolerance to high ethanol and sugar concentrations, keep *Z. mobilis* in the focus of biotechnological research over four decades. The complete genome sequence of *Z. mobilis* ZM4, consisting of a single circular chromosome of 2,056,416 bp, was reported by Seo et al. (2005), followed by the genomes of several other strains (Kouvelis et al., 2009; Pappas et al., 2011; Desiniotis et al., 2012). Its small genome size, together with high specific rate of sugar catabolism via the Entner–Doudoroff (ED) pathway, and a relatively simple central metabolic network, make *Z. mobilis* a promising candidate for metabolic engineering (Sprenger, 1996; Rogers et al., 2007). Currently, recombinant *Z. mobilis* capable of fermenting pentose sugars is regarded as a potential alternative to yeast and recombinant *Escherichia coli* for ethanol biofuel synthesis from agricultural and forestry waste (Dien et al., 2003; Panesar et al., 2006; Rogers et al., 2007; Lau et al., 2010).

In spite of the seeming simplicity of its metabolism, *Z. mobilis* is a bacterium with an interesting physiology (Kalnenieks, 2006), posing researchers some long-standing challenges. Its extremely rapid glucose catabolism, far exceeding the biosynthetic demands of the cell, and the presence of an active respiratory chain with a low apparent P/O ratio (Bringer et al., 1984; Strobdeicher et al., 1990; Kalnenieks et al., 1993) are major manifestations of its so-called uncoupled growth. There are serious gaps in our understanding of the mechanistic basis of uncoupled growth, and in particular, the reason for the low degree of coupling in the respiratory chain of *Z. mobilis*.

Mathematical modeling and *in silico* simulations are the most powerful tools of systems biology for understanding of complex metabolic phenomena, and often lead to novel, counterintuitive conclusions. A quantitative picture of physiology and metabolism is a key for rational, model-driven metabolic engineering. Some of the different metabolic modeling approaches that can support the design of novel metabolic engineering strategies are summarized in **Figure 1** (for reviews see: Schuster et al., 2000; Lin et al., 2010; Santos et al., 2011; Schellenberger et al., 2011; Rohwer, 2012). Compared with qualitative, pathway-oriented approaches, computational network analyses can enforce strict mass, energy and redox balancing and give an overall stoichiometric equation for predicted conversions (c.f. de Figueiredo et al., 2009). Here we outline recent advances and perspectives from applying such systems biology approaches to the physiology of *Z. mobilis*. We discuss some recent results gained by stoichiometric and kinetic modeling of its central metabolism, and their potential application to the design of novel substrate pathways, synthesis of novel products, and to the study of the uncoupled growth phenomenon *per se*.

RECONSTRUCTION OF *Z. mobilis* CENTRAL METABOLIC NETWORK

Two medium-scale (Tsantili et al., 2007; Pentjuss et al., 2013) and two genome-scale stoichiometric reconstructions of *Z. mobilis* (Lee et al., 2010; Widiastuti et al., 2010) have been reported so far, representing instances of the left and center panels of **Figure 1** respectively. These reconstructions were based on the available genome annotation (Seo et al., 2005; Kouvelis et al., 2009) and provided an overall picture of *Z. mobilis* metabolism. The recent reconstruction made by Pentjuss et al. (2013) was focussed solely on the reactions of central metabolism and for the first time for *Z. mobilis* provided simulation-ready model files. That

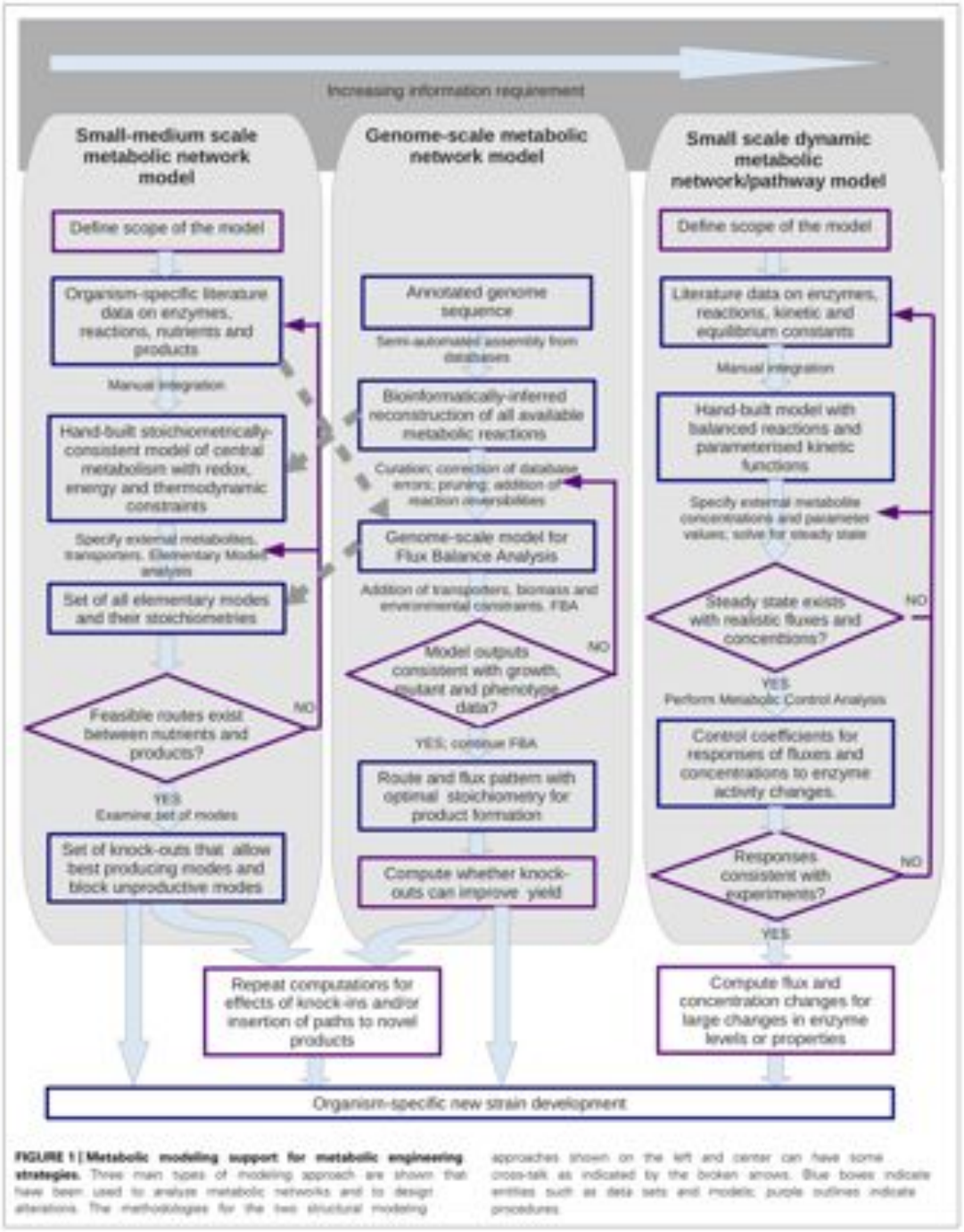

FIGURE 1 | Metabolic modeling support for metabolic engineering strategies. Three main types of modeling approach are shown that have been used to analyse metabolic networks and to design alterations. The methodologies for the two structural modeling approaches shown on the left and center can have some cross-talk as indicated by the broken arrows. Blue boxes indicate entities such as data sets and models; purple outlines indicate procedures.

decreased the scale, yet allowed an improvement in the accuracy of reconstruction, by combining the genome-derived information with the preexisting biochemical evidence on *Z. mobilis*, available mostly for the reactions of catabolism and central metabolism.

Notably, several key reactions of central metabolism, common for the majority of the chemoheterotrophic, facultatively anaerobic bacteria, are absent in *Z. mobilis*. The Embden–Meyerhof–Parnas (EMP) glycolytic pathway is not operating in this bacterium. Absence of the EMP pathway has been confirmed by [1-^{13}C]glucose experiments (Fuhrer et al., 2005), and furthermore, the gene for phosphofructokinase is lacking in the genome (Seo et al., 2005). *Z. mobilis* is the only known microorganism that uses the ED pathway anaerobically in place of the EMP glycolysis. Since the EMP pathway produces two ATP per glucose while the ED produces only one, it might seem that *Z. mobilis* suffers from ATP deficiency. However, it has been recently shown by means of thermodynamic analysis that, for a given glycolytic flux, the ED pathway requires significantly less enzymatic protein than the EMP pathway (Flamholz et al., 2013). On the other hand, the amount of the ED pathway enzymes in *Z. mobilis* cell is reported to be very high, reaching 50% of the cell's soluble protein (Algar and Scopes, 1985; An et al., 1991). The high level of expression of the pathway together with its inherent speed, therefore, makes ATP production by the *Z. mobilis* ED pathway very rapid and, in fact, excessive for the needs of cell. Energy dissipation in order to regenerate ADP is thus essential for its balanced operation (Kalnenieks, 2006).

The TCA cycle is truncated, and consists of two branches, leading to 2-oxoglutarate and fumarate as the end products (Bringer-Meyer and Sahm, 1989). The genes for the 2-oxoglutarate dehydrogenase complex and malate dehydrogenase are absent (Seo et al., 2005), and accordingly, ^{13}C-labeling patterns of 2-oxoglutarate and oxaloacetate do not support cyclic function of this pathway in *Z. mobilis* (de Graaf et al., 1999). Also, the pentose phosphate pathway is incomplete: transaldolase activity is lacking (Feldmann et al., 1992; de Graaf et al., 1999). The activity of 6-phosphogluconate dehydrogenase, the first reaction of the oxidative part of the pentose phosphate pathway, was reported to be very low (Feldmann et al., 1992). Subsequently, the corresponding gene (*gnd*) could not be identified in the sequenced genomes.

The aerobic redox cofactor balance and the function of electron transport chain represent yet another part of *Z. mobilis* metabolism that differs from that typically found in other bacteria. *Z. mobilis* is one of the few known bacteria in which both NADH and NADPH can serve as electron donors for the respiratory type II NADH dehydrogenase (ZMO1113; Bringer et al., 1984; Strohdeicher et al., 1990; Kalnenieks et al., 2008). Because of the truncated Krebs cycle, the ED pathway is the only source of reducing equivalents in catabolism, and therefore the electron transport chain competes for the limited NADH with the highly active alcohol dehydrogenases (Kalnenieks et al., 2006). Withdrawal of NADH from the alcohol dehydrogenase reaction would cause accumulation of acetaldehyde, which inhibits growth of aerobic *Z. mobilis* culture (Wecker and Zall, 1987). Nevertheless, this bacterium possesses a respiratory chain with high rates of oxygen consumption. The apparent P/O ratio of its respiratory chain is low (Bringer et al., 1984; Kalnenieks et al., 1993) though the mechanistic basis for that is not clear. However, for metabolic engineering purposes, an active, yet energetically inefficient electron transport has advantages for the needs of redox balancing during synthesis of novel products via metabolic pathways for which regeneration of $NAD(P)^+$ is essential, whereas the aerobic increase of biomass yield is unwanted.

QUEST FOR NOVEL SUBSTRATES AND PRODUCTS: STOICHIOMETRIC AND THERMODYNAMIC ANALYSIS

Much of the metabolic engineering in *Z. mobilis* has been devoted to broadening of its substrate spectrum and expanding its product range beyond bioethanol with a particular focus on the pathway of pentose sugar utilization for synthesis of bioethanol (Sprenger, 1996; Rogers et al., 2007). Advanced pentose-assimilating strains of *Z. mobilis* have been developed during the last couple of decades that can, in several respects, compete with the analogous recombinant strains of *E. coli* and *S. cerevisiae* (Lau et al., 2010). We were interested to explore the biotechnological potential of the low-efficiency respiratory chain of this bacterium for expanding its substrate and product spectrum.

Based on a medium-scale reconstruction of central metabolism (Pentjuss et al., 2013), stoichiometric modeling was used to search the whole solution space of the model, finding maximum product yields and the byproduct spectra with glucose, xylose, or glycerol as the carbon substrates for respiring cultures (**Figure 1**, left hand side). This was done by Flux Balance Analysis approach, using the COBRA Toolbox (Schellenberger et al., 2011). The stoichiometric analysis suggested several metabolic engineering strategies for obtaining products, such as glycerate, succinate, and glutamate that would use the electron transport chain to oxidize the excess NAD(P)H, generated during synthesis of these metabolites. Oxidation of the excess NAD(P)H would also be needed for synthesis of ethanol from glycerol.

It is essential, however, to complement the stoichiometric analysis with estimation of the thermodynamic feasibility of the underlying reactions. Glycerol utilization can serve as an example. Being a cheap, renewable carbon source, a byproduct of biodiesel technology, glycerol represents an attractive alternative substrate for *Z. mobilis* metabolic engineering. It is not expected to have serious growth-inhibitory effects, and also, little genetic engineering seems to be needed to make it consumable by *Z. mobilis*, and to channel it into the rapid ED pathway. Conversion of glycerol to ethanol by *Z. mobilis* would require expression of a heterologous transmembrane glycerol transporter and a glycerol kinase. Its genome contains genes for the two subsequent conversion steps, glycerolphosphate dehydrogenase and triose phosphate isomerase, leading to the ED intermediate glyceraldehyde-3-phosphate although, their overexpression might be needed. The further reactions from the glyceraldehyde-3-phosphate to ethanol represent a part of *Z. mobilis* natural ethanologenic pathway, and should be both rapid and redox-balanced. The extra NAD(P)H, generated by the glycerolphosphate dehydrogenase reaction could be oxidized by the respiratory chain. If succinate is the desired product

(Peréjaan et al., 2013), the extra reducing equivalents could be used for reduction of fumarate by the respiratory fumarate reductase.

The pathway from glycerol to glyceraldehyde-3-phosphate via phosphorylation and following oxidation and isomerization steps is presented in biochemistry textbooks as the pathway of glycerol catabolism after breakdown of triacylglycerols in higher animals and humans (see e.g., Lehninger Principles of Biochemistry, 6th edition, Fig. 17-4). Though feasible from the stoichiometric point of view, it reveals problems when subjected to thermodynamic analysis. The equilibrium of the glycerolphosphate dehydrogenase reaction appears to be shifted very much toward formation of glycerol phosphate. *In silico* kinetic simulations of glycerol uptake for a putative engineered *Z. mobilis* demonstrate a dramatic accumulation of glycerol-3-phospate, reaching concentrations of several molar even at a high rate of NAD(P)H withdrawal by the respiratory chain (Rutkis et al., unpublished). Apparently, while the estimated overall stoichiometry of aerobic glycerol conversions is correct, thermodynamic analysis suggests the need to search for alternative reaction sequences to avoid excessive intracellular accumulation of metabolites.

AEROBIC ELEMENTARY FLUX MODES OF THE PENTOSE PHOSPHATE PATHWAY

A metabolic network can function according to many different pathway options. Elementary flux mode (EFM) analysis has emerged as a systems biological tool that dissects a metabolic network into its basic building blocks, the EFMs (Schuster et al., 2000, 2002). All metabolic capabilities in steady states represent a weighted average of the EFMs, which are the minimal sets of enzymes that can each generate a valid steady state. The EFM approach has proved to be efficient for designing sets of knock-out mutations in order to minimize unwanted metabolic functionality in the producer strains. For example, in engineered *E. coli*, EMF-based mutation analysis helped to eliminate catabolite repression and to increase carbon flux toward the target product ethanol (Trinh et al., 2008).

By decomposing a network of highly interconnected reactions, the EFM analysis may reveal unexpected flux options. Recently we applied EFM analysis to the interaction between the ED, pentose phosphate pathway and respiratory chain in an engineered *Z. mobilis*, which expresses heterologous *gnd* and enzymes for pentose conversion, using the metabolic modeling package ScrumPy (Poolman, 2006). We were interested in the EFMs that such non-growing engineered *Z. mobilis* might employ for aerobic catabolism of glucose and xylose. Analysis revealed several EFMs in respiring cells (**Figure 2**) that have considerable interest for study of aerobic energy-coupling in this bacterium. With both monosaccharides, knocking out *edd* (encoding 6-phosphogluconate dehydratase), and overexpressing heterologous *gnd* (encoding 6-phosphogluconate dehydrogenase), would lead to generation of additional NAD(P)H and CO_2 in the pentose phosphate pathway, while lowering the ethanol yield. Yet, most importantly, decrease of the ethanol yield would not be accompanied by accumulation of acetaldehyde and acetoin.

Thus, a simple EFM analysis suggests how to modify *Z. mobilis* aerobic metabolism so that its electron transport chain would receive more reducing equivalents without accumulation of inhibitory byproducts. Strains with such metabolic modifications might be very useful for study of the mechanisms underlying the uncoupled mode of oxidative phosphorylation in this bacterium.

KINETIC MODELING OF THE ENTNER–DOUDOROFF PATHWAY

Despite the diverse studies of *Z. mobilis* physiology and genetics, little has been done so far to combine the accumulated knowledge in a form of kinetic model of central metabolism that would be comparable to the existing models for *E. coli* and yeast, and could be used to develop efficient metabolic engineering strategies (c.f. **Figure 1**, right-hand panel). A kinetic model reported by Altintas et al. (2006) focussed mainly on the interaction between the heterologous enzymes of pentose phosphate pathway and the native *Z. mobilis* ED glycolysis. Providing predictions for optimization of expression levels of the heterologous genes, this study contributed to strategies for maximizing xylose conversion to ethanol. However, the authors assumed constant intracellular concentrations of all adenylate cofactors. Since the ED pathway itself is a major player in ANP and NAD(P)(H) turnover, this might lead to erroneous conclusions on the pathway kinetics and restrict the range of model application. The recent kinetic model by Rutkis et al. (2013): (i) treated the cofactor levels as variables, making the interplay between adenylate cofactor levels and the pathway kinetics explicit, and (ii) introduced equilibrium constants in the kinetic equations to account for the reversibility of reactions more correctly. Metabolic control analysis (MCA) carried out with the model pointed to the ATP turnover as a major bottleneck, showing that the ATP consumption (dissipation) exerts a high level of control over glycolytic flux under various conditions (Rutkis et al., 2013).

Indeed, experimental studies of the ED pathway flux have shown that moderate overexpression of the ED pathway and alcohol dehydrogenase genes do not affect the glycolytic flux (Arfman et al., 1992; Snoep et al., 1995). Larger increases of the expression levels even caused a decrease in flux, exerting also a negative impact on *Z. mobilis* growth rate (Snoep et al., 1995). This clearly indicated that glycolytic flux in *Z. mobilis* must be controlled at some point(s) outside the ED pathway itself. The negative effects of overexpression apparently did not result from intrinsically negative flux control coefficients of the ED enzymes, but were attributable to the protein burden effect (Snoep et al., 1995), whereby overexpression of an enzyme with a small flux control coefficient caused reductions in the expression of other enzymes that have a greater influence on the flux. These results together with MCA studies on the kinetic model suggested that, due to the negligible flux control coefficients for the majority of reactions, single enzymes of the ED pathway should not be considered as prime targets for overexpression to increase the glycolytic flux in *Z. mobilis* (Rutkis et al., 2013). The calculated effects of several glycolytic enzyme (*gap*, *pgk*, *pgm*) and both alcohol dehydrogenase isoenzyme (*adhA* and *adhB*) overexpression, in accordance with previous experimental observations, predicted little or no increase of glycolytic flux (Arfman et al., 1992; Snoep et al., 1995). The somewhat higher flux control coefficient for the pyruvate decarboxylase (*pdc*) reaction suggested

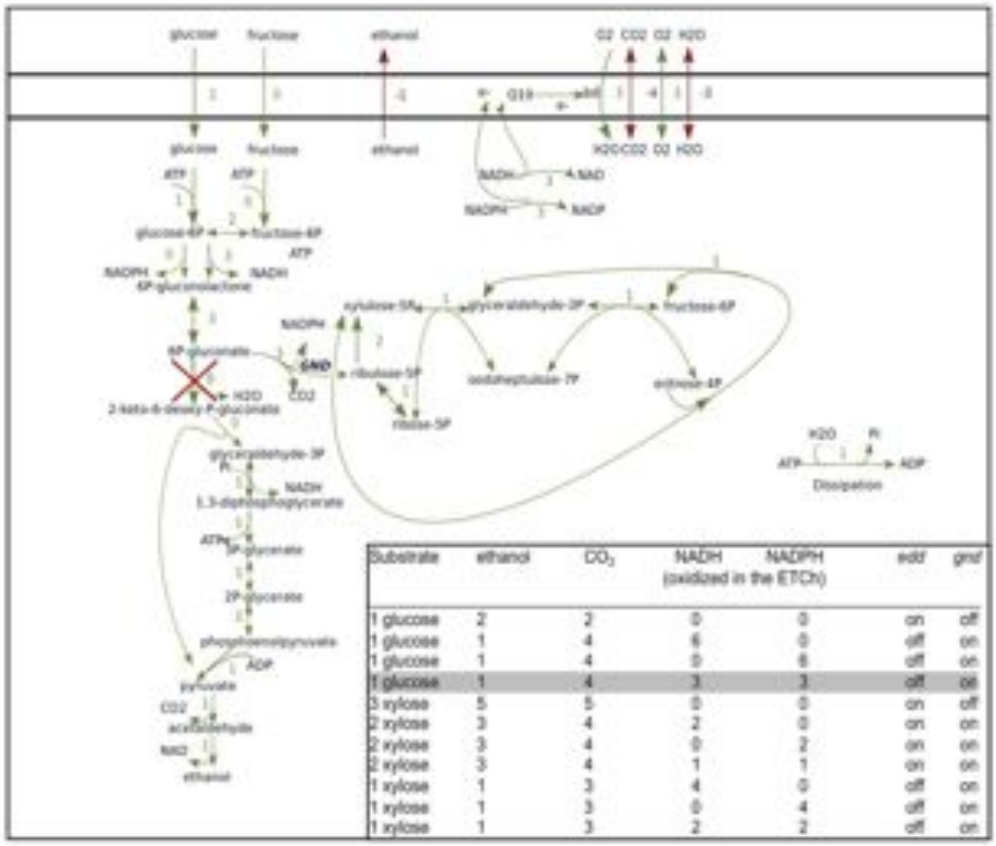

Substrate	ethanol	CO_2	NADH (oxidized in the ETCh)	NADPH (oxidized in the ETCh)	edd	gnd
1 glucose	2	2	0	0	on	off
1 glucose	1	4	6	0	off	on
1 glucose	1	4	0	6	off	on
1 glucose	1	4	3	3	off	on
3 xylose	5	5	0	0	on	off
2 xylose	3	4	2	0	on	on
2 xylose	3	4	0	2	on	on
2 xylose	3	4	1	1	on	on
1 xylose	1	3	4	0	off	on
1 xylose	1	3	0	4	off	on
1 xylose	1	3	2	2	off	on

FIGURE 2 | Elementary flux modes of aerobic glucose and xylose catabolism for a strain with engineered pentose phosphate pathway enzymes. Elementary flux mode for catabolism of glucose in cells with knocked-out *edd* and overexpressed heterologous *gnd* via the Entner-Doudoroff and pentose phosphate pathway, involving both NADH- and NADPH-oxidizing activity of the respiratory chain, is shown. ScrumPy modeling software EFM drawing algorithm (Pentjuss et al., unpublished) was used for visualization. Inset: complete list of elementary flux modes of glucose and xylose catabolism in *Z. mobilis*, involving the Entner-Doudoroff pathway, pentose phosphate pathway and the respiratory chain, with ethanol and carbon dioxide as the sole products. The explicitly shown elementary flux mode is shaded in gray.

that overexpression of this enzyme by more than 3-fold, might lead to an increase of glycolytic flux of almost 23% (Rutkis et al., 2013). However, quite the opposite was observed experimentally: approximately 10-fold increase of *pdc* was shown to slow down glycolysis by up to 25%, thereby implying that the protein burden might be a serious side effect of catabolic enzyme overexpression in *Z. mobilis*. Usually effects of protein burden are of minor importance in optimization of catabolic fluxes, due to relatively low concentrations of the enzymes in catabolic routes. This is not the case for *Z. mobilis* catabolism, however, since over 50% of the cell protein already is engaged in the function of the ED pathway (Algar and Scopes, 1985). Fortunately, flux control coefficient estimations still indicate a certain solution space for flux improvement: simultaneous overexpression of *pdc*, *eno*, *pgm* within the 3-fold range of initial enzyme activities (wich most probably would be below the putative protein burden threshold), has the potential to increase the glycolytic flux by up to 25% (to reach 6.6 *g* glucose, *g* dry wt^{-1}h^{-1}; Rutkis et al. (2013).

Obviously, another option would be to raise ATP dissipation. That could be done by overexpression of the H^+-dependent F_0F_1-ATPase, a major ATP-dissipating activity. Reyes and Scopes (1991) have estimated the F_0F_1-ATPase contribution being over 20% of the total intracellular ATP turnover. It should be noted, however, that overexpression of ATP-dissipating reaction(s) might disturb the intracellular ATP homeostasis, with successive suspension of glycolysis (by slowing down the first reaction of the ED pathway, phosphorylation of glucose). Co-response analysis indicates (Rutkis et al., 2013) that, at the highest glycolytic flux considered

(4.6 g/g/h), the cellular capacity to maintain the ATP homeostasis is close to its limit, since even 1% further increase of glycolytic flux due to rise of ATP dissipation would be associated with a 4% decrease in ATP concentration.

CONCLUSION

Although *Z. mobilis* metabolism has been subject to extensive research, and genome sequence data for several strains are now also available, it is only quite recently that modeling of its central metabolic network has started to gain momentum. These latest results of modeling *Z. mobilis* illustrate the relevance of combined stoichiometric, thermodynamic and kinetic analysis of central metabolism at different scales for microorganisms producing biorenewables. Concerted application of structural and dynamic modeling will help to identify targets for future metabolic engineering in a systematic manner, and provide novel insights into the biotechnological potential of this bacterium.

AUTHOR CONTRIBUTIONS

All authors have equally contributed to the manuscript and have accepted the final version to be published.

ACKNOWLEDGMENTS

This work was supported by the Latvian ESF projects 2009/0227/1DP/1.1.1.2.0/09/APIA/VIAA/128 and 2009/0138/1DP/1.1.2.1.2/09/IPIA/VIAA/004, and by the Latvian Council of Science project 536/2012.

REFERENCES

Algar, E. M., and Scopes, R. K. (1985). Studies on cell-free metabolism: ethanol production by extracts of *Zymomonas mobilis*. *J. Biotechnol.* 2, 275–287.

Altintas, M. M., Eddy, C. K., Zhang, M., McMillan, J. D., and Kompala, D. S. (2006). Kinetic modeling to optimize pentose fermentation in *Zymomonas mobilis*. *Biotechnol. Bioeng.* 94, 275–295. doi: 10.1002/bit.20843

An, H., Scopes, R. K., Rodriguez, M., Keshav, K. F., and Ingram, L. O. (1991). Gel electrophoretic analysis of *Zymomonas mobilis* glycolytic and fermentative enzymes: identification of alcohol dehydrogenase II as a stress protein. *J. Bacteriol.* 173, 5975–5982.

Arfman, N., Worrell, V., and Ingram, L. O. (1992). Use of the tac promoter and lacIq for the controlled expression of *Zymomonas mobilis* fermentative genes in *Escherichia coli* and *Zymomonas mobilis*. *J. Bacteriol.* 174, 7570–7578.

Bringer-Meyer, S., and Sahm, H. (1989). Junctions of catabolic and anabolic pathways in *Zymomonas mobilis*: phosphoenolpyruvate carboxylase and malic enzyme. *Appl. Microbiol. Biotechnol.* 31, 529–536.

Bringer, S., Finn, R. K., and Sahm, H. (1984). Effect of oxygen on the metabolism of *Zymomonas mobilis*. *Arch. Microbiol.* 139, 376–381.

de Figueiredo, L. F., Schuster, S., Kaleta, C., and Fell, D. A. (2009). Can sugars be produced from fatty acids? a test case for pathway analysis tools. *Bioinformatics* 25, 152–158. doi: 10.1093/bioinformatics/btn621

de Graaf, A. A., Striegel, K., Wittig, R. M., Laufer, B., Schmitz, G., Wiechert, W., et al. (1999). Metabolic state of *Zymomonas mobilis* in glucose-, fructose-, and xylose-fed continuous cultures as analysed by 13C- and 31P-NMR spectroscopy. *Arch. Microbiol.* 171, 371–385.

Desiniotis, A., Kouvelis, V. N., Davenport, K., Bruce, D., Detter, C., Tapia, R., et al. (2012). Complete genome sequence of the ethanol-producing *Zymomonas mobilis* subsp. *mobilis* centrotype ATCC 29191. *J. Bacteriol.* 194, 5966–5967. doi: 10.1128/JB.01398–1312

Dien, B. S., Cotta, M. A., and Jeffries, T. W. (2003). Bacteria engineered for fuel ethanol production: current status. *Appl. Microbiol. Biotechnol.* 63, 258–266. doi: 10.1007/s00253-003-1444-y

Felshansen, S., Sahm, H., and Sprenger, G. (1992). Pentose metabolism in *Zymomonas mobilis* wild-type and recombinant strains. *Appl. Microbiol. Biotechnol.* 38, 354–361.

Flamholz, A., Noor, E., Bar-Even, A., Liebermeister, W., and Milo, R. (2013). Glycolytic strategy as a tradeoff between energy yield and protein cost. *Proc. Natl. Acad. Sci. U.S.A.* 110, 10039–10044. doi: 10.1073/pnas.1215283110

Fuhrer, T., Fischer, E., and Sauer, U. (2005). Experimental identification and quantification of glucose metabolism in seven bacterial species. *J. Bacteriol.* 187, 1581–1590. doi: 10.1128/JB.187.5.1581–1590.2005

Kalnenieks, U. (2006). "Physiology of *Zymomonas mobilis*: some unanswered questions," in *Advances in Microbial Physiology*, Vol. 51, ed. R. K. Poole (London: Academic Press), 73–117. doi: 10.1016/S0065-2911(06)51002-1

Kalnenieks, U., de Graaf, A. A., Bringer-Meyer, S., and Sahm, H. (1993). Oxidative phosphorylation in *Zymomonas mobilis*. *Arch. Microbiol.* 160, 74–79.

Kalnenieks, U., Galinina, N., Strazdina, I., Kravale, Z., Pickford, J. L., Rutkis, R., et al. (2008). NADH dehydrogenase deficiency results in low respiration rate and improved aerobic growth of *Zymomonas mobilis*. *Microbiology* 154, 989–998. doi: 10.1099/mic.0.2007/012682-0

Kalnenieks, U., Galinina, N., Toma, M. M., Pickford, J. L., Rutkis, R., and Poole, R. K. (2006). Respiratory behaviour of a *Zymomonas mobilis* adhB::kanr mutant supports the hypothesis of two alcohol dehydrogenase isoenzymes catalysing opposite reactions. *FEBS Lett.* 580, 5084–5088. doi: 10.1016/j.febslet.2006.08.034

Kouvelis, V. N., Saunders, E., Brettin, T. S., Bruce, D., Detter, C., Han, C., et al. (2009). Complete genome sequence of the ethanol producer *Zymomonas mobilis* NCIMB 11163. *J. Bacteriol.* 191, 7140–7141. doi: 10.1128/JB.01084-09

Lau, M. W., Gunawan, C., Balan, V., and Dale, B. E. (2010). Comparing the fermentation performance of *Escherichia coli* KO11, *Saccharomyces cerevisiae* 424A(LNH-ST) and *Zymomonas mobilis* AX101 for cellulosic ethanol production. *Biotechnol. Biofuels* 3, 11. doi: 10.1186/1754-6834-3-11

Lee, K. Y., Park, J. M., Kim, T. Y., Yun, H., and Lee, S. Y. (2010). The genome-scale metabolic network analysis of *Zymomonas mobilis* ZM4 explains physiological features and suggests ethanol and succinic acid production strategies. *Microb. Cell Fact.* 9, 94. doi: 10.1186/1475-2859-9-94

Liu, S., Agren, R., Bordel, S., and Nielsen, J. (2010). Use of genome-scale metabolic models for understanding microbial physiology. *FEBS Lett.* 584, 2556–2564. doi: 10.1016/j.febslet.2010.04.052

Panesar, P. S., Marwaha, S. S., and Kennedy, J. F. (2006). *Zymomonas mobilis*: an alternative ethanol producer. *J. Chem. Technol. Biotechnol.* 81, 623–635. doi: 10.1002/jctb.1448

Pappas, K. M., Kouvelis, V. N., Saunders, E., Brettin, T. S., Bruce, D., Detter, C., et al. (2011). Genome sequence of the ethanol-producing *Zymomonas mobilis* subsp. *mobilis* lectotype strain ATCC 10988. *J. Bacteriol.* 193, 5051–5052. doi: 10.1128/JB.05395-11

Pentjuss, A., Odzina, I., Kostromins, A., Fell, D. A., Stalidzans, E., and Kalnenieks, U. (2013). Biotechnological potential of respiring *Zymomonas mobilis*: a stoichiometric analysis of its central metabolism. *J. Biotechnol.* 165, 1–10. doi: 10.1016/j.jbiotec.2013.02.014

Poolman, M. G. (2006). ScrumPy: metabolic modelling with python. *Syst. Biol.* 153, 375–378. doi: 10.1049/ip-syb:20060010

Reyes, L., and Scopes, R. K. (1991). Membrane-associated ATPase from *Zymomonas mobilis*: purification and characterization. *Biochim. Biophys. Acta* 1068, 178–178.

Rogers, P., Lee, K., Skotnicki, M., and Tribe, D. (1982). Ethanol production by *Zymomonas mobilis*. *Adv. Biochem. Eng.* 23, 37–84.

Rogers, P. L., Jeon, Y. J., Lee, K. J., and Lawford, H. G. (2007). *Zymomonas mobilis* for fuel ethanol and higher value products. *Adv. Biochem. Eng.* 108, 263–288. doi: 10.1007/10_2007_060

Rohwer, J. M. (2012). Kinetic modeling of plant metabolic pathways. *J. Exp. Bot.* 63, 2275–2292. doi:10.1093/jxb/ers080

Rutkis, R., Kalnenieks, U., Stalidzans, E., and Fell, D. A. (2013). Kinetic modelling of *Zymomonas mobilis* Entner-Doudoroff pathway: insights into control and functionality. *Microbiology* 159, 2674–2689. doi: 10.1099/mic.0.071340-0

Santos, F., Boele, J., and Teusink, B. (2011). A practical guide to genome-scale metabolic models and their analysis. *Methods Enzymol.* 500, 509–532. doi: 10.1016/B978-0-12-385118-5.00024-4

Schellenberger, J., Que, R., Fleming, R. M. T., Thiele, I., Orth, J. D., Feist, A. M., et al. (2011). Quantitative prediction of cellular metabolism with constraint-based models: the COBRA Toolbox v2.0. *Nat. Protoc.* 6, 1290–1307. doi: 10.1038/nprot.2011.308

Schuster, S., Fell, D. A., and Dandekar, T. (2000). A general definition of metabolic pathways useful for systematic organization and analysis of complex metabolic networks. *Nat. Biotechnol.* 18, 326–332. doi: 10.1038/73786

Schuster, S., Hilgetag, C., Woods, J. H., and Fell, D. A. (2002). Reaction routes in biochemical reaction systems: algebraic properties, validated calculation procedure and example from nucleotide metabolism. *J. Math. Biol.* 45, 153–181. doi: 10.1007/s002850200143

Seo, J.-S., Chong, H., Park, H. S., Yoon, K.-O., Jung, C., Kim, J. J., et al. (2005). The genome sequence of the ethanologenic bacterium *Zymomonas mobilis* ZM4. *Nat. Biotechnol.* 23, 63–68. doi: 10.1038/nbt1045

Snoep, J. L., Yomano, L. P., Westerhoff, H. V., and Ingram, L. O. (1995). Protein burden in *Zymomonas mobilis*: negative flux and growth control due to overproduction of glycolytic enzymes. *Microbiology* 141, 2329–2337.

Sprenger, G. A. (1996). Carbohydrate metabolism in *Zymomonas mobilis*: a catabolic highway with some scenic routes. *FEMS Microbiol. Lett.* 145, 301–307.

Strohdeicher, M., Neuss, B., Bringer-Meyer, S., and Sahm, H. (1990). Electron transport chain of *Zymomonas mobilis*. Interaction with the membrane-bound glucose dehydrogenase and identification of ubiquinone 10. *Arch. Microbiol.* 154, 536–543.

Trinh, C. T., Unrean, P., and Srienc, F. (2008). Minimal *Escherichia coli* cell for the most efficient production of ethanol from hexoses and pentoses. *Appl. Environ. Microbiol.* 74, 3634–3643. doi: 10.1128/AEM.02708-07

Tuantili, I. C., Karim, M. N., and Klapa, M. I. (2007). Quantifying the metabolic capabilities of engineered *Zymomonas mobilis* using linear programming analysis. *Microb. Cell Fact.* 6, 8. doi: 10.1186/1475-2859-6-8

Wecker, M. S. A., and Zall, R. R. (1987). Production of acetaldehyde by *Zymomonas mobilis*. *Appl. Environ. Microbiol.* 53, 2815–2820.

Widiastuti, H., Kim, J. Y., Selvarasu, S., Karimi, I. A., Kim, H., Seo, J. S., et al., (2010). Genome-scale modeling and in silico analysis of ethanologenic bacteria *Zymomonas mobilis*. *Biotechnol. Bioeng.* 455–465. doi: 10.1002/bit.22903

Conflict of Interest Statement: The authors declare that the research was conducted in the absence of any commercial or financial relationships that could be construed as a potential conflict of interest.

Received: 16 November 2013; paper pending published: 29 December 2013; accepted: 21 January 2014; published online: 05 February 2014.

Citation: Kalnenieks U, Pentjuss A, Rutkis R, Stalidzans E and Fell DA (2014) Modeling of Zymomonas mobilis central metabolism for novel metabolic engineering strategies. Front. Microbiol. 5:42. doi: 10.3389/fmicb.2014.00042

This article was submitted to Microbial Physiology and Metabolism, a section of the journal Frontiers in Microbiology.